National Library
of Canada

Acquisitions and
Bibliographic Services Branch

395 Wellington Street
Ottawa, Ontario
K1A 0N4

Bibliothèque nationale
du Canada

Direction des acquisitions et
des services bibliographiques

395, rue Wellington
Ottawa (Ontario)
K1A 0N4

Your file Votre référence

Our file Notre référence

NOTICE

The quality of this microform is heavily dependent upon the quality of the original thesis submitted for microfilming. Every effort has been made to ensure the highest quality of reproduction possible.

If pages are missing, contact the university which granted the degree.

Some pages may have indistinct print especially if the original pages were typed with a poor typewriter ribbon or if the university sent us an inferior photocopy.

Reproduction in full or in part of this microform is governed by the Canadian Copyright Act, R.S.C. 1970, c. C-30, and subsequent amendments.

AVIS

La qualité de cette microforme dépend grandement de la qualité de la thèse soumise au microfilmage. Nous avons tout fait pour assurer une qualité supérieure de reproduction.

S'il manque des pages, veuillez communiquer avec l'université qui a conféré le grade.

La qualité d'impression de certaines pages peut laisser à désirer, surtout si les pages originales ont été dactylographiées à l'aide d'un ruban usé ou si l'université nous a fait parvenir une photocopie de qualité inférieure.

La reproduction, même partielle, de cette microforme est soumise à la Loi canadienne sur le droit d'auteur, SRC 1970, c. C-30, et ses amendements subséquents.

Canada

Surface Modifying Macromolecules for Enhancement of Polyethersulfone Pervaporation Membrane Performance

by

Phạm Vũ Anh

A thesis submitted to the School of Graduate Studies and Research

in partial fulfillment of the requirements for the degree of

MASTER OF APPLIED SCIENCE

in the Deparment of Chemical Engineering

University of Ottawa

August 1995

ISBN 0-612-07856-6

UNIVERSITÉ D'OTTAWA
UNIVERSITY OF OTTAWA

ABSTRACT

Polysulfones and their chemical derivatives are known to be versatile materials for the preparation of membranes. However, their potential use in the fabrication of pervaporation membranes has not been fully explored. The objective of this work was to modify the surface of polyethersulfone membranes in order to render them more useful in pervaporation for the removal of volatile organic compounds (VOC) from aqueous solutions.

Surface Modifying Macromolecules (SMMs) were designed and developed as surface modifiers of asymmetric polyethersulfone (PES) membranes. Eight SMM polymers were synthesized in triplicate using methylene bis-*p*-phenyl diisocyanate (MDI), polypropylene oxide (PPO) and polyfluoroalcohol (BA-L). They represented a 2^3 factorial design used to study the effects of reactant stoichiometry, prepolymer reactant concentration and chain length of the polyfluoroalcohol on the SMM properties and reproducibility of the SMM synthesis. The bulk SMM polymers were characterized with differential scanning calorimetry (DSC), gel permeation chromatography (GPC) and elemental analysis. The compatibility between PES and SMM polymers was studied by DSC.

The average molecular weight of SMM polymers, determined by GPC, were in the range of 1.0×10^4 to 3.5×10^4. As predicted by theoretical considerations, SMMs were found to have migrated to the PES surface, rendering it more hydrophobic. This migration effect was confirmed by water droplet contact angle measurements and X-ray photoelectron spectroscopy (XPS). Opaqueness of PES/SMM films and results of DSC showed that SMM was either immiscible or partially miscible with PES.

Preliminary pervaporation studies indicated that the addition of SMMs improved the selectivity of PES membranes, used in the separation of chloroform/water mixtures by 150 to 240%, depending on the chemical formulation of the SMM. In several cases, SMMs also improved the permeation rate. From a preliminary assessment of the changes in membrane surface and bulk characteristics, the surface chemistry and energetics were observed to contribute an important role in inducing the membranes' enhanced properties.

However, further information regarding bulk structure and microphase separation of the SMM within the PES matrix (among other possible factors such as membrane structure, membrane pore size or membrane solubility characteristics) will be required to better comprehend the mechanism of action of the SMM materials.

Kính tặng bố mẹ, Bác sĩ Phạm Ngọc Đức và Dược sĩ Vũ Tường Vân
và Thắm...

ACKNOWLEDGMENTS

The author is grateful for the support, guidance and suggestions of Professors J.P. Santerre and T. Matsuura throughout this research. Special thanks are extended to Mr. Daniel Duguay for his comments and challenging views, Professor A.Y. Tremblay for his constructive ideas, Dr. David Cooney for his guidance in thermal analysis techniques, Mr. Y. Fang for sharing some of the pervaporation results, and especially Ms. Phạm thị Thắm for the many hours she spent helping to edit the drafts of this thesis. The author also wishes to thank the assistance of the support staff at the Department of Chemical Engineering and the research personnel of the Taichman Laboratory at the Heart Research Institute.

The author wishes to thank the National Science and Engineering Research Council for the financial support, and Dr. M. Day of the Institute for Environment Chemistry, National Research Council, Ottawa for the use of thermal analysis equipments. The equipments and technical support provided by the Industrial Membrane Research Institute and the Cardiovascular Devices Division, University of Ottawa Heart Institute are also greatly appreciated.

Finally, the author wishes to thank his parents, brothers and sister for their support and understanding during the course of this research.

TABLES OF CONTENTS

LIST OF TABLES

LIST OF FIGURES

Chapter 1

INTRODUCTION

1.1 Volatile organics : the problem

Groundwater contaminated with a low concentration (in the range of parts per million, ppm) of volatile organic compounds (VOC) is the most common type of hazardous water contamination (Brewer, 1991). VOC are also common industrial chemicals, and their separation from various liquid or gaseous waste streams is important in waste reduction and control (Narbaitz and Benedeck, 1986; Amy et al., 1987; Levenston Assoc. et al., 1991). Techniques such as air stripping, activated carbon adsorption and UV-peroxide oxidation are being used successfully to purify water, but with some deficiencies (Brewer, 1991). Air stripping transfers the contaminants from one phase to another. Activated carbon adsorption has a variable response to contaminants, and the spent activated carbon may pose a secondary hazardous solid waste problem. UV-peroxide oxidation and other advanced oxidation schemes are very effective, but are also expensive and energy intensive.

1.2 The membrane separation solution

Recovery of valuable organics is always a preferable means for pollution control; however, this path is seldom economical for standard methods where the concentration of the organics is low (<10,000 ppm). Several membrane separation technologies offer possible alternatives that could overcome some of the deficiencies associated with existing technologies for water and air pollution reduction, and for VOC recovery and reuse. These technologies include membrane separation via pervaporation of liquid streams followed by compression-induced condensation, and vapor permeation of gaseous streams. Figure 1-1 shows the range of VOC concentrations where pervaporation is applicable. The development of more efficient membranes and the ease of membrane manufacturing could expectedly make this the technology of choice.

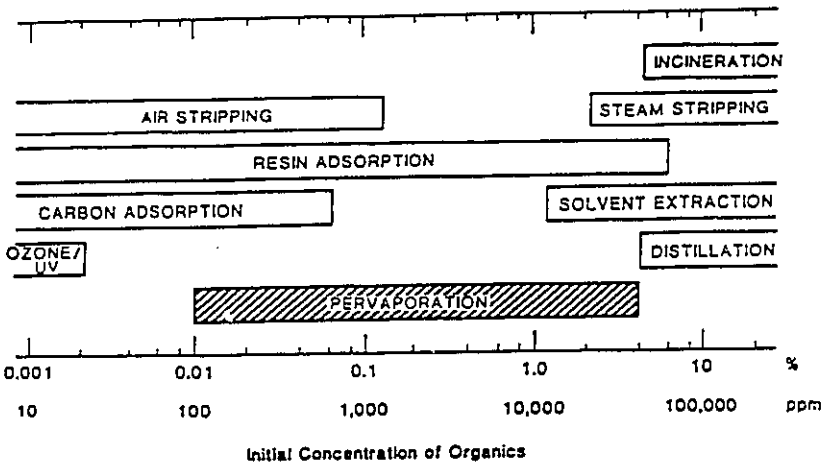

Figure 1 - 1 : Commercial methods of removing VOC from aqueous streams (Ho and Sirkar, 1992, p. 152)

1.3 Membrane pervaporation and vapor permeation

The removal of volatile organics by pervaporation and by vapor permeation has been reviewed recently by Huang (1991). Pervaporation is a process where the permeant undergoes a phase change from liquid to vapor as it passes through a selective membrane. In vapor permeation, the feed is first evaporated to a saturated state prior to membrane contact. The permeate side of the membrane is kept under vacuum or in contact with a stream of sweeping inert gas, and the permeate is collected by condensation. In both cases, separation is possible because of difference(s) between the behaviour of permeants in the membrane. Differences have been observed with respect to permeation rate (Huang and Rhim, 1991) and affinity for the membrane (Yoshikawa et al., 1984a,b).

Néel (1991) suggested that the transition from the liquid to vapor state is a multistage process that is much more complex than a single vaporization step, and the composition of the pervaporate differs widely from that of the mixed vapor obtained after equilibrium conditions. Hence, pervaporation is a non-equilibrium process. In conjunction with an appropriate membrane, it can efficiently separate azeotropic mixtures. The mixtures to be separated can be of water/organic or organic/organic type. According to the feed composition (Huang, 1991), the pervaporation process is referred to as the dehydration of an organic liquid, the removal of organics from a water stream, or the separation of two organic liquids.

Initially, pervaporation was studied using a dense, homogeneous membrane; however, the low permeation rate obtained prevented its development into an industrial application. The development of the "phase-inversion" membrane making method by Loeb and Sourirajan in the 1960's, which produced a characteristic high-flux asymmetric membrane, provided a possible solution for overcoming this low permeation rate problem (Néel, 1991). Research on membranes has since continued with emphasis on both new materials and their related processing techniques.

There is yet a systematic method for choosing the correct material(s) to make a membrane for a specific application. Most of the time, materials and membranes are evaluated by trial and error, or based on experience (Kesting, 1971; Matsuura, 1993). Koops and Smolders (1991) have provided comprehensive articles describing common observations and rules of thumb, as well as some strategies in the selection of material for pervaporation membranes. In general, membranes made from hydrophobic elastomeric polymers have been known to be highly selective toward organics and thus are effective in removing VOC from water by pervaporation (Koops and Smolders, 1991). To date, most of the applied developments have been with polydimethylsiloxane (PDMS) or silicone rubber material (Fleming and Slater, 1992). Composite membranes, having a thin selective layer of PDMS, have been used industrially. For example, a German company, Gesellschaft Für Trenntechnik (GFT), has successfully developed a pervaporation process for the dealcoholization of beers, wines, and liquors using PDMS composite membranes (Escudier et al., 1988). Processes for the removal and recovery of trace organics from groundwater and industrial waste water using composite PDMS membranes are also commercially available (Bengston and Boddeler, 1988; Kaschemekat et al., 1988).

1.4 Research motivations and methods

The development of membrane based separations consists of three major stages: (i) material selection or development, (ii) membrane making from the selected material and (iii) membrane module development (Kesting, 1971; Matsuura, 1993). The successful

completion of each stage depends on two factors: economics and engineering. Evaluation of the economic aspect is based on the cost of membrane development and the market in which the developed membrane will compete as a solution to a problem. Most often, the high cost of the membrane is associated with the special engineering methods necessary for maintaining membrane productivity. For example, PDMS membranes require chemical treatment to control swelling due to the absorption of feed components at a particular operating temperature. This swelling is responsible for loss of productivity (Blume and Baker, 1987; Eustache and Histi, 1981).

The efficient use of membranes requires large surface areas (Kesting, 1971; Matsuura, 1993). However, PDMS composite membranes, due to their insufficient mechanical properties, need special physical configurations for modules. Since these modules usually do not allow for a high surface to volume ratio, many modules are required (Blume and Baker, 1987), and the resulting additional capital cost contributes to the limited use of these membranes. The use of PDMS based membranes will diminish further due to their low solvent resistance, which contributes to swelling and loss of selectivity (Eustache and Histi, 1981). Therefore, there is a need to develop a membrane which has good selectivity for organics, while not having the disadvantages of PDMS based membranes.

Potential solutions to meet this need include the optimization of existing membrane manufacturing methods, development of new materials, and modification of existing materials. There is a limit as to what process optimization can do; for example, it can not change the mechanical properties of the PDMS membrane. Justification for the development of new materials is often not practical since the current market size for pervaporation is small, and there is not a concise understanding of which material characteristics correlate with the separation properties of the membrane.

Modifying the surface of existing membranes seems to offer both engineering and economic feasibility. In particular, modification of membranes which are made from conventional materials like polyethersulfone (PES), polyetherimide (PEI) or polysulfone

(PS) will enjoy the additional advantage of using the existing industrial membrane manufacturing facilities. The hypothesis is that significant changes to the pervaporation membrane selectivity toward organic compounds and permeation rate can be achieved by modifying the surface hydrophobicity of the membrane. This hypothesis is based on two general observations: firstly, it is well documented that surface chemistry and morphology play an important role in permeant transport (Kesting, 1971; Matsuura, 1993), and secondly, membrane hydrophobicity favors organic selectivity (Koops and Smolders, 1991; Fleming and Slater, 1992). Furthermore, the reverse application of this hypothesis is supported by studies for dehydration by pervaporation, where water selectivity is of importance. Yoshikawa et al. (1984a, 1984b) have shown that the hydrophilicity of a membrane is the determinant factor in water selectivity. Using this result, Huang and Xu (1988), Huang et al. (1988) and Xu and Huang (1988) have modified the surface of membranes to increase hydrophilicity and have successfully improved the water selectivity of their membranes.

The purpose of this work then is to modify the conventional membranes in order to change their surface energetics, so that the surface hydrophobicity would be equal to or greater than that of PDMS. Moreover, Koops and Smolders (1991) concluded that hydrophobic polymers like polyethylene, polypropylene, polytetrafluoroethylene or polyvinylfluoride, which lack hydrophilic groups, have a low selectivity for water/organic and organic/organic liquid mixtures. These authors suggested that the possible reason lies in the absence of strong interactions between permeants and membrane to create a differential driving force. They have also suggested that permeation and separation can only take place in the amorphous parts of the semi-crystalline polymers, with separation based on differences in size and shape of the permeants. If these authors are correct, modifying the hydrophobicity of conventional amorphous polymer surfaces should increase the selectivity.

Glassy and amorphous polymers like PES, PEI and PS also offer good control over pore characteristics which, along with affinity, determine the overall selectivity of a membrane (Matsuura, 1993). Hence, a surface modification technique on membranes

made from these conventional materials could produce better separation characteristics by providing a means for adjusting the affinity factor (i.e. hydrophobicity).

Surface modification techniques have been used to improve the transport properties of membranes in a variety of processes. Some of these techniques include radiation grafting polymerization in membrane distillation (Wu et al., 1992); chemical coating (Stengaard, 1988), electron radiation (Nyström, 1989) and surface fluorination in ultrafiltration (Hvid et al., 1991; Keszler, 1991; Sedath et al., 1993); plasma polymerization or deposition in reverse osmosis (Lai and Chao, 1990; Li et al., 1990) and surface fluorination in gas separation (Mohr et al., 1991). In pervaporation, efforts have been concentrated on controlling the swelling and/or the hydrophilicity of membranes used in dehydration. Some of the methods applied include grafting (Huang and Xu, 1988), cross-linking (Huang et al., 1988; Xu and Huang, 1988; Kang et al., 1990) and plasma polymerization (Inagaki et al., 1988; Masuoka et al., 1992).

All of the above mentioned methods are potentially useful for modifying polymer surface energetics, but there are some deficiencies associated with each of them. An ideal technique would provide flexibility in application and ample controllability to prevent over-modification to the point of damaging the polymer surface. It also has to limit its modification to the surface, so that the bulk properties of the polymer are kept relatively intact. Plasma techniques and surface fluorination can not be easily controlled, and the mechanism of these processes are not yet fully understood; hence, surfaces produced by these methods usually encounter problems such as irreproducibility and irreversible surface damage (Néel, 1991). Cross-linking is only useful for producing solvent resistant surfaces; its use in modifying the surface energetics is rare. Chemical coating and grafting require specific conditions which somewhat limit their uses. An attractive alternative is the use of surface active additives as a component of the membrane casting solution. This method offers advantages such as simplicity of application, and better control with regard to reproducibility. To date, the use of this technique in membrane fabrication has not been openly reported in the literature.

The driving force for minimization of interfacial energy is universal to all condensed phase of matters (Somorjai, 1981). The phenomenon whereby a surface active component in a polymeric mixture determines the final polymer's surface characteristics has been reported by Hu and Sung (1980) and Ratner and Paynter (1984). Minimization of surface tension by reorientation of the lower surface energy segment at the polymer surface for a multi-component system, (i.e. copolymers), has been reported by Kasemura et al. (1978, 1979, 1987a, 1987b, 1987c). The concept of adding a surface active component into a polymer mixture to minimize polymer surface energy has been hypothesized and applied successfully by Kasemura et al. (1993) for epoxy resin, and by Ward et al. (1984), Ward (1989), Ratner et al. (1984), Kober and Wesslén (1992) in developing bio-compatible materials.

1.5 Scope of the research

The objective of this work is to develop surface active additives to be used for the fabrication of pervaporation membranes using conventional materials, specifically PES. These surface active additives would improve surface hydrophobicity of PES. The modified PES membrane would ultimately have better separation characteristics than currently available membranes. The initial concept was to take advantage of the low surface energy characteristics of the new Zonyl^{TM} intermediates (Figure 1-2) by synthesizing surface active additives with these molecules. In many ways, the use of the Zonyl^{TM} materials is similar to the recent work of Schmidt et al. (1994), where these materials were coated and chemically stabilized to generate a new low energy non-stick surface.

$$F\text{-}(CF_2)_m\text{-}CH_2\text{-}CH_2\text{-}OH$$

Figure 1 - 2: Chemical structure of Zonyl^{TM} Intermediates.

According to previous work (Ward et al., 1984; Kasemura et al., 1993), the most effective surface active additive possesses an amphipathic structure. In this particular

case, this means that it has both polar and non-polar polymer blocks. These investigators also made the following general observations:

(i) The surface of a polymer modified by a surface active additive can be saturated with the additives at relatively low concentration (< 5% w/w), and the modified surface properties would be those of the additives (Ward et al, 1984).

(ii) Surface active additives usually possess segments that are compatible with the polymer in which they are dispersed. This factor is crucial for the longterm stability of the additives at the surface (Ward et al, 1984; Kasemura et al., 1993).

(iii) The degree of surface modification depends on the molecular weight of the additive (Ward et al, 1984; Ward, 1989), the miscibility of the additive (Kasemura et al., 1993) and the nature of the low surface energy segment.

The Zonyl fluorohydrocarbons (also called polyfluoroalcohol) can be used as starting materials for the synthesis of polyurethane block copolymers that could have the physical properties of a polyurethane elastomer and hydrophobicity that surpasses that of PDMS and PTFE, since the Zonyl^{TM} intermediates can induce a critical surface tension of 3-5 dynes/cm in comparison to 18.5 for PTFE and 21-24 for PDMS (DuPont Co., 1988). Yu, Okkema and Cooper (1990) have synthesized and characterized polyfluoro-alkyletherurethanes. Their results showed that it was possible to synthesize polyurethane containing fluoroalkyl groups which have different physical characteristics, such as tensile strength and elongation, and that possess a low surface energy characteristic due to the orientation of the fluoro-segment at the surface. The successful incorporation of fluorine based moieties at the membrane surface would also enhance thermal and oxidative stability (Munekata, 1988) and yield good chemical resistance (Hunston et al., 1978).

The surface active additives in this work will be called surface modifying macromolecules (SMMs). The hypothetical structure of an SMM is composed of two parts: a main body chain resulting from a polyaddition reaction of diisocyanate and polymeric diol to form a prepolymer, and a surface active part, which is the result of the

end-capping reaction of Zonyl^{TM} intermediate molecules with the isocyanate terminated prepolymer. The proposed synthesis scheme along with the hypothetical structure is shown in Figure 1-3.

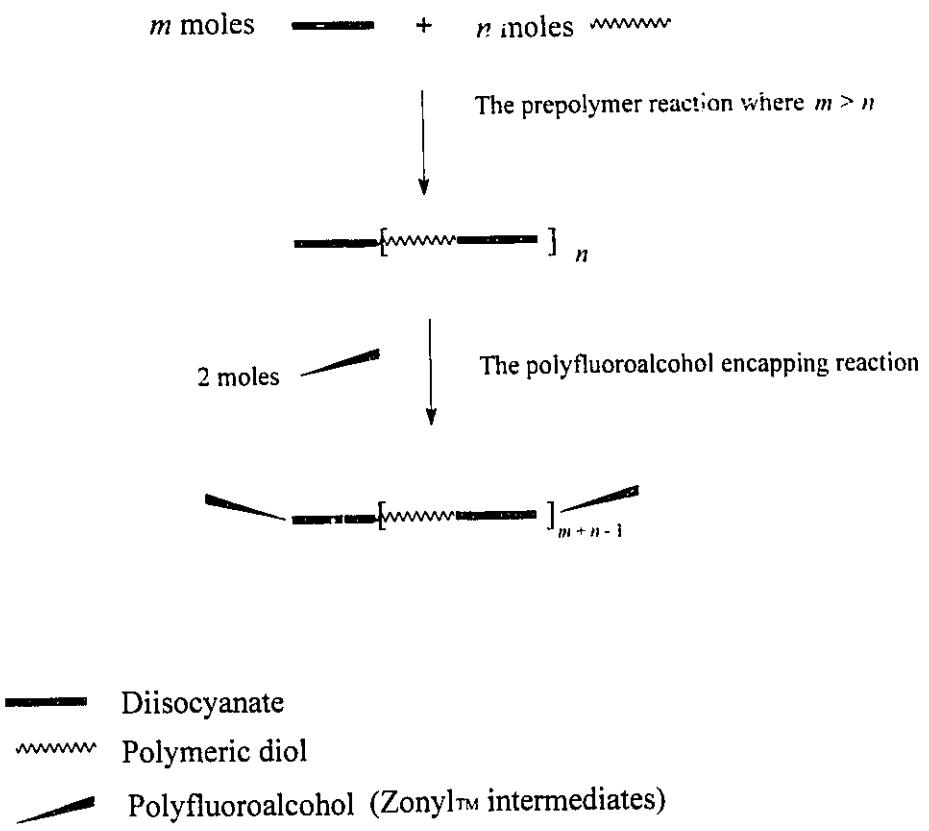

Figure 1 - 3 : The proposed scheme for SMM synthesis

The research will study three aspects of the SMM materials: (i) material characteristics of the SMMs, (ii) surface modification and polymer/SMM compatibility, and (iii) relationship between surface characteristics and separation properties. The first two aspects can be somewhat determined experimentally, but the needed functional relationship between the surface characteristics and separation properties of a membrane is not yet fully understood. Moreover, it is logical to suspect that there exists a chance that the optimum in membrane performance does not coincide with the optimum in surface modification, even if surface properties can be manipulated with the use of

surface active additives such as SMMs. For this reason, a trial and error approach as illustrated by the flowchart in Figure 1-4 has been adopted for this work.

The primary concern is to obtain a reasonably reproducible SMM, so that reliable membrane testing can be carried out. To evaluate the reproducibility, bulk properties of the SMMs such as the glass transition temperature (T_g), component composition, relative average molecular weight and its distribution will be compared. Afterward, further studies with respect to the surface modification of PES and bulk behaviour of the PES/SMM mixtures will be carried out. These properties can be studied with surface characterization techniques like X-ray photoelectron spectroscopy (XPS), contact angle measurements, and differential scanning calorimetry (DSC) to determine the thermal characteristics for the PES/SMM mixtures.

From the theoretical structure of an SMM (Figure 1-3), it is logical to expect that the bulk of the design function (i.e. surface properties) of these materials comes from their end-groups, which, in traditional materials, become significant only when the size of the polymer chain is within a certain range (Rosen, 1982; Danusso et al. ,1993). Hence, one of the important results to be determined is the effect(s) of the SMM molecular weight on surface modification and pervaporation characteristics. Other effect(s) may be due to the chemical nature and composition of the end-groups and the main chain.

The objectives of this research are therefore:

(i) To synthesize SMMs based on a fixed set of reactants and to indentify the variables of synthesis which control SMM properties.

(ii) To identify the parameters which yield the most reproducible SMM(s).

(iii) To assess the effect(s) of SMM molecular weight and fluorinated characteristics on the surface modification and bulk properties of PES.

(iv) To demonstrate the influence(s) of various SMMs, with different molecular weight and fluorinated characteristics, on pervaporation characteristics of the modified PES membranes.

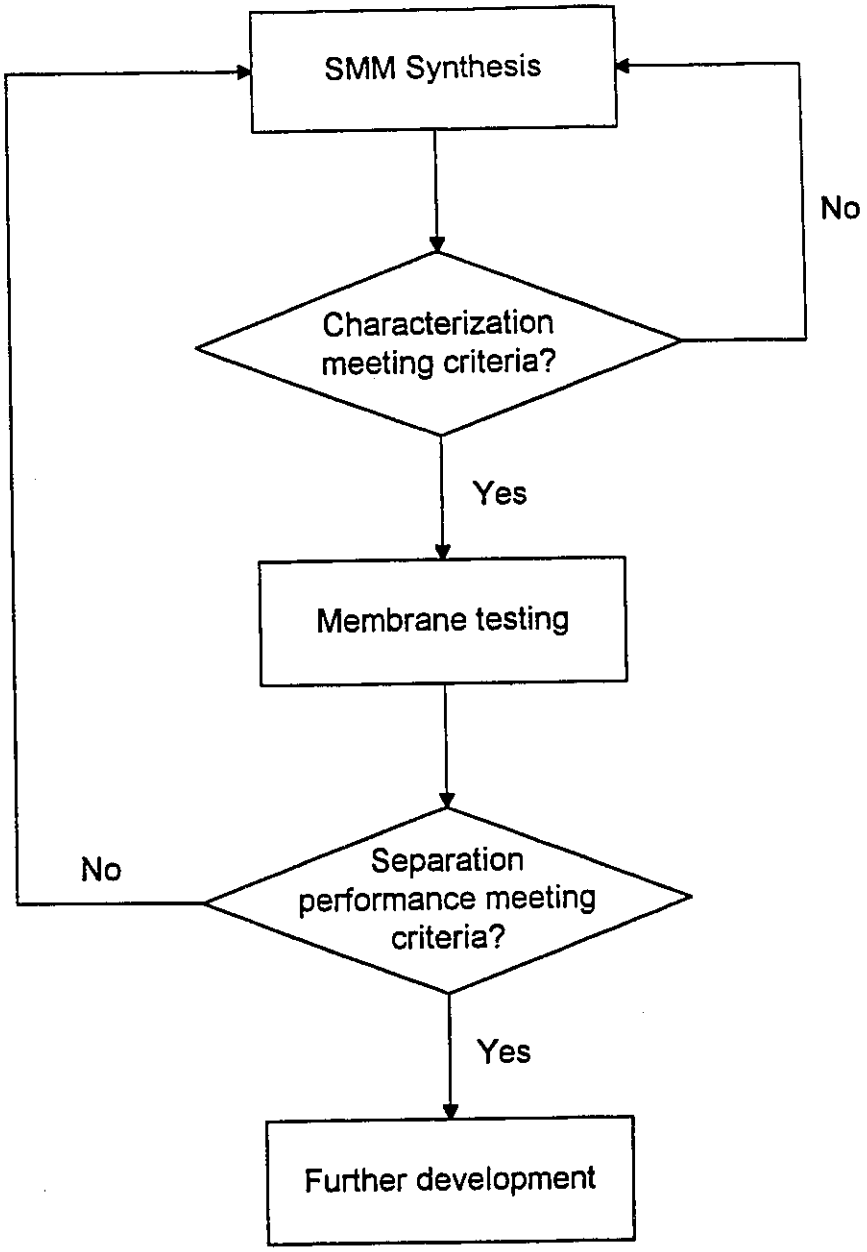

Figure 1 - 4 : The SMM-membrane development process.

Chapter 2

THEORETICAL BACKGROUND

The concept of adding surface modifying macromolecules (SMMs) into the membrane casting solution of a conventional thermoplastic polymer to produce a membrane surface with hydrophobic character has been described in the introduction. This membrane will hypothetically have enhanced organic selectivity relative to membranes made without SMM. As described previously, the development of an SMM does not follow a rigid theoretical approach; however, there are four theoretical aspects which would serve as the basis for qualitative assessment of what an SMM should be and for quantitative evaluation of the potential parameters which are of engineering importance. These aspects include: (i) the thermodynamics of interfacial phenomena, (ii) the thermodynamics of polymer blends or mixtures, (iii) the polyurethane chemistry which governs the synthesis of an SMM, and (iv) the theory of pervaporation. The important points of each aspect will be presented; they will serve as a basis for the experimental design and discussion of results.

2.1 Thermodynamics of interfacial phenomena

There are a number of good books and reviews available on the thermodynamics of interfacial phenomena (Aveyard and Haydon, 1973; Davies and. Rideal, 1963; Bikerman, 1970; Somorjai, 1981; Andrade, 1985). This section deals with the definitions and semantics of commonly encountered terms as well as the fundamental phenomena of the interface.

Surface phenomena are commonly described by terms such as surface free energy, surface tension, surface stress and interfacial energy. A clear understanding of some of these expressions is sometimes confused with their historical meanings. For example, before the introduction of the energy concept, surface tension had been used to describe the tendency of surface films to minimize surface areas, and the word surface really

means interface (Davies and Rideal, 1963). Thus, when describing the various thermodynamic terms and quantities in surface phenomena, they must be clearly understood and appropriately defined.

The thermodynamic property of the surface is characterized mainly by the reversible work γ (gamma) to create a unit area of surface at constant temperature (T), volume (V), and chemical potential of component i (μ_i). It is only under certain conditions that γ is equal to the surface free energy, and it is not the surface stress. Although γ is widely called surface tension, its meaning has little physical significance in many situations (Davies and. Rideal, 1963). The γ of a newly created surface is defined as

$$\gamma \equiv \frac{dw}{dA} \tag{2.1}$$

i.e. the specific surface work to create dA new surface area. The thermodynamics of interfaces (Table 2-1) is essentially the same as the thermodynamics of homogeneous systems, except that the work term in the latter will include all of the γdA components for the heterogeneous (interface-containing) systems.

When a new surface area, dA, is created, there is a possibility that a number of molecules, dN, move to or from the surface region. This movement introduces the concept of surface excess or deficiency of component i :

$$\Gamma_i \equiv \frac{dN_i}{dA} \equiv \text{surface excess of component } i \,. \tag{2.2}$$

The expressions for surface energy (E), surface Gibbs free energy (G), and surface Helmholtz free energy (F) can be developed from basic thermodynamic equations (Table 2-1) with $dN_i=\Gamma_i dA$:

$$\begin{aligned} (dE)_{S,V} &= \gamma dA + \sum \mu_i \Gamma_i dA \\ (dG)_{T,P} &= \gamma dA + \sum \mu_i \Gamma_i dA \\ (dF)_{T,V} &= \gamma dA + \sum \mu_i \Gamma_i dA \end{aligned} \tag{2.3}$$

Table 2 - 1: Summary of Basic Reversible Thermodynamic Equations for Single-Component, Multi-component, and Surface-Containing Systems (Andrade, 1985, p. 251).

Quantity	Single-component "surface-free" system	Open or multiple component system— no surface	Open system with surface[b]
Internal Energy, E	$dE = T\,dS - P\,dV$	$dE = T\,dS - P\,dV + \sum_i \mu_i\,dN_i$	$T\,dS - P\,dV + \sum_i \mu_i\,dN_i + \gamma\,dA$
Enthalpy, H	$dH = T\,dS + V\,dP$	$dH = T\,dS + V\,dP + \sum_i \mu_i\,dN_i$	$T\,dS + V\,dP + \sum_i \mu_i\,dN_i + \gamma\,dA$
Helmholtz free energy, F	$dF = -S\,dT - P\,dV$	$dF = -S\,dT - P\,dV + \sum_i \mu_i\,dN_i$	$-S\,dT - P\,dV + \sum_i \mu_i\,dN_i + \gamma\,dA$
Gibbs free energy, G	$dG = -S\,dT + V\,dP$	$dG = -S\,dT + V\,dP + \sum_i \mu_i\,dN_i$	$-S\,dT + V\,dP + \sum_i \mu_i\,dN_i + \gamma\,dA$
		$\left(\frac{\partial G}{\partial N_i}\right)_{T,P,N_j} \equiv (\mu_i)$ = chemical potential	$dN_i/dA \equiv \Gamma_i$ = surface excess $\sum \mu_i\,dN_i = \sum \mu_i \Gamma_i\,dA$

[a] In the absence of other forms of work, e.g., electrical, magnetic, gravitational, etc.
[b] For more than one type of surface, replace $\gamma\,dA$ by $\sum_i \gamma_i\,dA_i$.

The corresponding specific energy and specific free energies are defined by Andrade et al. (1985) as

$$\left(\frac{\partial E}{\partial A}\right)_{S,V} \equiv e_s = \gamma + \sum \mu_i \Gamma_i \equiv \text{specific surface energy}$$

$$\left(\frac{\partial G}{\partial A}\right)_{T,P} \equiv g_s = \gamma + \sum \mu_i \Gamma_i \equiv \text{specific surface Gibbs free energy}$$

$$\left(\frac{\partial F}{\partial A}\right)_{T,V} \equiv f_s = \gamma + \sum \mu_i \Gamma_i \equiv \text{specific surface Helmholtz free energy} \qquad (2.4)$$

$\gamma = e_s = g_s = f_s$ if and only if $\Gamma_i = 0$ (applicable for pure substance) and at constant T,P,S,V. In general, the surface Helmholtz and Gibbs free energy and the surface energy are different quantities. γ is generally not f_s, g_s or e_s although it may be equal to one, both or all three of these quantities under special conditions. Specific Gibbs free energy is preferred to represent the specific surface work and specific surface free energy, since pressure is generally more constant than volume in a heterogeneous system. These quantities are commonly expressed in ergs/cm^2 or mJ/m^2, as well as dynes/cm or N/m.

The process of forming a new surface can be divided into two parts (Davies and Rideal, 1963):

(i) The phase must be displaced to expose the new surface

(ii) Atoms in the surface plane rearrange to assume their equilibrium positions.

In liquids, parts one and two happen almost instantaneously, and the creation of the new surface produces γ or the reversible work to form the new surface. In solids, part two may occur slowly or not at all. Due to low atomic mobility, a solid can be stretched or compressed without changing the number of atoms at the surface; however, the distance of separation between atoms is altered, resulting in surface stress. In a multi-component system, part two can be combined with the migration of atoms to or from the interface, i.e. the development of surface excesses or deficiencies, Γ_i. In a single-component system, $\Gamma_i = 0$, unless there is a change in density near the surface. Therefore, in a

single-component system, γ is both the specific Gibbs free energy and the specific Helmholtz free energy at constant density, and can be called specific surface free energy. When $S = 0$ (i.e. no restructuring), γ will also be called the specific surface free energy.

From basic thermodynamics, using either the Gibbs or Guggenheim treatment of interfaces, it can be shown that

$$(d\gamma)_T = -\sum \Gamma_i d\mu_i \tag{2.5}$$

where the surface excess of component i, $\Gamma_i \equiv N_i / A$. Equation 2.5 is the Gibbs adsorption equation, a fundamental equation of surface chemistry which relates the surface excess of components with the change in surface energy. If $\Gamma_i > 0$, i is concentrated at the surface zone and the phenomenon is called adsorption. If $\Gamma_i < 0$, there is a deficiency of i at the surface and is referred to as negative adsorption.

The energy necessary to create a new surface is always positive (Gibbs, 1928). This means that a solid or a liquid would have a lower total energy if there were no surface. The magnitude of the specific surface energy , γ, depends on the chemical bonding of the solid or liquid (Somorjai, 1981). Metals possess the highest specific surface energy, whereas fluorinated hydrocarbons are among those with the lowest specific surface free energy (Table 2-2). This positive surface energy provides the thermodynamic driving force for changes in the surface's shape and chemical composition. Condensed systems, in equilibrium, minimize their total surface energy by adopting shapes with the smallest possible surface area (Somorjai, 1981). Surface free energy can also be minimized by certain substances covering the surface (Somorjai, 1981). This is one of the reasons why a high energy metal surface is readily covered by low energy organic compounds. In an environment where there are many components of different specific surface energy, a hierarchical composition of the surface can be found (Figure 2-1), where the lowest specific surface energy component occupies the outermost layer. Wetting or lack of adhesion is determined by whether the spreading of one type of molecule on the surface reduces or increases the total surface free energy (Somorjai, 1981).

Table 2 - 2 : Specific surface free energies of selected solids and liquids (Somorjai, 1981, p. 31).

Material	γ (ergs/cm^2)	T (°C)
W (solid)	2900	1727
Nb (solid)	2100	2250
Au (solid)	1410	1027
Ag (solid)	1140	907
Ag (liquid)	879	1100
Fe (solid)	2150	1400
Fe (liquid)	1880	1535
Pt (solid)	2340	1311
Cu (solid)	1670	1047
Cu (liquid)	1300	1535
Ni (solid)	1850	1250
Hg (liquid)	487	16.5
LiF (solid)	340	−195
NaCl (solid)	227	25
KCl (solid)	110	25
MgO (solid)	1200	25
CaF_2 (solid)	450	−195
BaF_2 (solid)	280	−195
He (liquid)	0.308	−270.5
Na (liquid)	9.71	−195
Xenon (liquid)	18.6	−110
Ethanol (liquid)	22.75	20
Water (liquid)	72.75	20
Benzene (liquid)	28.88	20
n-Octane (liquid)	21.80	20
Carbon tetrachloride (liquid)	26.95	20
Bromine (liquid)	41.5	20
Acetic acid (liquid)	27.8	20
Benzaldehyde (liquid)	15.5	20
Nitrobenzene (liquid)	25.2	20
Perfluoropentane (liquid)	18.6	−110

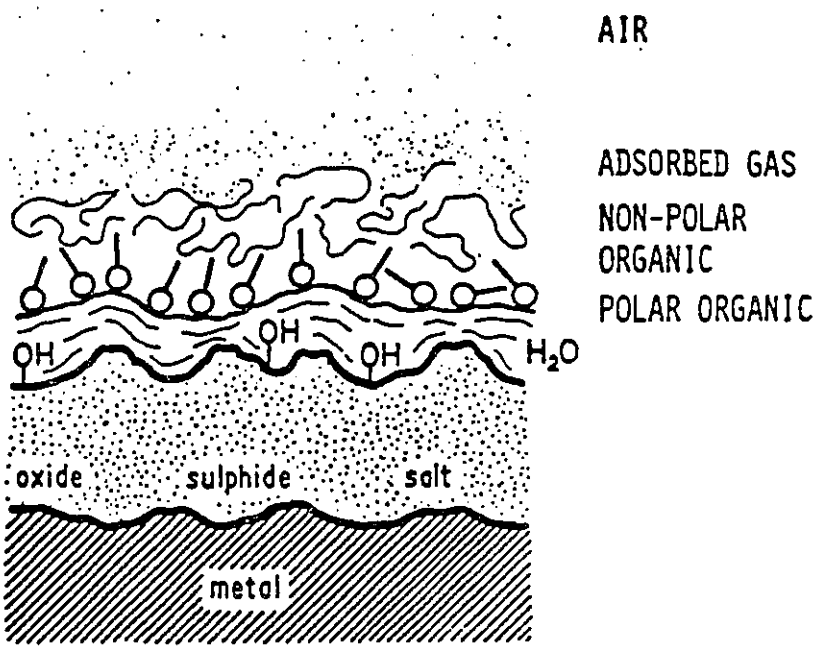

Figure 2 - 1 : Hierarchy of spontaneously adsorbed layers on a metal or other high-energy surfaces (Andrade, 1985, p. 255).

In polymer systems, the analysis of interfacial phenomena is much more complex because these systems are not in equilibrium. Polymer systems are dynamic and environmentally dependent due to the large molecular weight and thermodynamic heterogeneities such as local chain motion, partial crystallinity or mixed phase domain(s). When a polymer surface is created, the start and completion of the two-part process of phase displacement and equilibration may be somewhere between those of an ideal liquid and solid. The hierarchy of components based on their specific surface energy is also present in polymer systems (Hu and Sung, 1980; Ratner and Paynter, 1984). Minimization of interfacial energy in a polymer system by rearrangement of the low surface energy components can occur in two ways, depending on polymer type and how it was processed. In copolymers, the interfacial segment possessing a low surface energy will orient itself according to the environment in which it is exposed to (Hu and Sung, 1980). In melt processing and solution processing or when there is sufficient mobility of polymers, the components with the lowest surface energy will segregate at the interface (Hu and Sung, 1980). This effect has been exploited successfully to synthesize low surface energy materials.

Polymer surface modification using surface active additives is governed by two factors. One factor is thermodynamics, which requires that the modifier has a lower specific surface energy than that of the bulk polymer. The second factor is the kinetics of surface accumulation, which is thought to depend on polymer miscibility whenever polymers are blended (Kasemura et al., 1993).

2.2 Polymer blends and miscibility

Polymer miscibility affects the amount of SMM which can be mixed into the casting solution. It also affects the distribution of the SMM in the surface. If the bulk polymer and the SMM are miscible, then the demixing process would be slow, and the ability of the SMM to accumulate at the interface decreases. The advantage of having a miscible SMM-polymer system is in obtaining a homogeneous membrane. An immiscible SMM-polymer would have fast surface accumulation, but would also result in phase separation

in the membrane. Another important aspect which is related to polymer miscibility is the stability of the SMM in the membrane. Intuitively, immiscible pairs will have low stability and thus are undesirable.

The subject of blending polymers is discussed in a number of books and reviews (Paul, 1993; Paul and Newman, 1978; Krause, 1978). In the following sections, some descriptions of the terms and fundamental concepts of blending polymers will be presented to demonstrate the importance of this aspect on the development of the SMM.

2.2.1 Characteristics of miscible blends

Miscible blends are homogeneous at the polymer segment level, and single phase blends are usually optically transparent. The resulting properties of a miscible blend will be at least as good as the composition weight average of pure components. It was often concluded that miscibility among polymer-polymer pairs is a rare exception; however, recent research has shown that this statement is somewhat overstated (Paul, 1993). Significant advances have been made in understanding the origin of the interactions governing miscibility, quantifying their thermodynamic parameters and learning how to control them through molecular structure (Paul and Newman, 1978). Advances in this area for copolymers were attained by using binary interaction models to properly account for both the intermolecular and intramolecular interactions among monomer units (Paul and Newman, 1978).

2.2.2 Immiscible blends

Immiscible blends have phase domains that consist, in the limiting case, of the corresponding pure components. Unlike composites, their phase morphology is not predetermined because all phases are fluid during processing (Paul and Newman, 1978). Also in many cases, there is a high interfacial tension between the components in the melt or solution that leads to an unstable or uncontrolled phase morphology (Paul and Newman, 1978).

2.2.3 Thermodynamic considerations

Miscibility of polymer mixtures is best understood and should only be defined in thermodynamic terms. However, techniques for critically and unambiguously examining the thermodynamics of miscible polymer-polymer mixtures are very limited (Paul and Newman, 1978). Results from techniques such as neutron scattering studies of polymer mixtures have shown promise in fulfilling the need for conceptual and quantitative studies (Kirste and Lehnen, 1976; Krause et al., 1976; Ballard et al., 1976).

In a typical experiment, one polymer in the mixture is considered to be a 'solute' in the other, and the 'solution' is studied via neutron scattering in a manner similar to classical light scattering of polymer in a solvent (Flory, 1953). Scattering intensities have been measured as a function of 'solute' concentration and scattering angle, and subsequently analyzed by a Zimm plot. In these studies, the analysis gave the correct molecular weight for the 'solute' polymer, which is the confirmation that these 'solutions' are classical ones, having miscibility in a true thermodynamic sense (Paul and Newman, 1978). Furthermore, it was found that the radius of gyration of the solute polymer has the size predicted in both bulk or dilute solution, as well as having similar molecular weight dependence. This observation provided the first conclusive evidence to suggest that conformations in polymer-polymer solution are substantially the same as those in other better understood polymer states (Paul and Newman, 1978). It also implies that the segments of the two polymers are more or less in random contact, as solvent molecules and polymer segments mix together (Flory, 1953). This kind of behaviour, however, was observed only for blends that show a single glass transition temperature (T_g) (Stein et al., 1974). The use of a single glass transition temperature as a criterion for indicating blend miscibility has since been accepted as a somewhat fundamentally justified measurement of miscibility (Paul and Newman, 1978).

2.2.4 Effect of molecular weight

The unique factor that affects the thermodynamics of polymer blends, compared to other systems, is the large molecular weight of both components. In general, the qualitative thermodynamic argument, which limits miscibility to a rare occurrence in

polymer blends, recognizes that the entropy of mixing ΔS_{mix} in the free energy of mixing expression, Equation 2.6, will be very small since a large molecular weight leads to a smaller number of moles for the respective polymers in the blend.

$$\Delta G_{mix} = \Delta H_{mix} - T\Delta S_{mix} \tag{2.6}$$

While the negative sign of the combined entropy favors mixing, it is usually too small since the heat of mixing ΔH_{mix} is generally thought to be positive, at least for relatively polar systems.

The Flory-Huggins polymer solution theory (Flory, 1953), although inadequate in some cases, provides a useful first approximation for the terms in Equation 2.6. This theory gives the free energy of mixing of polymers A and B:

$$\Delta G_{mix} = RTV\left\{\frac{\phi_A \ln \phi_A}{V_A'} + \frac{(1-\phi_A)\ln(1-\phi_A)}{V_B'} + \chi_{AB}\phi_A(1-\phi_A)\right\} \tag{2.7}$$

where ϕ_A is the volume fraction of A, V_i' is the molar volume of i , and χ_{AB} is an interaction parameter related to the heat of mixing, which is positive for endothermic systems.

In the special case where both polymers have the same molecular weight M and density ρ, and when χ_{AB} is replaced by an equivalent parameter $2\rho/M_{CR}$, where M_{CR} will be a critical molecular weight (Paul, 1978), Equation 2.7 can be rewritten as:

$$\Delta G_{mix} = \frac{\rho VRT}{M_{CR}}\left\{\frac{M_{CR}}{M}\left[\phi_A \ln \phi_A + (1-\phi_A)\ln(1-\phi_A)\right] + 2\phi_A(1-\phi_A)\right\} \tag{2.8}$$

Thermodynamic stability for a one phase mixture exists only when Equation 2.9 is satisfied.

$$\left(\partial^2 \Delta G_{MIX} / \partial \phi^2\right)_{T,P} > 0 \tag{2.9}$$

M_{CR} is the critical molecular weight where this condition is no longer satisfied for all compositions. When $M<M_{CR}$, the condition of Equation 2.9 is fulfilled for all compositions. When $M>M_{CR}$, a stable one phase mixture can exist at the extremities of the composition range; this is called partial miscibility.

The χ_{AB} parameter can be estimated from the solubility parameter δ_A and δ_B (unit ≡ $(cal/cm^3)^{1/2}$, or $(J/cm^3)^{1/2}$) if the compounds are relatively non-polar. For the special case where the polymers have similar M and ρ, M_{CR} is given by (Krause, 1978):

$$M_{CR} = 2\rho RT / (\delta_A - \delta_B)^2 \qquad (2.10)$$

When the solubility parameters differ by 1.0 $(cal/cm^3)^{1/2}$, M_{CR} is less than 1200 at 25°C; however, when the two polymers are matched more closely and this difference is 0.1 $(cal/m^3)^{1/2}$, M_{CR} rises to about 120,000. Thus polymer molecular weight has a strong influence on miscibility for systems that have an endothermic heat of mixing. The situation is different for exothermic systems.

The consequence of all these considerations is that the miscibility of non-polar polymers of substantial molecular weight occurs only when the solubility parameters are precisely matched. Needless to say, it will be very difficult to find miscible polymer pairs by matching similar chemical structure or solubility parameters, unless the molecular weight is low since the enthalpy of mixing can at best approach zero. If specific interactions between polar groups are involved, the enthalpy of mixing can be negative (exothermic mixing); consequently, ΔG_{mix} will be negative in spite of the small entropy. These interactions may arise from a variety of mechanisms such as dipole-dipole forces, but it is useful to think in terms of donor and acceptor groups in analogy to hydrogen bonding. It is possible then to select two polymers having chemical moieties within or attached to the chains which have the proper *complementary dissimilarity* to yield an exothermic heat of mixing. There will still be an endothermic contribution from the dispersive interactions or Van der Waals forces, between the remaining parts of the structure that do not specifically interact (Paul and Newman, 1978).

The design criteria are such that the SMM must be stable in the dispersed phase, but it must be moderately incompatible in order to allow for surface modification to occur. So if the SMM chemistry favors miscibility, the potential for surface modification will decrease as the macromolecules will be retained in the 'miscible matrix'. Balancing miscibility and surface modification requires the knowledge of both the molecular weight and the *complimentary chemical dissimilarity.*

2.2.5 Models for predicting the T_g of a miscible polymer blend

Over the years, numerous equations have been used to relate the glass transition temperatures of completely miscible polymer-polymer and polymer-plasticizer mixtures to component properties and mixture composition (Gordon and Taylor, 1952; Fox, 1956; Couchman, 1978; Couchman and Karasz, 1978; Chow, 1980). Some of these equations are empirical, while others are based on theoretical considerations. Couchman and Karasz (1978) have obtained an equation based on the continuity of mixture entropy at T_g. This equation, which appears to be applicable in several systems, reduces under certain conditions to other well known expressions such as the simple rule of mixtures, the logarithmic rule of mixtures or the Fox equation (Cortázar et al., 1987). The Couchman and Karasz equation attempts to relate the T_g of a polymeric mixture with the composition and properties of the pure components. The equation is written as follows:

$$\ln\left(\frac{T_g}{T_{g1}}\right) = \left[w_1 \Delta Cp_2 \ln\left(\frac{T_{g2}}{T_{g1}}\right)\right] / \left[w_1 \Delta Cp_1 + w_2 \Delta Cp_2 \right. \qquad (2.11)$$

where T_g is the glass transition temperature of the mixture, and T_{g1}, T_{g2} are those of the pure components; ΔCp is the difference in specific heat between the liquid and glassy states at T_g, w is the weight fraction, and component (1) is that having the lower glass transition temperature.

The application of this equation requires the values for ΔCp, which are not readily available in the known literature. However, Equation 2.11 may be simplified by taking into account the Simha-Boyer empirical rule which states that for a number of polymers,

$T_g \Delta Cp$ is approximately constant (Simha and Boyer, 1962). So Equation 2.11 is transformed into:

$$\ln\left(\frac{T_g}{T_{g1}}\right)=\left[w_2 \ln\left(\frac{T_{g2}}{T_{g1}}\right)\right]/\left[w_1\left(\frac{T_{g2}}{T_{g1}}\right)+w_2\right] \tag{2.12}$$

In the limiting case where $T_{g1}=T_{g2}$, Equation 2.12 may be transformed into the Fox equation:

$$1/T_g = w_1/T_{g1} + w_2/T_{g2} \tag{2.13}$$

On the other hand, if $\Delta Cp_1 = \Delta Cp_2$, Equation 2.11 reduces to the logarithmic rule of mixtures:

$$\ln T_g = w_1 \ln T_{g1} + w_2 \ln T_{g2} \tag{2.14}$$

If the T_g ratio of the two components is not far from unity, Equation 2.14 may be modified to give the additive rule of mixtures:

$$T_g = w_1 T_{g1} + w_2 T_{g2} \tag{2.15}$$

2.3 Polyurethane chemistry

The SMMs in this work will be synthesized based on polyurethane chemistry, which is classified as a type of step-growth polymerization (Cowie, 1991). Polyurethanes were first reported by Bayer in 1937 (Bayer et al., 1942; Bayer, 1947), and by Kinke and co-workers in 1939 (Kinke et al., 1950). They can be viewed as mixed amide-esters of carbonic acids. Thus, polyurethanes have intermediate properties between those of polyesters and polyamides. Polyurethanes can be synthesized by various methods (Figure 2-2) and are widely used in the areas of adhesives, coatings, flexible and rigid foams, elastomers, fibers, waterproofing, thermoset resins, thermoplastic molding compounds, rubber vulcanization, silicon and boron polymers, and the preparation of poly(2-oxazolidone) resins (Lelah and Cooper, 1986).

Polyurethanes are composed of short, alternating blocks of soft and hard segment units. The soft segment is typically a polyester-, polyether-, or polyalkyl-diol having

molecular weight between 500 and 5000. The hard segment is normally an aromatic diisocyanate that has been polymerized with a low molecular weight diol or diamine, called the chain extender, to produce an oligomeric aromatic urethane or urethane-urea segment of molecular weight between 300 and 3000. The macroglycol and the chain-extended diisocyanate combine to form an $(AB)_n$ type block copolymer (Figure 2-3). Within the large range of molecular weight and molar ratios possible for each type of segment, a broad spectrum of physical properties can be found. These materials can be very brittle and hard, or they can be soft and viscous, or anywhere in between.

2.3.1 Isocyanate chemistry

The formation of urethane bonds in polyurethane elastomers as well as the SMM synthesized in this work relates to the isocyanate group which possesses an electronic structure consisting of several resonance structures in equilibrium(Equation 2.16):

$$[\ R{-}N{=}C{=}O \ \leftrightarrow \ R{-}N^{-}{-}C^{+}{=}O \ \leftrightarrow \ R{-}N{=}C^{+}{-}O^{-}\ ] \qquad (2.16)$$

Because of multiple resonance structures, several classes of reactions involving the isocyanate group are possible. Reaction can occur across the C=N bond in a variety of ways, including adduct formation, oligomerization, cycloaddition and insertion reactions. Of these, only oligomerization and insertion are important in the formation of polyurethanes. Reactions involving the C=O bond are less important, and the formation of carbodiimides is an exception. A detailed description of isocyanate chemistry has been given by Patai (1977).

Principal reactions

The primary reaction in the polymerization of isocyanates is the insertion reaction. The reaction mechanism proceeds by a nucleophilic attack on the carbon center in the isocyanate group, as shown in Equation 2.17 for the reaction of an alcohol with an isocyanate.

$$\begin{array}{l} R{-}\overset{\curvearrowleft}{N}{=}\underset{\uparrow}{C}{=}O \\ \qquad\quad \uparrow \\ \qquad H{-}\ddot{O}{-}R' \end{array} \quad \rightarrow \quad R{-}NH{-}COO{-}R' \qquad (2.17)$$

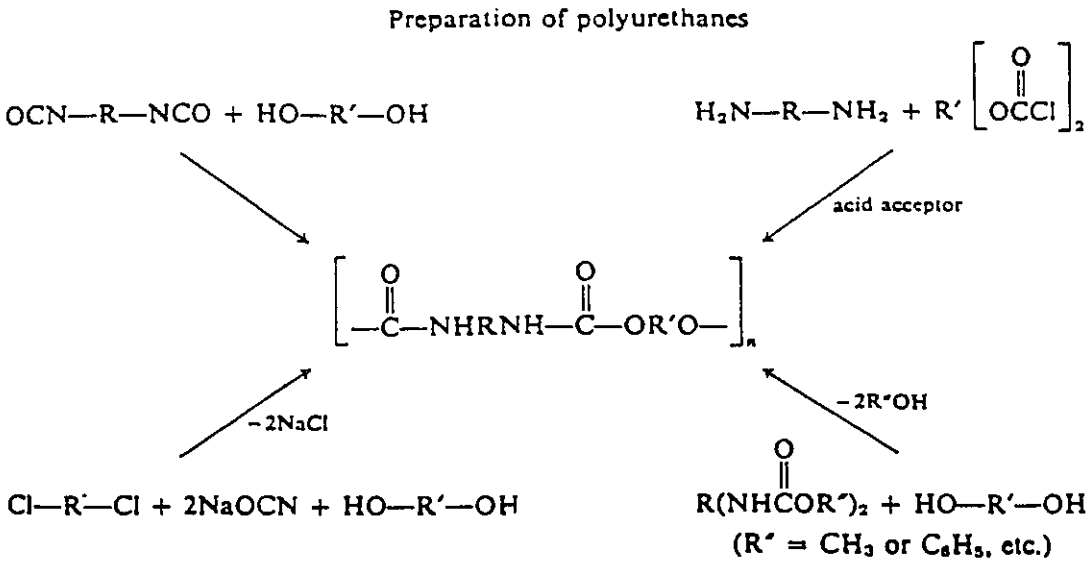

Figure 2 - 2 : Preparation of polyurethanes (Lelah and Cooper, 1986, p.233).

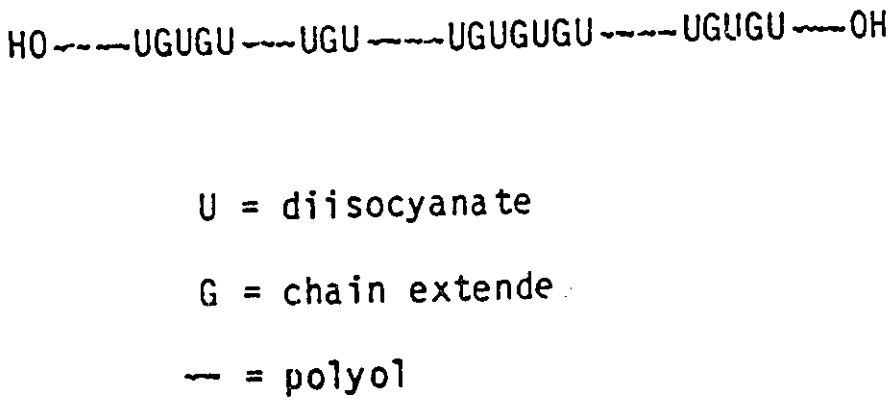

Figure 2 - 3 : Segmented polyurethane structure (Lelah and Cooper, 1986, p. 22).

The product of this reaction contains a carbamate ester linkage, which is more commonly known as a urethane linkage. Isocyanates can react with amines in a similar fashion to form urea linkages:

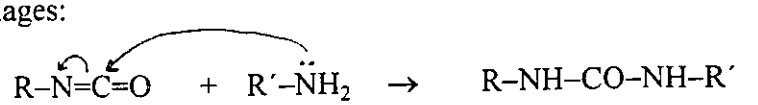

$$R\text{–}N{=}C{=}O \quad + \quad R'\text{–}NH_2 \quad \rightarrow \quad R\text{–}NH\text{–}CO\text{–}NH\text{–}R'$$

Polymers which contain both urethane and urea linkages are known as polyurethaneureas.

The reaction between isocyanate and water is a special case of an alcohol/isocyanate reaction (Equation 2.18)

$$R\text{–}N{=}C{=}C \; + \; H_2O \; \rightarrow \; R\text{–}NH\text{–}COOH \; \rightarrow \; R\text{–}NH_2 \; + \; CO_2 \qquad (2.18)$$

Water is sometimes desirable in the production of polyurethane foam because of the CO_2 produced. The amine product from this reaction further reacts with an isocyanate group to form a urea linkage. There are cases where water is used as an impurity to affect the molecular weight and mechanical properties of the final polymer (Gogolewski, 1989).

Side reactions

Undesirable side reactions in the synthesis of polyurethane block copolymers include insertion reactions, oligomer formation and, to some extent, the formation of carbodiimides (Patai, 1977). Both the urethane linkage and urea linkage are capable of nucleophilic attack on the isocyanate, especially at elevated temperatures. The products of these reactions are called allophanates and biurets, respectively, as shown in Equations (2.19) and (2.20).

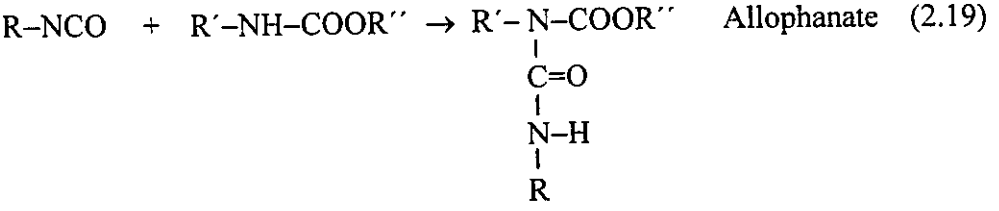

$$R\text{–}NCO \quad + \quad R'\text{–}NH\text{–}COOR'' \; \rightarrow \; R'\text{–}\underset{\displaystyle C{=}O}{\underset{|}{\overset{|}{N}}}\text{–}COOR'' \qquad \text{Allophanate} \qquad (2.19)$$

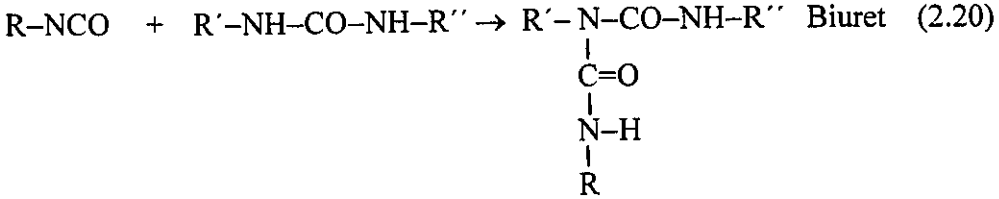

$$R\text{–}NCO \quad + \quad R'\text{–}NH\text{–}CO\text{–}NH\text{–}R'' \; \rightarrow \; R'\text{–}\underset{\displaystyle C{=}O}{\underset{|}{\overset{|}{N}}}\text{–}CO\text{–}NH\text{–}R'' \qquad \text{Biuret} \qquad (2.20)$$

Allophanate or biuret formation results in the chemical cross-linking of the polymer chains. Often, an excess of isocyanate functionality is used in polymerization to promote cross-linking in the post-curing period, after the product has been formed in its final stage.

The second type of side reaction involving the isocyanate group is the formation of oligomeric species, under special conditions. Dimers (uretidine diones) may be formed from aromatic isocyanates. Trimers (isocyanurates) can be produced from both aliphatic and aromatic isocyanates. The dimer reaction is readily reversible above 150° C, whereas the trimer is a stable complex even at relatively high temperatures. The formations of dimer and trimer is as follows:

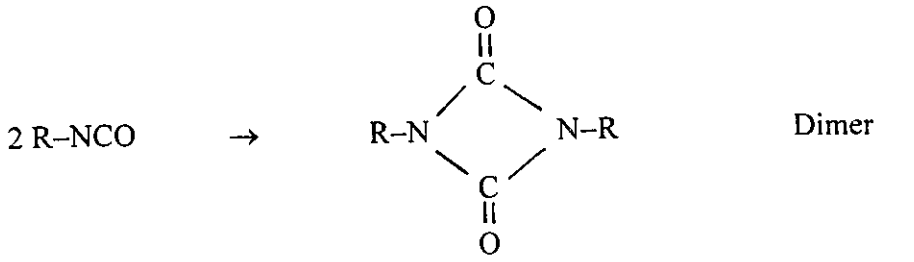

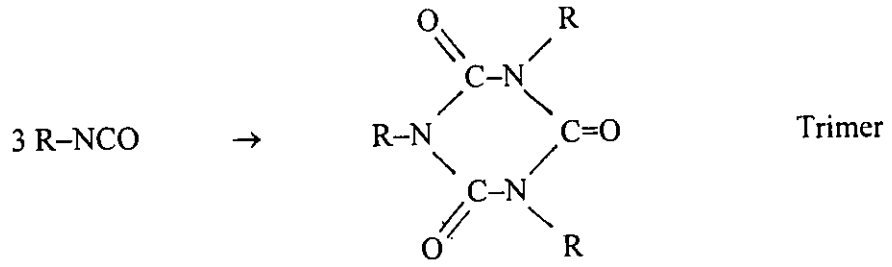

Kinetics of Isocyanate reactions

The hydroxyl-isocyanate reactions can be catalyzed by a variety of catalytic systems (Reegan and Frisch, 1971). Since catalysts are not used in this work, the information on catalysis is not presented. Information on the subject can be found in a number of

reviews and books (Reegan and Frisch, 1971; Lelah and Cooper, 1986; Gogolewski. 1989).

The rate of both catalyzed and uncatalyzed isocyanate insertion reactions experimentally follow second-order kinetics, although with small deviations. The uncatalyzed reaction between the hydroxyl group and the isocyanate group has been well characterized by Baker and Holdsworth (1947), Baker and Gaunt (1949). For the reaction mechanism

$$\text{R–NCO} + \text{R}'\text{–OH} \underset{k_{-1}}{\overset{k_1}{\rightleftharpoons}} \text{R}'\text{–O}^{+}\text{–H} \,|\, \text{R–N=C–O}^{-} \xrightarrow{k_2} \text{R–NH–CO–OR}' \quad (\text{OH})$$

the governing rate equation is

$$\frac{-d[NCO]}{dt} = \frac{-d[OH]}{dt} = \frac{k_1 k_2 [OH]^2 [NCO]}{k_{-1} + k_2 [OH]} \tag{2.21}$$

For $k_1 << k_2$, this becomes a standard second order rate equation, which is usually the case in practice. The kinetics of amine-isocyanate reaction is apparently different than that of the hydroxyl-isocyanate reaction (Brady and Narinesingh, 1971). This is probably due to the autocatalytic effect of the product since a urea linkage contains two secondary amines in close proximity.

2.3.2 Phase separation in polyurethane block copolymer

Polyurethane block copolymers generally display a two-phase microstructure. This phase separation is believed to result in the superior physical and mechanical properties of these materials (Lelah and Cooper, 1986; Gogolewski, 1989). Experimental techniques (Gogolewski, 1989) such as electron spectroscopy, small-angle X-ray scattering, and others such as infrared dichroism, dynamic mechanical analysis, and differential scanning calorimetry have been used to characterize the polyurethanes and have confirmed the following characteristics of polyurethane block copolymers (Lelah and Cooper, 1986; Gogolewski, 1989):

(i) The hard, rigid isocyanate segments segregate to glassy or semicrytalline domains, commonly called hard domains.

(ii) The macroglycol soft segments form an amorphous or semicrytalline matrix in which the hard domains are dispersed at low to moderate hard-segment content.

(iii)The hard domains act as multi-functional cross-linking sites and as reinforcing fillers, resulting in materials which possess both high modulus and elastomeric behavior.

(iv)The driving force for the segregation into domains is provided by the chemical incompatibility of the hard and soft segments.

Factors affecting the degree of phase separation include hydrogen bonding between the urethane linkages and the carbonyl or ether functionality, segment length, segment polarity and crytallizability, overall chemical composition, and mechanical and thermal history (Gogolewski, 1989). Several visual models have been derived from experimental data, some of which are shown in Figures 2-4 and 2-5.

2.3.3 Polyurethane block copolymer synthesis

Methods

Most polyurethanes are formed using a prepolymer method, where the polymer is formed in two stages (Figure 2-6) (Lelah and Cooper, 1986; Gogolewski, 1989). Initially, the diisocyanate and polyol react to form an intermediate oligomer of molecular weight 1000 to 5000. This prepolymer then reacts with a diol or diamine chain extender to form the final high molecular weight polymer. This step is usually called the chain-extension stage. An alternate procedure for polyurethane synthesis is a one-step process. In this method, the entire polymer formation is carried out by simultaneously mixing together polyol, diiocyanate, and chain extender in the presence of suitable catalysts.

Synthesis media

Many laboratory polyurethanes are synthesized in solution (Lelah and Cooper, 1986; Gogolewski, 1989). The choice of solvent may affect the rate of reaction. In general,

slower reactions occur in solvents that can complex with active hydrogen compounds or catalysts. as compared to those in solvents that cannot associate with reactant or catalyst. Ideally, the solvent must be chosen such that it will not interfere with the synthesis. Common solvents used in the synthesis include N,N-dimethylacetamide (DMAC), dimethylformamide (DMF), tetrahydrofuran (THF), and dimethylsulfoxide (DMSO). In most commercial productions, solvent free bulk polymerization techniques are used. where reactant phase compatibility and inter-phase diffusion processes are believed to affect the synthesis. The difference in synthesis conditions alters both the rate and yield of various reactions from laboratory to commercial production scale.

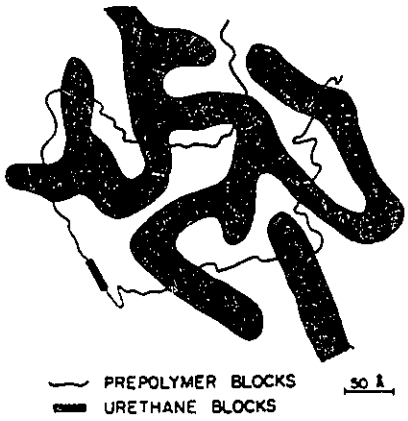

Figure 2 - 4 : Representation of domain structures in a segmented copolymer (Lelah and Cooper, 1986, p. 37).

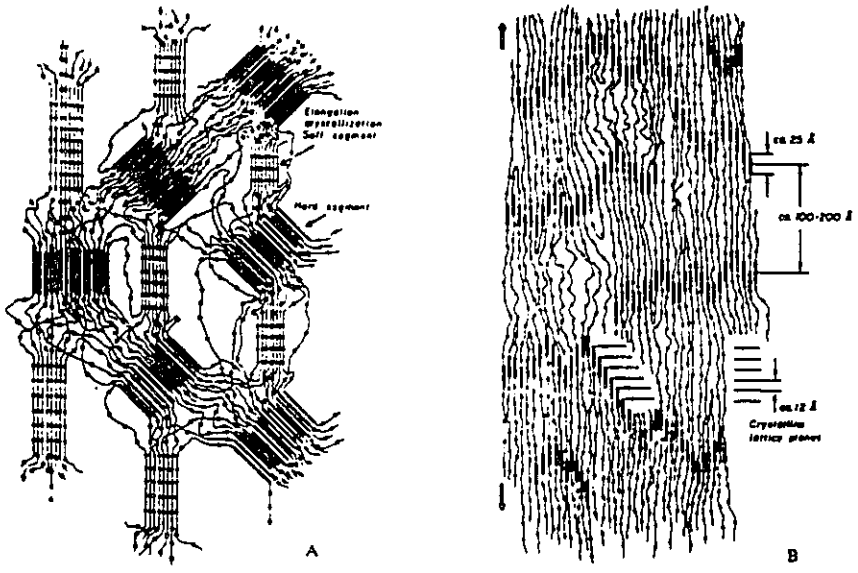

Figure 2 - 5 : Morphological model for extended polyurethane elastomer domain structure. (A) structure at 200% elongation; (B) structure of material annealed at 500% elongation (Lelah and Cooper, 1986, p. 37).

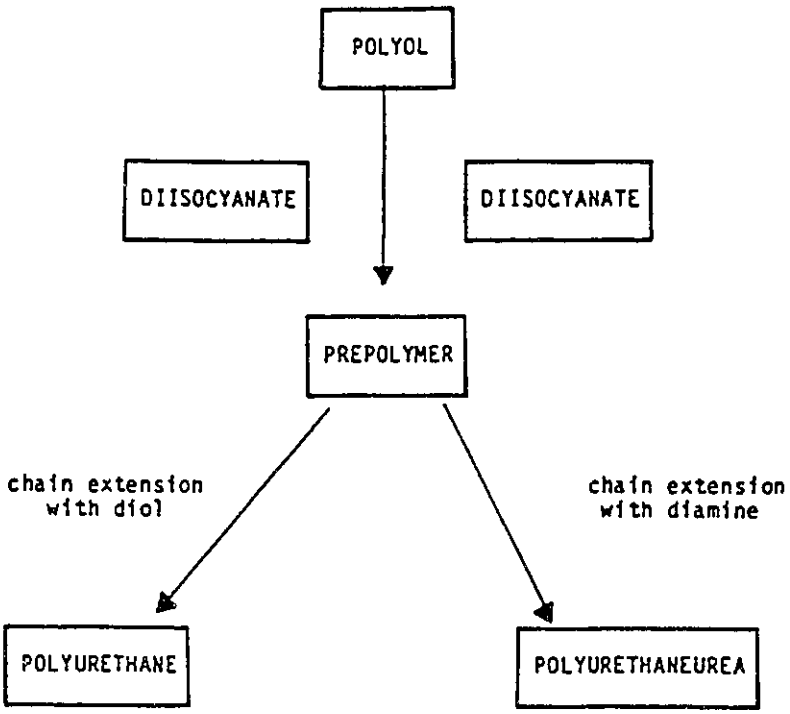

Figure 2 - 6 : Two-stage technique for the synthesis of polyurethanes and polyurethaneureas (Lelah and Cooper, 1986, p. 32).

Carothers equation

W.H. Carothers proposed a simple equation relating the number average degree of polymerization x_n to a quantity p_e describing the extent of the reaction for linear polycondensations such as the chain growth reaction between the isocyanate group and the alcohol or amine group in polyurethane synthesis.

If N_o is the original number of molecules present in an A-B monomer system and N_t is the number of all molecules remaining after time t, then the total number of functional groups of either A or B which have reacted is $(N_o - N_t)$. At time t, the extent of reaction p_e is given by

$$p_e = (N_o - N_t)/N_o \quad \text{or} \quad N_t = N_o(1 - p_e) \tag{2.22}$$

given that $x_n = N_o/N_t$, combining with Equation 2.22 gives the Carothers equation,

$$x_n = 1/(1 - p_e). \tag{2.23}$$

For the A-A + B-B reaction, Equation 2.23 is also valid, given that there are initially $2N_o$ molecules.

The Carothers equation predicts that a high extent of reaction is very important in yielding a high enough degree of polymerization. For example, a p_e value of 0.95 yields $x_n = 50$, whereas $x_n = 100$ occurs when $p_e = 0.99$.

Chain growth, to produce high molar mass materials, becomes increasingly difficult as the reaction proceeds (Cowie, 1991). This is due to a number of reasons: (i) the difficulty in ensuring the precise equivalence of the reactive groups in the starting materials when two or more types of monomer are used, (ii) the decreasing frequency of functional groups meeting and reacting as their concentration diminishes, and (iii) the increasing likelihood of interference from side reactions.

The control of the chain growth reaction can be affected by rapidly cooling the reaction at the appropriate stage, or by adding calculated quantities of monofunctional materials. More usefully, a precisely controlled stoichiometric imbalance of the reactants

in the mixture can provide the desired result. This can be expressed in an extension of the Carothers equation as,

$$x_n = (1 + r) / (1 + r - 2rp_e) \qquad (2.24)$$

where r is the ratio of the number of molecules of the limiting reactant to that of the excess reactant. When a monofunctional additive is used, r is defined as the ratio $N_A/(N_{BB} + 2N_B)$ where N_B is the number of monofunctional molecules added.

In practice, $p_e = 1$ is rarely achieved, nor is it a perfect stoichiometric balance. The consequences of this are shown in Figure 2-7 where x_n is plotted as (a) a function of p_e, calculated from Equation 2.23 , and (b) as a function of the stoichiometric ratio for p_e = 1.000, 0.998 and 0.950 calculated from Equation 2.24.

Segment length distributions

The molecular weight distribution or polydispersity of the majority of soft segments used in a polyurethane block copolymer synthesis is often narrow ($M_w/M_n < 1.3$), and the physical properties of the final polymer are relatively independent of the polydispersity of the soft segments (Lelah and Cooper, 1986). Unfortunately, this observation is not applicable for hard segments. The hard segment size distribution is governed by a number of factors, including the synthetic procedure and the degree of completion of the polymerization reaction. The distribution of hard segment size for a complete conversion of the reactants follows the most probable distribution for condensation reactions. For fractional conversion, the distribution of size is not the most probable. This is because there is a difference in the rate of reaction among the primary, secondary and higher order isocyanate groups, with primary isocyanates being the fastest.

The distribution of sequence lengths at conversions greater than 10% for a two-step solution polymerization obeys the relation (Harrell, 1969):

$$N_{si} = N_{st}\,\alpha^{i-1} \qquad (2.25)$$

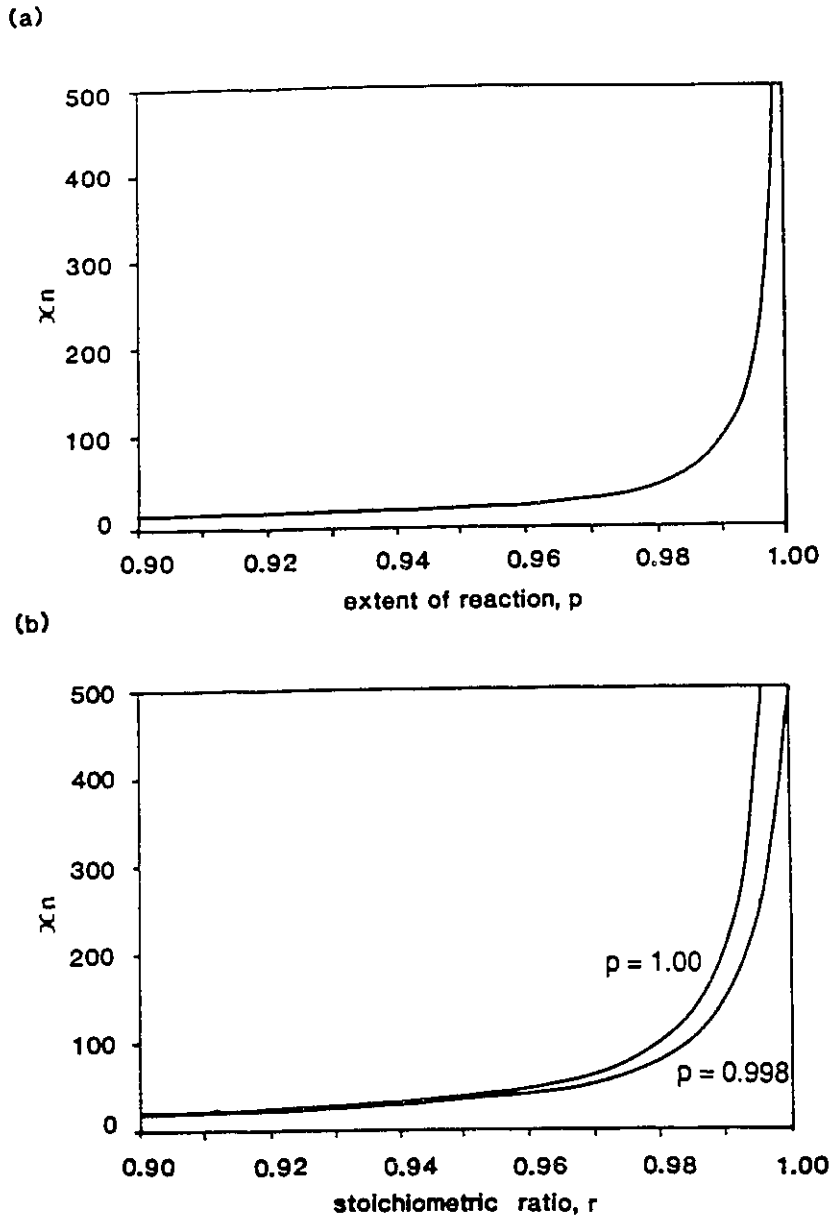

Figure 2 - 7 : Variation of the degree of polymerization x_n (a) as a function of p_e, calculated from Equation 2.23 , and (b) as a function of the stoichiometric ratio for p_e = 1.000 and 0.998 calculated from Equation 2.24 (Cowie, 1991, p. 33).

where i is the number of diisocyanate /chain extender pairs, N_{si} is the number of segments containing i pairs, N_{st} is the total number of segments, and α is a function of the total conversion only. The two-step polymerization produces a more narrow molecular weight distribution than does a single-step polymerization. The one-step reaction results in hard segments with a heterogeneity index (M_w/M_n) approaching two, for long average hard-segment lengths. It has been found that a decrease in the breadth of the hard segment size distribution has significantly increased the tensile modulus of a polyurethane (Harrell, 1969). Also, it has been suggested that the total molecular weight has little effect on the physical properties, when the total chain molecular weight exceeds a M_n of 25,000 (Schollenberger and Dinbergs, 1973). At this level, the size, size distribution and composition of the individual segments determine the macroscopic properties of the material (Schollenberger and Dinbergs, 1973).

Finally, if a monofunctional group is to be reacted with various isocyanate groups (i.e. primary, secondary, or higher) such as in synthesizing SMMs, then the distribution would logically and possibly depend on whether the monofunctional group affects the overall kinetics or not. A monofunctional group which adversely changes the overall kinetics will ultimately affect the overall size distribution of the resulting material. Hence, a polyurethane block copolymer which has some monofunctional components such as an SMM could possibly be associated with problems in terms of reproducibility of properties and general material characteristics.

2.3.4 Materials for synthesis and their effects on properties

High molecular weight polyurethane block copolymers have been synthesized and used in a variety of applications. The effects of the type of isocyanate, macroglycol and chain extender used has been investigated by many workers (Lelah and Cooper, 1986; Gogolewski, 1989). From a mechanical property perspective, the following starting materials which have been used in polyurethane block copolymer synthesis and their general effects on the material properties are described (Lelah and Cooper, 1986; Gogolewski, 1989).

Isocyanates

The two most commonly used isocyanates are toluene diisocyanate (TDI) and methylene bis-*p*-phenyl diisocyanate (MDI) (Lelah and Cooper, 1986; Gogolewski, 1989). MDI generally has higher reactivity than TDI, and polymers based on MDI may have better physical properties. MDI is also crystalizable while TDI is not. Other isocyanates that could also result in high performance polymers include: naphthalene diisocyanate (NDI) and 3,3′-bitoluene diisocyanate. Aromatic diisocyanates and polymers made from them are somewhat unstable toward light. Also available are aliphatic isocyanates, which include 1,6-hexane diisocyanate (HDI), isophorone diisocyanate (IPDI), and methylene bis (p-cyclohexyl isocyanate) (H_{12}MDI). The chemical structures of common commercial diisocyanates are shown in Figure 2-8.

Chain extenders

There are two classes of chain extenders: aromatic and aliphatic diols and diamine (Lelah and Cooper, 1986; Gogolewski, 1989). Aliphatic chain extenders generally yield softer materials than aromatic chain extenders (this is due to the tendency of hard segments containing aromatic chain extenders to posess a greater volume fraction of the material which make up the hard segment). Materials chain extended with a diamine usually display superior properties compared to similar polymers with the equivalent diol chain extender. For aliphatic chain extenders, the number of carbons in the extender backbone influences the strength of the final polymer (Gogolewski, 1989). In general, a highly crytalline hard domain leads to a polyurethane with improved physical characteristics. As well, it is easier to crystallize a hard segment containing even numbers of carbon in the chain extender (Gogolewski, 1989).

Polyol soft-segments

Polyols available for copolymer synthesis include polyethers, polyesters, polyalkyls, and polydimethylsiloxanes (Lelah and Cooper, 1986; Gogolewski, 1989). Traditionally, polyurethanes have been synthesized with polyester and polyether soft-segments.

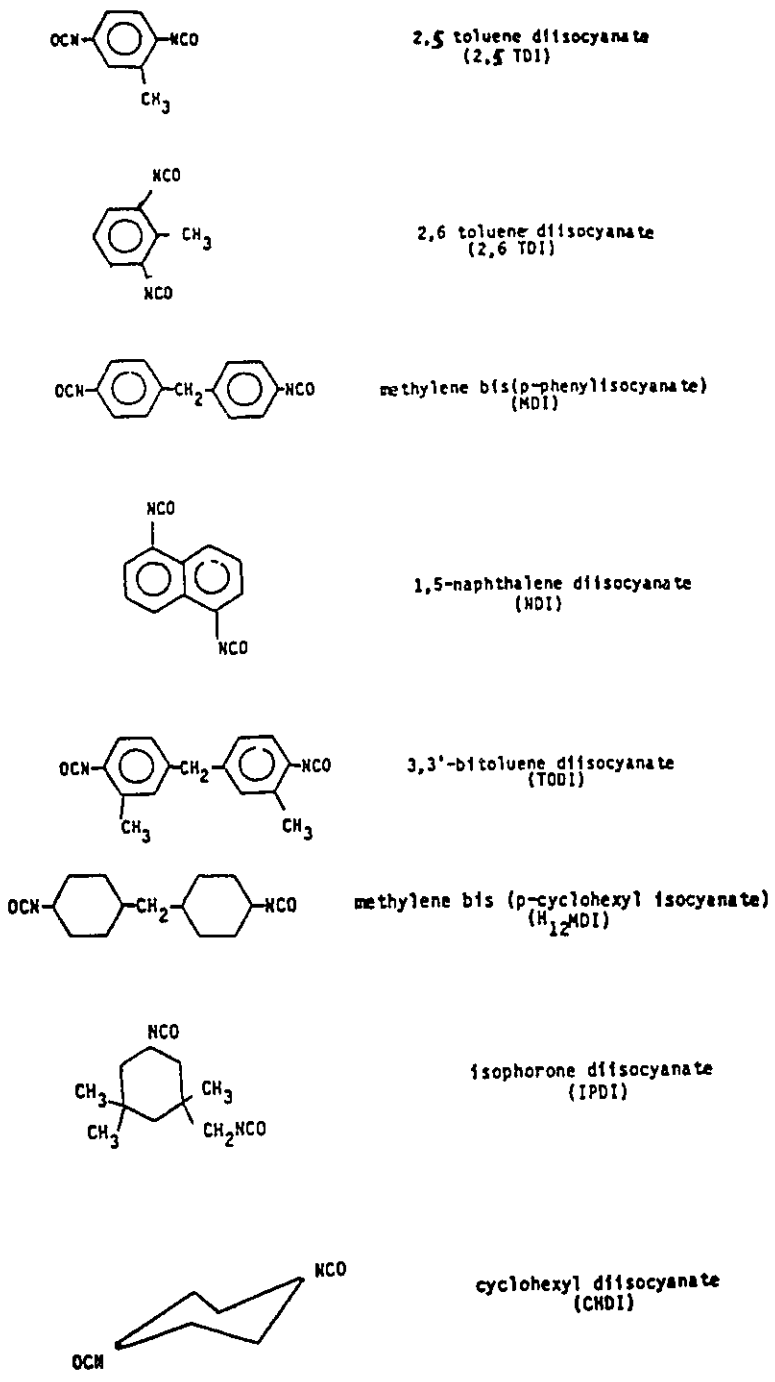

Figure 2 - 8 : Typical diisocyanates used for polyurethane synthesis (Lelah and Cooper, 1986, p. 29).

Polyester based urethanes possess relatively good mechanical properties; however, they are also susceptible to hydrolytic cleavage at the ester linkage. On the other hand, polyether based materials show relatively high resistance to hydrolytic cleavage. Materials based on the polyether polyols display various characteristics. For example, polyethylene oxide (PEO) based materials show poor resistance to water uptake, apparently because of their hydrophilic properties, whereas polypropylene oxide (PPO) based materials are typically soft. The preferred polyether based materials have been synthesized with polytetramethylene oxides (PTMO), which gives the best physical properties. These materials show good hydrolytic stability and water resistance. For applications where environmental stability of the polyurethane block copolymer (e.g. at extreme temperature and pressure) is a major concern, polyalkyl glycol based materials offer a better alternative to the relatively less stable polyether and polyester based polyurethane block copolymers. Some common polyols and their chemical structures are shown in Figure 2-9.

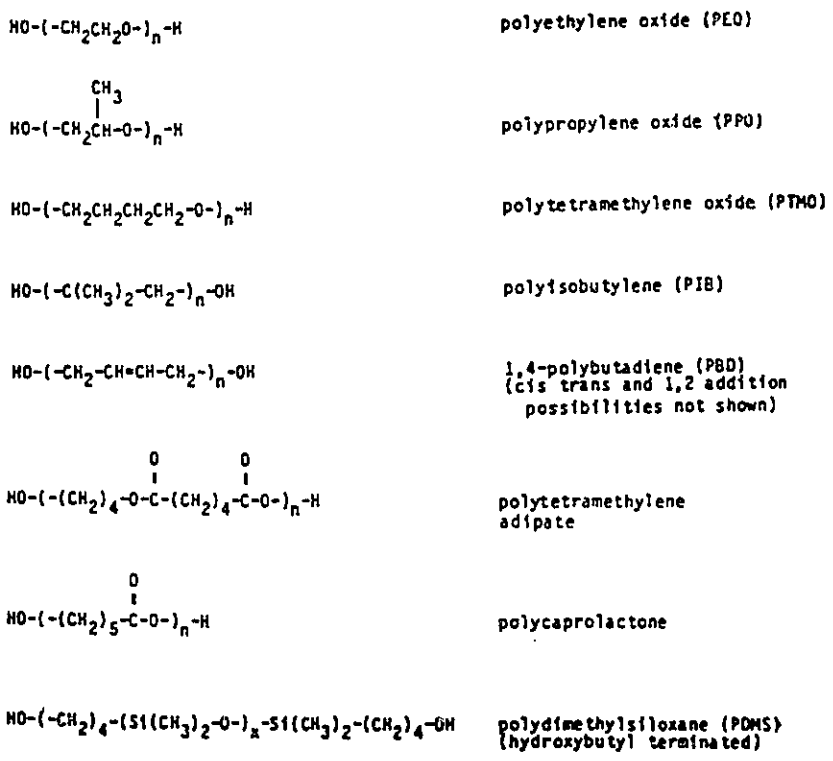

Figure 2 - 9 : Typical polymeric diol soft segments used for polyurethane synthesis (Lelah and Cooper, 1986, p. 30).

2.4 Theoretical aspects of pervaporation

In order to identify the relationship between the characteristics of the SMMs developed in this study and the pervaporation studies carried out in conjunction with this thesis, it will be helpful to review the current theories regarding the mechanism of transport of the permeants through pervaporation membranes. Huang and Rhim (1991) have reviewed the characteristics of pervaporation membrane separation, including common theoretical models and some general assessments regarding the effects of process conditions (Huang and Rhim, 1991). Many mechanisms of transport are available (Huang, 1991), but there is none which can be applied universally. The most accepted mechanism is the solution-diffusion model (Lee, 1975; Mulder and Smolders, 1984), where the permeant is believed to first dissolve in the polymer of the membrane; it then diffuses through the polymer and desorbs from the other side of the membrane. This model will be described briefly later in this section, but first, some theoretical principles of the permeation of single and binary liquids through dense, homogeneous membranes will be introduced.

2.4.1 Permeation of a single liquid

The permeation of a single permeant through a dense homogeneous membrane is studied to obtain the intrinsic transport property of a given membrane material. This permeation can be satisfactorily described by Fick's law with a diffusion coefficient which depends on concentration (Binning et al., 1961; Long, 1965; Huang and Jarvis, 1970). The permeation rate of a permeant through a membrane hence depends on its solubility and diffusivity in the polymer.

The steady-state permeation can be described by a form of Fick's law:

$$J^* = -D\frac{dC}{dx} \tag{2.26}$$

where J^* is the permeation flux, D is the diffusivity, and dC/dx is the concentration gradient across the membrane. The diffusivity D depends strongly on the concentration of the permeant in the membrane and can take many forms. The most common is

$$D = D_0 \exp(\tau C) \tag{2.27}$$

where D_0 is the diffusion coefficient at zero concentration, τ is the plasticizing coefficient and C is the concentration of the permeant sorbed in the polymer. Substituting Equation 2.27 into Equation 2.26, rearranging and integrating with the boundary condition gives

$$J^* \int_0^L dx = -D_o \int_{C_1}^{C_2} \exp(\tau \cdot C) dC \tag{2.28}$$

where L is the membrane thickness, C_1 and C_2 are the concentration of permeant in the polymer at the upstream and the downstream side, respectively. At steady state:

$$J^* = \frac{D_o}{\tau L}[\exp(\tau C_1) - \exp(\tau C_2) \tag{2.29}$$

and the concentration profile is then

$$C = \frac{1}{\tau}\left[\exp(\tau C_1) - \frac{x}{L}\left[\exp(\tau C_1) - \exp(\tau C_2)\right]\right] \tag{2.30}$$

where C_1 can be determined by the equilibrium sorption of liquid in the polymer. C_2 is essentially zero, if the downstream is maintained under vacuum and the desorption rate is independent of diffusion.

Direct measurement of the concentration in the membrane is difficult, so it will be more convenient if the concentrations could be related to a readily measurable quantity like pressure. If thermodynamic equilibrium is assumed to exist at the upstream and downstream interfaces, then the concentrations can be written as $C_1 = C^*(P^o)$ and $C_2 = C^*(P_2)$. P^o is the saturated vapor pressure of the liquid at the operating temperature, and P_2 is the pressure in the vapor side. Here, $C^*(P)$ is a function of pressure with some parameters depending on temperature and the nature of polymer and permeant (Huang and Rhim, 1991). Thus, Equation 2.29 and Equation 2.30 can be expressed in term of P^o and P_2. The permeability Q_p is then

$$Q_p = \frac{D_o}{\tau \Delta P}\left[\exp(\tau C_1) - \exp(\tau C_2)\right] = \frac{J^* L}{\Delta P} \tag{2.31}$$

where $\Delta P = P^o - P_2$. For most polymer-solvent systems, the static equilibrium relationship $C^*(P)$ obeys either

$$C^*(P) = P \cdot \exp(\tau C) \tag{2.32}$$

or Henry's law

$$C^*(P) = S^* P \tag{2.33}$$

where S^* and τ are constants which depend only on the temperature and the nature of the system.

2.4.2 Permeation of binary components

A satisfactory quantitative explanation of binary permeation through polymeric membranes is not yet a reality. However, some qualitative assessments are available. In general, the effect of a mixture's composition on the permeation rate and selectivity is very noticeable (Huang and Rhim, 1991), and its study is complicated by the possible inter-relation of causes and effects. The permeation rate of one component, for example, could be influenced negatively or positively by the presence of the other component (Huang and Lin, 1968; Brun et al., 1985). In terms of selectivity, its order of magnitude was found to be lower than the ratio of the permeation rates of pure components (Huang and Rhim, 1991). This behaviour is usually attributed to the plasticizing effect of the permeants on the membrane. Hence, a linear dependence of the permeant diffusivity is not suitable to account for large plasticizing effects. Many investigators (Huang and Lin, 1968; Brun et al., 1985; Mulder and Smolders, 1985; Rautenbach and Albrecht, 1980) suggested that the diffusivity of each component is a function of permeant concentration which is related to the free volume of the polymer. This free volume, in turn, depends on the local composition of the ternary system permeant *i* / permeant *j* / membrane.

The membrane selectivity of a binary system can be expressed in terms of a separation factor α, defined as the ratio of concentration of components *i*, *j* in the permeate over that in the feed:

$$\alpha_{i/j} = \frac{(y_i / y_j)}{(x_i / x_j)}. \tag{2.34}$$

The selectivity and permeation rate of a membrane usually behave in opposite ways; that is, when one factor increases, the other decreases (Huang and Rhim, 1991). Hence, it is useful to define a composite performance index that will take into account both. Huang and Rhim (1991) defined a pervaporation index (PSI) to be the product of separation factor and the permeation rate:

$$PSI = J_i \cdot \alpha_{i/j} \tag{2.35}$$

This index is useful as a comparative value to evaluate membranes.

2.4.3 The solution-diffusion model of pervaporation

The most widely accepted transport mechanism for pervaporation is the solution-diffusion model (Lee, 1975; Mulder and Smolders, 1984) which can be divided into three steps:

(i) Sorption of permeant(s) onto the membrane at the upstream side.

(ii) Diffusion of permeant(s) through the membrane.

(iii)Desorption into a vapor phase at the downstream side.

Hence, the selectivity and permeation rate are governed by the solubility and diffusivity of each component of the feed mixture to be separated. Mulder et al. (1985) suggested that in liquid mixtures, separation is possible because the membrane can preferentially transport one component over the other, even if the driving forces are equal. However, this statement is still debatable. Nevertheless, the prediction of selectivity is often difficult since the transport of one component through the membrane is affected by the presence of the other component(s), as in the case of binary permeation.

Solubility is a thermodynamic property, while the diffusivity is a kinetic property. Thus, the coupling of transport of permeants can be divided into two parts, a thermodynamic part and a kinetic part (Brun et al., 1985). In the thermodynamic part, the

concentration change of one component in the membrane due to the presence of another component is caused by mutual interactions between the permeants in the membrane, as well as by interactions between the individual components and the membrane material. For the kinetic part, coupling is due to the effect of the concentration on the diffusion coefficients of the permeants in polymers.

Vaporization on the permeate side of the membrane (desorption step) is generally considered to be a fast, non-selective step if the partial pressure is kept low (Aptel et al, 1976; Huang and Rhim, 1991). It has been shown that the permeate flux remained unaltered, but then suddenly decreased and became dependent on the rate of vaporization when the pressure approached the partial vapor pressure of the liquid component (Aptel et al, 1976; Huang and Rhim, 1991).

There are several relationships, which are usually derived from the Flory-Huggins thermodynamic theory, to describe the equilibrium sorption of low molecular weight components in polymers (Flory, 1953). These include (i) the sorption of pure liquid in amorphous polymer, (ii) the sorption of binary liquid mixture in an amorphous polymer, (iii) the sorption of pure liquid in crosslinked polymer, and (iv) the sorption of pure liquid in a semi-crystalline polymer (Huang and Rhim, 1991). The expression for the sorption of pure liquid in an amorphous polymer describes the sorption behaviour as largely dependent on the interaction parameter χ_{iP} between the permeant and the polymer. This parameter generally increases as the affinity between the permeant and the polymer decreases. For the binary sorption, the interaction parameters are generally concentration dependent. The expression for pure liquid sorption in crosslinked polymer reflects the restriction on swelling, which results in a decrease of the concentration of liquid in the polymer. For the sorption of pure liquid in a semi-crystalline polymer, the expression accounts for the decrease in component concentration by assuming that the crystallites can be considered as physical crosslinks, having the same effects as chemical crosslinks. In addition, the model assumes that crystallites are impermeable to permeants.

Most of the diffusion models or mechanisms can be considered as either 'molecular' or 'free volume' models. The former theory interprets the diffusion process in terms of the specific postulated motions of permeant molecules and polymer chains (Dibenedetto, 1963; Dibenedetto and Paul, 1964; Paul and Dibenedetto, 1965). The latter is based on an oversimplified view of molecular processes, but relates the diffusion coefficients to the free volume ('hole') of the system on the basis of fluctuation analysis (Vrentas and Duda, 1976 & 1977). The diffusion coefficient, in most cases, depends on the concentration of the components in the membrane. Several common expressions are summarized by Huang and Rhim (1991).

According to the solution-diffusion model, the flux of a component i through the membrane can be described by the product of concentration, mobility and driving force (Lonsdale et al., 1965; Merten, 1966). The driving force in membrane pervaporation, as in most membrane processes, is the gradient of chemical potential. For component i, the flux can be expressed as

$$J_i = -C_i B_i \frac{d\mu_i}{dx} \tag{2.36}$$

where C_i is the concentration, B_i is the mobility and μ_i is the chemical potential. At constant temperature, Equation 2.36 can be written as

$$J_i = -C_i B_i \left(RT \frac{d \ln a_i}{dx} + V_i \frac{dP}{dx} \right)_T \tag{2.37}$$

where V_i is the molar volume of component i. Since the pressure difference between the upstream and downstream phase is about one bar in pervaporation processes (Huang and Rhim, 1991), the term concerning differential change in pressure can be neglected. Equation 2.37 hence reduces to

$$J_i = -C_i B_i RT \frac{d \ln a_i}{dx} \tag{2.38}$$

If the diffusion coefficient of component i in the membrane is taken as

$$D_i = RTB_i \tag{2.39}$$

then Equation 2.37 further reduces to

$$J_i = -C_i D_i \frac{d \ln a_i}{dx} \tag{2.40}$$

In the case of a polymeric membrane and a binary liquid mixture (i.e. a ternary system), the chemical potentials can be obtained from Flory-Huggins thermodynamics (Flory, 1953).

Chapter 3

MATERIALS AND EXPERIMENTAL METHODS

3.1 Overview

The experimental part is arranged chronologically into four sections which presents: (i) the synthesis of SMMs, (ii) the characterization of SMMs for bulk properties, (iii) the bulk and surface characterization of SMM/PES blends, and (iv) the preparation of membranes with SMM and evaluation of pervaporation performance. In the section concerning the synthesis (section 3.3), there are a number of physical variables which could theoretically affect the resulting polymer. These include temperature, reaction time, stirring rate, the dimension of the stirring blade or bar, solvent type, reactant type, reactant stoichiometry and reactant concentration. On the other hand, the membrane preparation part (section 3.5) involves a number of important factors which influence the final products. These include solution viscosity, thickness of casted layer, evaporation temperature and time, and the nature of the gelation medium. While it is beyond the scope of this work to study the variables specific to the preparation of membranes, this thesis will carefully examine the relation between SMM synthesis variables and the various properties of the SMM and SMM/PES mixtures.

3.2 Materials

The materials which have been used in the synthesis of SMM and the membrane pervaporation experiments are listed in Table 3-1.

3.3 Synthesis of surface modifying macromolecules

3.3.1 Preparation of Materials

The chemical structures of the synthesis reagents are given in Figure 3-1a. Methylene bis-*p*-phenyl diisocyanate was purified before use by vacuum distillation at 0.025 mmHg (the procedure can be referenced from Perrin and Armarego (1988)). Purified MDI was

stored in a moisture controlled refrigerator. Polypropylene diol of average molecular weight 425 was purified by degassing at 0.5 mmHg for 24 hours before use to remove any absorbed moisture. BA-L is a polyfluoroalcohol (and a type of Zonyl^{TM} intermediate) with a variable number of (CF_2) repeating units (Figure 3.1a). It was received as a mixture of polyfluoroalcohols with m ranging from 4 to 12. It was distilled at 0.025 mmHg to yield three physically distinct fractions. The fractions were stored in moisture controlled refrigerator prior to use. A description of each fraction is listed in Table 3-2. Fractions Low (m = 4-8) and High ($m \geq 10$) were used in this work. N,N-dimethylacetamide was used as the reaction solvent and was distilled at 0.5 mmHg within 24 hours of the reaction.

Table 3 - 1: Materials for SMM synthesis and membrane pervaporation experiments

Material	Abbreviation	Average M_w or Formula weight (g/mole)	Descriptions	Supplier*
Methylene bis-*p*-phenyl diisocyanate	MDI	250.26	White, solid	Eastman Kodak
Polypropylene diol	PPO	425	Colorless, viscous liquid	Aldrich Chemicals
Zonyl BA-L^{TM}	BA-L	443	Yellow-brown, viscous liquid	DuPont Chemicals
Polyethersulfone (Victrex 4800P)	PES	$1.0 \times 10^{5\dagger}$	White, powdered solids	ICI Advanced Materials
Polyvinyl-pyrrolidone	PVP	1.0×10^{4}	Light yellow, powder	Sigma Chemicals
Chloroform	—	119.5	Colorless, liquid	BDH Chemicals
N,N-dimethyl-acetamide	DMAC	87.12	Colorless, liquid	Aldrich Chemicals
1,1,2-trichloro-1,2,2trifluoroethane	TCTFE	187.38	Colorless, liquid	HPLC grade, BDH Chemicals

†Determined by Gel permeation chromatography using polystyrene standards

*The suppliers' addresses are provided in Appendix F

3.3.2 Experimental design (Sachs, 1984)

Through preliminary work, three variables were suspected to significantly affect the molecular weight and properties of the SMMs: (i) the reactant stoichiometry, (ii) the chemical nature of the polyfluoroalcohol (Zonyl^{TM} intermediates) and (iii) the concentration of the reactants at the prepolymer stage of the synthesis procedure. The choices on the level of stoichiometry and reaction concentration was somewhat arbitrary; however, to some extent was based on the ability of the synthesized molecule to blend with the PES material.

Table 3 - 2 : Physical data for Zonyl BA-L

BA-L fraction	m*	weight fraction of fluorine †	Vapor temperature range at 0.025 mmHg (°C)	Average M_W	Physical state
Low	4-8	0.546	50-55	443	colorless liquid
Medium	8-10	N/D	60-65	490	soft, white solid
High	≥10	0.658	70-90	589	white solid

* approximate number of (CF_2) unit based on DuPont's literature (DuPont Co., 1988), see Figure 3-1a
† determined by elemental analysis
N/D : not determined

A factorial experimental design was used to study the effects of the three variables on the bulk properties and reproducibility of the SMMs,. A two level, three variables study (2^3) was produced. Table 3-3 summarizes the experiments in factorial design. Each experiment was conducted three times in order to obtain an average for the different conditions. The high (+) and low (-) values for each of the variables were chosen based on preliminary synthesis work which sought to define SMM molecular weight and properties that would enable their mixing with PES. This latter work was qualitative and is not further described in this thesis.

(i) For reactant stoichiometry, a '+' represents '3:2:2' diisocyanate:polyol:BA-L mole ratio, whereas a '-' represents a '2:1:2' ratio.

(ii) For the chemical nature of the BA-L, a '+' represents the 'High' fraction of BA-L distillation, whereas a '-' represents the 'Low' fraction.

(iii) For the reactant concentration in the prepolymer stage: a '+' represents 0.3 mmol/mL of diisocyanate and 0.2 mmol/mL of polypropylene diol for the 3:2:2 formula ratio;

while for the 2:1:2 formula, a '+' represents 0.2 mmol/mL of diisocyanate and 0.1 mmol/mL of polypropylene diol. The '-' indicates reactant concentrations equal to 75% of those for the '+' case.

Table 3 - 3 : Factorial design matrix for the three variable study on the synthesis of SMMs. The plus (+) and minus (-) signs represent specific changes in the level of the variable involved. A plus represents a high value, whereas a minus represents a low value.

Experiment No.	SMM†	Stoichiometry	Type of polyfluoroalcohol	Prepolymer reactant concentration
1	MPB322HN	+	+	+
2	MPB322HR	+	+	-
3	MPB322LN	+	-	+
4	MPB322LR	+	-	-
5	MPB212HN	-	+	+
6	MPB212HR	-	+	-
7	MPB212LN	-	-	+
8	MPB212LR	-	-	-

† See nomenclature in Table 3-4.

The responses for the changes in variables are the polystyrene equivalent average molecular weight, polydispersity, weight percent of MDI, PPO and BA-L High or Low in the SMM, and thermal characteristics of SMM such as onset T_g, mid-point T_g, T_g width and apparent change in specific heat capacity at T_g (ΔCp). The reproducibility of the SMMs was evaluated using an average standard error for each of these responses, with an overall average error for each SMM calculated from all responses. The average error over three replicates for each response was calculated according to Equation 3.1, whereas the overall average error was evaluated by Equation 3.2.

$$\%\ Error\ of\ Response = \frac{\sigma \times 100}{Mean_{response} \times \sqrt{n}} \qquad (3.1)$$

$$Average\ overall\ error = \frac{\sum_{i=1}^{p} Error\ of\ response_i}{p} \qquad (3.2)$$

where σ is the standard deviation from the $Mean_{response}$, n is the number of observations, and p is the number of responses. The integer defining 'i' in equation 3.2 are arbitrarily assigned to the individual responses. The overall error was used to determine which of the variables, or a combination of them, is important in controlling the SMM reproducibility.

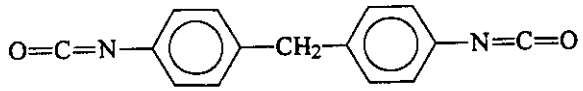

methylene bis-*p*-phenyl diisocyanate (MDI

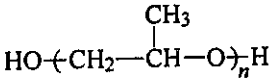

polypropylene diol (PPO)

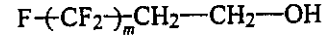

Zonyl BA-L intermediate (BA-L)

(a)

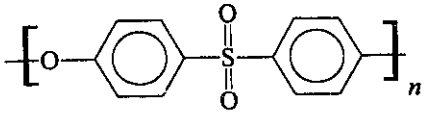

Victrex 4800P polyethersulfone (PES)

(b)

Figure 3 - 1 : Structures of chemicals (a) Methylene bis-phenyl diisocyanate (MDI), Polypropylene diol (PPO) and Zonyl™ BA-L intermediates (BA-L) for synthesis; (b) Victrex 4800P polyethersulfone (PES).

The factorial design generated eight experiments, and each was repeated three times to yield eight triplicate SMMs. MDI, PPO and BA-L were the only reactants used in the synthesis of SMMs. Thus, their nomenclature adopted the general form:

MPBijkXY(n)

Where *MPB* stands for MDI, PPO and BA-L; *i,j* and *k* represents the stoichiometry used for the three reactants, respectively; *X* is the type of BA-L fraction used (H ≡ High, L ≡ Low); and *Y* is the prepolymer reactant concentration (N ≡ normal, R ≡ reduced). The number *n* in parenthesis represents the batch number for the synthesis. For example, an SMM with the code MPB322HN(1) represents the polymer made from reacting MDI, PPO and BA-L, using a 3:2:2 mole ratio, with the 'High' fraction of BA-L at reactant concentration of 0.3 mmol/mL MDI and 0.2 mmol/mL PPO; the batch number is (1). Without the synthesis batch number (e.g. MPB322HN), the notation signifies a general class of SMMs sharing the same synthesis formula and reaction method. The reaction stoichiometry, fraction of BA-L and the amounts of reactants used for the synthesis of the 24 SMMs are listed in Table 3-4.

Table 3 - 4 : SMM synthesis data

SMM	Reactant (mmol)			
	MDI	PPO	BA-L	BA-L fraction
MPB322HN	30	20	20	High
MPB322HR	22.5	15	15	High
MPB322LN	30	20	20	Low
MPB322LR	22.5	15	15	Low
MPB212HN	20	10	20	High
MPB212HR	15	7.5	15	High
MPB212LN	20	10	20	Low
MPB212LR	15	7.5	15	Low

3.3.3 SMM synthesis

The eight triplicate SMMs were synthesized using a two-step solution polymerization procedure, as illustrated in Figure 3-2. All reactions were carried out under dry nitrogen atmosphere and stirring rate.

To a solution of PPO in 50 mL dry DMAC, preheated to 40 °C in a glass reactor, was added MDI in 50 mL DMAC. The resulting prepolymer mixture was stirred at 40-50 °C

for three hours. Then BA-L High or Low in 50 mL of DMAc was quickly added, and the resulting mixture was allowed to stir at room temperature for approximately 15 hours.

The SMM had to be precipitated from the solution and purified before use. The SMM was precipitated slowly in distilled water, washed three times with distilled water to leach out trace solvent and water-soluble unreacted components. The SMM was then dried in air- circulating oven at 50°C for 2 days. Once dry, the SMM was ground into fine particles and then washed with 1,1,2-trichloro-1,2,2-trifluoro-ethane (HPLC grade, 3 × 50 mL) to remove traces of unreacted polyfluoroalcohol. The final purified material was then dried in an air-circulating oven at 50° C for two days, followed by vacuum drying at 0.5 mmHg and 50° C for one additional day to remove all traces of volatile components.

3.4 Material Characterizations

3.4.1 Molecular weight characterization

Determining the absolute average molecular weight of a copolymer is always more difficult compared to that of a homopolymer (Cowie, 1991). Absolute techniques (Cowie, 1991) such as end-group analysis, those based on colligative property changes or those based on light scattering of the polymer molecules, permit a direct calculation of the average molecular weight from experimentally measured quantities which are defined by theoretical relations. However, the heterogeneous nature of a copolymer can introduce irregularities which render the determination of these theoretical relations difficult.

Very often, the molecular weight of a copolymer is reported as a relative or equivalent value. The method used in this work is gel permeation chromatography (GPC), where the sample's molecular weight was determined relative to well defined polystyrene standards. The operative principle of a gel permeation column is size exclusion, with the smaller molecules retained longer in the column (Cowie, 1991). Using this principle, GPC also provides the distribution of the molecular weight. The quantity Q measured by the GPC detector is proportional only to the *mass* concentration of the polymer at the column

outlet (Q is independent of molecular weight (M)) (Rosen, 1982), as shown in Equation 3.3

$$Q = kc \tag{3.3}$$

where Q = detector readout, k = proportionality constant, and c = mass concentration of polymer, g/cm^3. Thus a GPC curve consists of a plot of Q (usually in arbitrary scale divisions) versus v, the elution volume. Quantitative information is determined by knowing the relation between M and v based on a calibration curve of known monodispersed polymer molecular weight standards.

Molecular weight averages may be approximated directly from the GPC curve by breaking the curve into arbitrary volume increments Δv. The number of moles of polymer in a volume increment Δv is n_i (Rosen, 1982):

$$n_i = c_i \Delta v / M_i \tag{3.4}$$

where c_i = polymer mass concentration in the ith volume increment and M_i = molecular weight of the polymer in the ith volume increment (assumed essentially constant over small Δv). Because $c_i = Q_i / k$ (Equation 3.3)

$$n_i = Q_i \Delta v / k M_i \tag{3.5}$$

Therefore

$$M_n = \frac{\sum_i n_i M_i}{\sum_i n_i} = \frac{\sum_i Q_i}{\sum_i (Q_i / M_i)} \tag{3.6}$$

and

$$M_w = \frac{\sum_i n_i M_i^2}{\sum_i n_i M_i} = \frac{\sum_i Q_i M_i}{\sum_i Q_i} \tag{3.7}$$

where M_n is the number average molecular weight, and M_w is the weight average molecular weight.

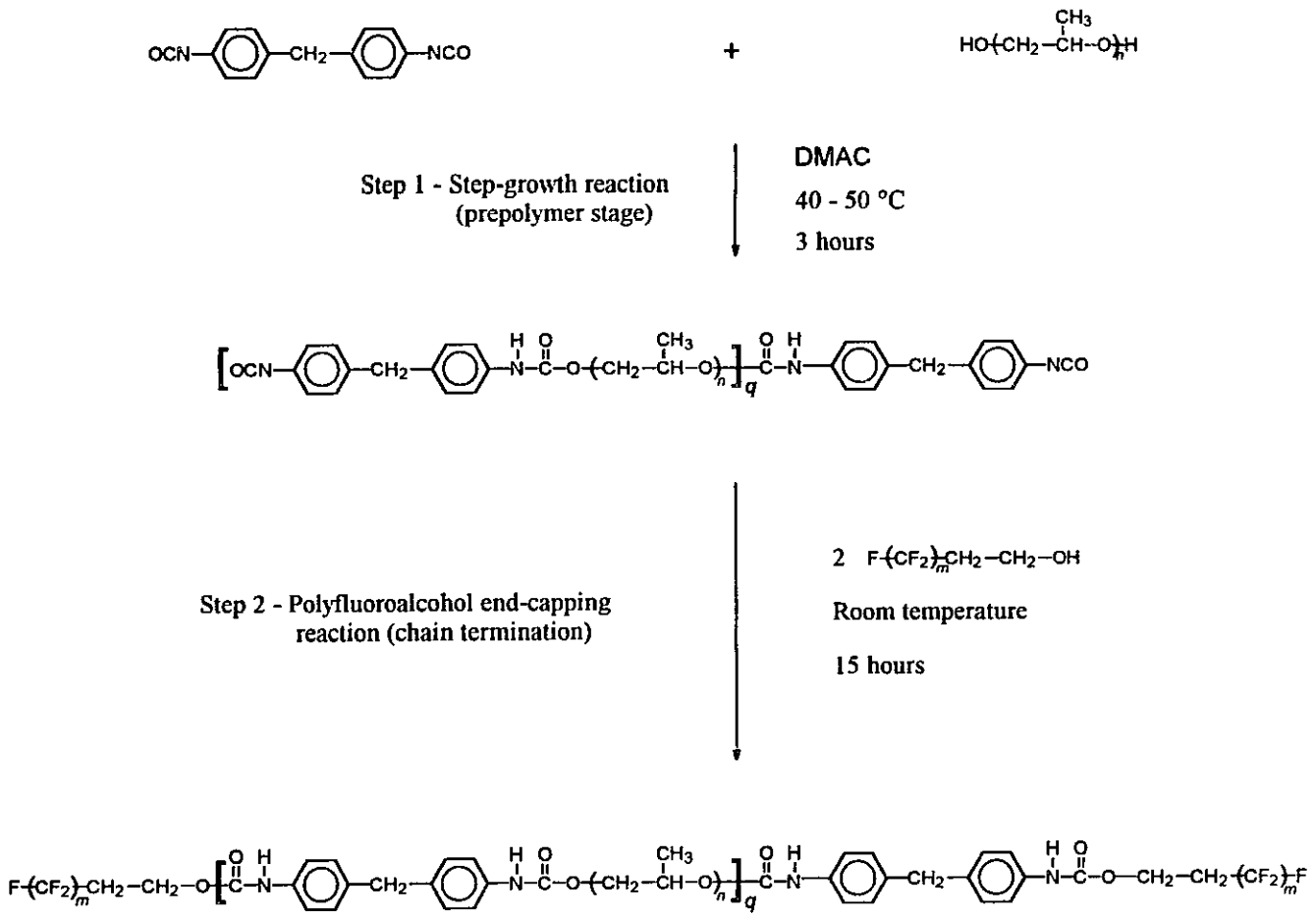

Figure 3 - 2 : The proposed reaction scheme for the SMM synthesis.

Based on polystyrene M_i standards, the equivalent average molecular weights of SMM and PES were determined by GPC. Three Waters Ultrastyragel columns (10^3, 10^4 and 10^5 Å pore sizes) and a differential refractive index detector (Waters 410) were used. The solvent phase was dimethylformamide (supplied by BDH, HPLC grade), containing 0.05 M LiBr (LiBr was used to minimize polymer strain entanglement). The flow rate was 1 mL/min, and the column temperature was kept at 80 °C.

3.4.2 Differential scanning calorimetry (DSC)

A solid polymer can exist in various states: random, ordered or semi-ordered. Polymers which are in a random state are called amorphous, whereas those which show some degree of order are classified as semi-crystalline (Cowie, 1991). As heat is supplied to a polymer sample, its coils will gain energy and more mobility. The temperature at which the ordered structure of the polymer coils disappears is the melting point (T_m). The temperature at which the amorphous polymer becomes rubbery is called the glass transition temperature (T_g).

The thermodynamic value of T_g is still under debate (Rosen, 1982). T_g was thought to be associated with the temperature at which two types of molecular motions in an amorphous polymer mass start: (i) translational motion of entire molecules, which permits flow, and (ii) cooperative movement of segments of molecules approximately 40 to 50 carbon atoms in length, permitting flexing and uncoiling (Rosen, 1982). Thus, T_g is a property of the polymer and is reflective of how the macromolecules which make up the polymer arrange themselves. T_g also reflects of a change in the specific heat capacity between the glassy and rubbery states, and it is difficult to define this change accurately (Brandrup and Immergut, 1989).

Differential scanning calorimetry (DSC) was used to determine thermal characteristics of SMM and PES/SMM blends. Three components characterizing T_g (°C) are reported in this work: (i) the onset T_g which is the temperature at which the transition started, (ii) the T_g width which is the range of temperature for the transition and (iii) the mid-point T_g, defined as the temperature at which half of the total change in specific heat

capacity has occurred. The convention for reporting the mid-point T_g was suggested by Brandrup and Immergut (1989) and has been used by several authors (Shultz and Young, 1983; Shultz et al., 1983; Aubin and Prud'homme, 1988; Burns and Kim, 1988). In addition, the apparent change in specific heat capacity at T_g (ΔCp) for each SMM was calculated from DSC data as employed by Shultz and Young (1983), Shultz et al. (1983), Aubin and Prud'homme (1988), and Burns and Kim (1988). ΔCp [J/(g.°C)] was determined according to the following relation (Charsley and Warrington, 1992):

$$\Delta Cp = \Delta H / \Delta T \tag{3.8}$$

where ΔH (J/g) is the total heat flow to the sample at T_g (°C) and ΔT (°C) is the difference in temperature between the liquid and glassy state (final T_g - onset T_g). The graphical method used to determine T_g values and a sample calculation of ΔCp can be found in Appendix C.

A DuPont DSC 910 system (located at the laboratory of Dr. M. Day, Institute for Environmental Chemistry, National Research Council, Ottawa, Ontario) equipped with a low temperature cell was used. DSC experiments were performed on 5-10 mg samples under nitrogen purge [50 mL/min] from -50 to 260°C[1] with a heating rate of 20 °C/min, where SMM were in powder form and actual PES and PES/SMM films or membranes were used. The following steps were carried out:

(i) The sample was first heated to 260 °C followed by an isothermal period (10 minutes at 260°C) to remove any traces of solvent and to relax the polymers.

(ii) The sample was cooled to -50°C at 40 °C/min with liquid nitrogen and then heated to 260°C at 20 °C/min.

Steps (i) and (ii) were repeated until the glass transition temperature (T_g) values from successive experiments did not differ more than 1°C (usually not more than three cycles). The analysis of thermograms was done using DuPont General V.4.0D software.

[1] Random thermal gravimetric analysis showed that most SMMs degraded at temperature > [360 - 400°C]

3.4.3 Contact angle measurements

The relative hydrophobicity of a surface can be qualitatively determined by measuring the contact angles of a water drop deposited onto it. The contact angle depends on the chemistry, roughness and heterogeneity of the surface (Johnson and Dettre, 1969). For a given system in thermodynamic equilibrium (stable or metastable), Gibbs (1928) analysis predicted that there would be only one contact angle. This situation only arises for an idealized smooth, homogeneous and non-deformable surface. In the absence of, or with a negligible, gravitational field, a free liquid drop will adopt a spherical shape which minimizes the free energy of the system. When in contact with either a solid or liquid substrate, it will take the shape which minimizes the free energy of the system. Gibbs (1928) demonstrated that minimizing the free energy requires the minimization of the sum

$$\gamma_{lg} A_{lg} + \gamma_{sg} A_{sg} + \gamma_{sl} A_{sl} \tag{3.9}$$

where γ is surface or interfacial tension, A is an area and the subscripts *lg*, *sg* and *sl* refer to liquid-vapor, solid-vapor and solid-liquid interfaces, respectively. For a plane, homogenous, non-deformable surface, the minimization yields the equation

$$\gamma_{lg} \cos\theta = \gamma_{sg} - \gamma_{sl} \tag{3.10}$$

where θ is the contact angle. Equation 3.10 is known as the Young's equation. The angle which a drop assumes on a solid surface is the result of a balance between the cohesive forces in the liquid and the adhesive forces between solid and liquid (Johnson and Dettre, 1969). If there were no interaction between solid and liquid, the interfacial tension would be the sum of the two surface tension γ_{sg} and γ_{lg}, and the contact angle would be 180°. Hence the closer a given contact angle to this limiting value, the less interaction will be between the liquid and the solid. In the presence of an interaction, the liquid will spread until Equation 3.10 is satisfied.

As previously discussed, real systems are rarely in thermodynamic equilibrium. This is even more pronounced in the case of polymer surfaces. A fundamental characteristic of wetting is the ability of a liquid drop to adopt many different stable angles on a solid surface. Two relatively reproducible angles are the largest and the smallest, which are

called the advancing angle θ_{adv} and the receding angle θ_{rec}, respectively. The names advancing and receding come from the method employed for measuring these two angles. The difference, $\theta_{adv} - \theta_{rec}$, is called the hysteresis.

The force exerted by the solid on the liquid can be active or passive. Active forces are those which cause the liquid to spread. Passive forces are those which resist movement of the drop's periphery. The advancing contact angle (θ_{adv}) characterizes the ability of a given liquid to spread on a surface; the receding contact angle (θ_{rec}) characterizes the breaking of the liquid spread or a measure of passive forces (Andrade, 1985; Johnson and Dettre, 1969). The balance between active and passive forces can be readily visualized in Figure 3-3, where a drop of a given liquid was deposited on a surface with an increasing angle of inclination. As the force of gravity pulls the liquid, there is a gradual build up of a forward angle (θ_a') and reduction of the trailing angle (θ_r'), but the drop's periphery will not move until the exertion of gravity is high enough to cause the drop to move and assume a new position. The forward and the tailing angles at which the sudden movement of the drop's periphery occurs are the advancing and receding angles, respectively (Johnson and Dettre, 1969). Johnson and Dettre (1969) refer to the balance of active and passive forces by the solid surface to resist the movement of the drop's periphery as an energy barrier, characteristic of a given surface.

There are two kind of hysteresis: (i) true classical thermodynamic hysteresis which is time independent, and (ii) kinetic hysteresis which is time dependent (Johnson and Dettre, 1969; Andrade et al., 1985). The thermodynamic hysteresis of a given real surface has been linked to its roughness and heterogeneity (Johnson and Dettre, 1969; Andrade et al., 1985). On the other hand, the kinetic hysteresis shows changes in hysteresis as a function of the rate of measurement and is due to swelling and penetration effects, surface mobility and reorientation and possibly surface deformation (Andrade et al., 1985). To properly minimize the kinetic hysteresis, controlled rate of measurement (i.e. controlled rate of liquid addition and withdrawing) or repeat cycle of measurement

until achieving constant measurement (e.g. by using the Wilhelmy plate technique (Johnson and Dettre, 1969; Andrade et al., 1985)) is usually used.

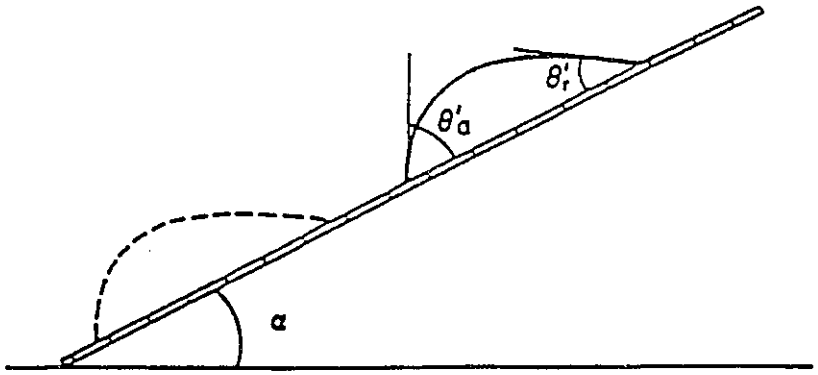

Figure 3 - 3 : Configuration of a liquid drop on an inclined surface.

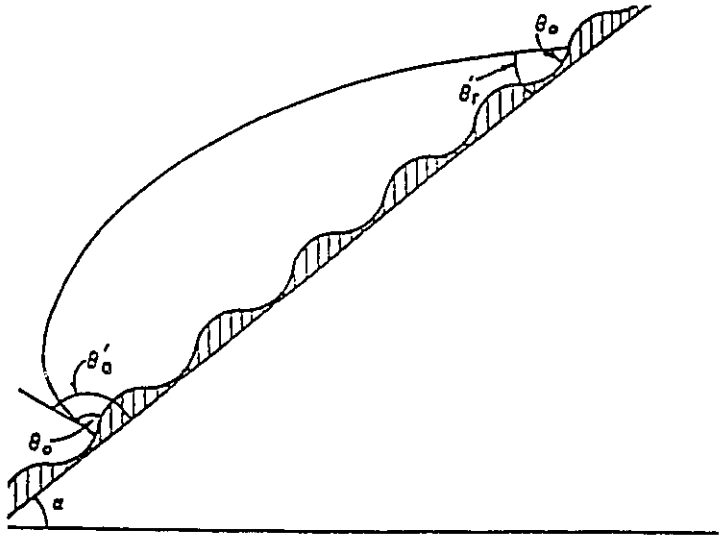

Figure 3 - 4 : Configuration of a liquid drop on a rough surface. Adapted from Johnson and Dettre 1969).

In this work, proper account for kinetic hysteresis was not possible due to the limitation of equipment available and the relatively large number of samples to be studied. However, the subject of kinetic hysteresis of the surfaces produced in this work is certainly of interest since swelling and penetration effects, surface mobility and

polymeric membranes (c.f. section 2.4). For the time being, kinetic hysteresis was assumed to be small (the assumption will be validated by the measurement protocol described later in this section, and the hysteresis measured was assumed to be due mainly to thermodynamic phenomena.

Hysteresis of contact angles due to surface roughness is illustrated in Figure 3-4. Clearly, the true contact angle is θ_o, but only the apparent advancing (θ'_a) and receding contact angles (θ'_r) can be directly measured. Several investigators have modeled this type of hysteresis, but the results obtained are considered difficult to use (Andrade et al., 1985). The most general study has been done by Johnson and Dettre (1964) through a thermodynamic study of a concentric surface roughness model by using Gibbs treatment of the equilibrium surface and assuming it to be correct (Figure 3-5). The general finding was that increasing the roughness increases advancing contact angles and decreases receding angles, resulting in higher hysteresis. This result agreed well with several experimental results (referenced in Johnson and Dettre, 1969; Andrade et al., 1985). In cases where the surface is glassy or optically smooth (i.e. the size of a generic 'valley' is less than 0.5 μm), the effect of surface roughness on hysteresis can be considered negligible (Johnson and Dettre, 1969; Andrade et al., 1985).

Surface heterogeneity can also cause hysteresis (Johnson and Dettre, 1969; Andrade et al., 1985). Figure 3-6 illustrates a surface composed of zones having different surface energetics. The islands in Figure 3-6, for example, represent low surface energy areas or high water contact angles. As a drop's periphery advances over such a surface, the edge of the liquid tends to stop at the boundaries of the islands. Johnson and Dettre (1964) studied a model surface consisting of concentric circular regions of alternating intrinsic contact angles, θ_1 and θ_2. Their model is shown in Figure 3-7. The heterogeneities were assumed to be very small compared to the dimensions of the liquid drop. Their theoretical analysis yielded the following conclusions which are useful in interpreting experimental data:

(i) Advancing angles are more reproducible on predominantly low-energy surfaces whereas receding angles are more reproducible on predominantly high-energy surfaces.

(ii) Advancing contact angles alone do not give a reliable measure of surface coverage. A 10 or 90% coverage (by a low energy monolayer) gives about the same advancing contact angle.

(iii) An advancing angle is a good measure of the wettability of the low-energy part of the surface and a receding angle is more characteristic of the high energy part.

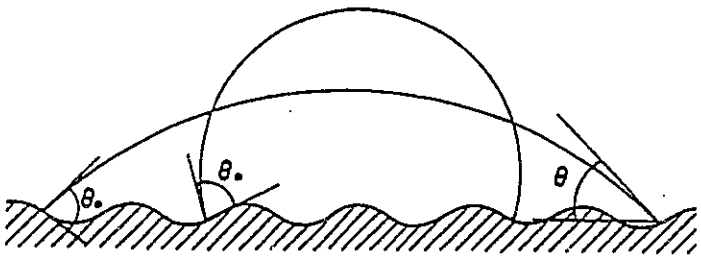

Figure 3 - 5 : Side view of Johnson and Dettre surface roughness model (1964). Adapted from Johnson and Dettre (1969).

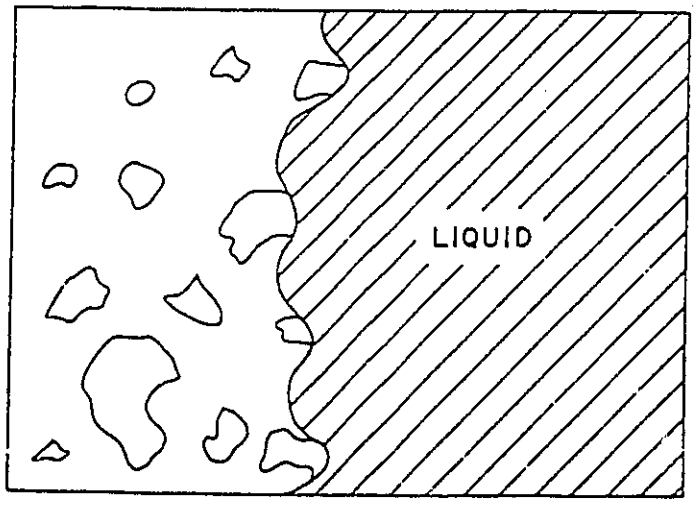

Figure 3 - 6 : A typical heterogeneous surface. Adapted from Johnson and Dettre (1969).

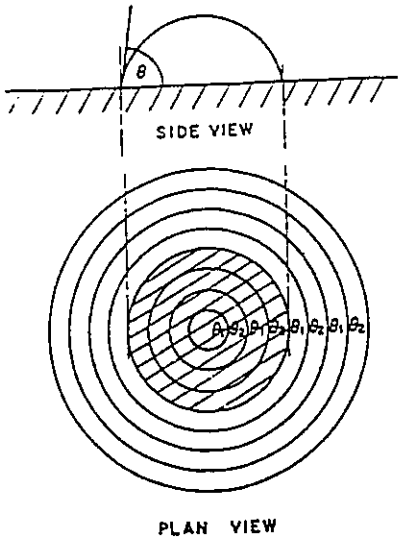

Figure 3 - 7 : Johnson and Dettre model (1964) of concentric surface heterogeneity. Adapted from Johnson and Dettre (1969).

Films for contact angle measurements were prepared on glass slides. The slides were soaked chromic acid solution for 24 hours and rinsed with distilled water, followed by drying in 100° C oven prior to use. Casting solutions were allowed to stand at room temperature for 48 hours for detection of any phase separation. Solutions forming a single phase were filtered through a 0.5 μm pore size Teflon® membrane filter prior to film casting.

PES and PES/SMM films were prepared from casting solutions consisting of 25 wt.% PES, and 0, 0.5, 1.0 or 2.0 wt.% SMM in distilled DMAC solvent. The filtered solution was cast onto a clean glass slides to form a thin film. The slide was then placed into an air circulating oven at 110° C for 10 minutes, followed by drying at room temperature for 24 hours in a dry-air circulating oven and an additional 24 hours of drying under vacuum

(room temperature, ~1 mmHg). Contact angles for each surface were measured immediately following the drying procedure.

Contact angle measurements for films prepared from membrane casting solution were cast from solutions containing different SMM compositions and also containing poly(vinyl pyrrolidone) as an additive (for more information see section 3.5.2 of this chapter). These studies were carried out to investigate the effect of PVP on the function of the SMM. The protocol to prepare films for contact angle measurements from these solutions were the same as described above.

Water θ_{adv} and θ_{rec} values of PES and PES/SMM films were measured using a Ramé-Hart, Model A-100 goniometer. Distilled water was purified using a Barnstead NANOpure II unit, and the initial water drop (2.0×10^{-4} mL) was deposited onto the film surface with a Ramé-Hart, Model 100-10 microlitre gas tight syringe. The volume of the drop was slowly increased and then decreased by adding water to and withdrawing water from it, using the microsyringe. The procedure was repeated three times prior to contact angle measurements. On the third water addition, a contact angle reading, just prior to the sudden movement of the three phase interface, was recorded as the θ_{adv} value. Water was then withdrawn until the onset of another sudden movement of the three phase interface to give the θ_{res} reading. A total of two slides were prepared for the PES solution and for each of the PES/SMM solutions. Ten readings were performed at random locations on the surface of each slide. After these sets of readings were taken, the films were then used for X-ray photoelectron spectroscopy measurements.

3.4.4 X-ray photoelectron spectroscopy (XPS)

The surfaces of PES/SMM films used in contact angle measurements were also characterized by XPS, done by the Centre for Biomaterials, University of Toronto, Toronto, Ontario. Films were marked for the side exposed to air and were separated from glass slides by immersion in distilled water. They were then dried by a solvent exchange procedure involving four consecutive overnight immersions in aqueous solutions of increasing ethanol concentrations (25, 50, 75 and 100 vol.% ethanol). After the last

immersion, the films were dried under vacuum for 24 hours at room temperature and then washed with 1,1,2-trichloro-trifluoroethane (TCTFE, HPLC grade) (2 x 1 minute rinses) to remove traces of silicone contamination. After drying under vacuum for 24 hours at room temperature, each sample was then put in an aluminum dish, covered with a non-lint tissue, placed inside a sterile plastic pouch, and sent for analysis. It was assumed that the drying procedure used and the application of high vacuum in the XPS analysis reduced the amounts of TCTFE to a non-interfering level.

The XPS information for samples is composed of two parts: low and high resolution spectra. At low resolution, information regarding elemental composition in terms of relative atomic percent is obtained. At high resolution, chemical bond types can be detected by measuring the relative binding energy shift. The reference for the high resolution data for this work was the C-C shift, and the relative importance of each type bond and the corresponding structure were given as a percentage. For the low resolution data, the relative intensities was standardized with respect to the intensity of the element carbon, whereas the high resolution data were standardized with respect to the C-C shift signal. Standardized results are common practices with investigators using XPS (Feast and Munro, 1987.

The XPS spectra were obtained on a Leybold MAX 200 XPS system. Unmonochromatized Mg K_α x-ray radiation was used as the excitation source. The source was run at 12 kV and 25 mA. Atomic percentages of the elements present were derived from spectra run in a low-resolution mode (pass energy = 192 eV) which were normalized to unit transmission of the electron spectrometer. The spectral regions of interest were also run in a high-resolution mode (pass energy = 48 eV). Binding energy and peak areas were obtained by use of the routines provided with the spectrometer. The energy scale of the spectrometer was calibrated to the Ag $3d_{5/2}$ and Cu $2p_{3/2}$ peaks at 368.3 eV and 932.7 eV, respectively. The binding energy scale was then shifted to place the C 1s feature present at 285.0 eV. Large-area analysis was performed (2×4 mm or 4×7 mm) so that exposure of the samples to the X-rays would be minimized while sufficient signal-to-noise ratios could be obtained for the spectral features. Low and high-

resolution data were collected at two take-off angles (θ'') 15° and 90° (see Figure 3-8 for illustration of θ''). The layer characterized at the 90° take-off angle was representative of the top 10 nm of the surface, while that characterized at the 15° take-off angle was representative of the top 2 nm of the surface. Relatively speaking, the difference between the information at the 15° and 90° represented a surface depth profile from a deeper layer (90°) to a more shallow layer (15°).

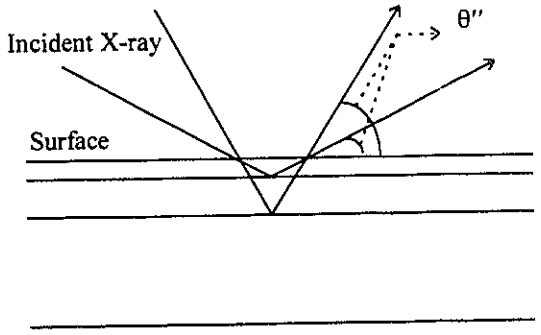

Figure 3 - 8 : Dependence of sampling depth on varying take-off angle (θ'') (Clark, 1978, p. 318).

3.4.5 Elemental analysis

Bulk elemental composition for each SMM was determined at Guelph Chemical Laboratory (GCL), Guelph, Ontario, Carbon (C), Nitrogen (N) and Fluorine (F), content of each type of SMM was reported as a weight percent. The summarized protocols used for each element was supplied by GCL and are reported as follows:

(i) For Carbon and Nitrogen: the samples were analyzed using a PERKIN ELMER 240 Elemental Analyzer where a weighed sample was combusted in an oxygen atmosphere at 950°C. The sample was then reduced by passing through copper at 650°C. The combustion products (CO_2, N_2) were then analyzed automatically using a standard technique of gas chromatography. The percent carbon and nitrogen were deduced from a calibration constant using National Bureau of Standards (NBS) standards of known percent carbon and nitrogen.

(ii) For fluorine: a weighed sample was covered with sodium peroxide, then combusted in an oxygen rich atmosphere using a Shöniger oxygen flask with distilled water as the

absorbing solution. After filtering, an aliquot of this solution was titrated with thorium nitrate using Alizarin Red S as an indicator. The fluorine concentration was then calculated from the volume of titrant used.

The elemental analysis method is convenient for the determination of individual monomer content in copolymer(s) if one component contains an element not present in the second one (Dobkowski, 1987). In this work, the element nitrogen (N) is associated with the urethane bond in the main chain of an SMM and is uniquely related to the MDI component, while the element fluorine (F) is only associated with the polyfluoroalcohol. For a binary system, every element can be balanced according to the following equations:

$$f_1 + f_2 = 1 \tag{3.11}$$

$$w'_{Y1} f_1 + w'_{Y2} f_2 = w'_{Ym} \tag{3.12}$$

where f_1 and f_2 are the weight fraction of components 1 and 2, respectively; w'_Y is the weight fraction of a given element Y in the material; subscripts 1, 2 and m denote component 1, 2 and their mixture (in copolymer), respectively. The weight fraction of a given component, e.g. 2, is

$$f_2 = (w'_{Ym} - w'_{Y1}) / (w'_{Y2} - w'_{Y1}) \tag{3.13}$$

If only one component contains the element Y, i.e. $w'_{Y1} = 0$, then

$$f_2 = w'_{Ym} / w'_{Y1} \tag{3.14}$$

Equation 3.13 can be extended to multi-component systems, i.e.

$$f_i = w'_{Ym} / w'_{Yi} \tag{3.15}$$

if element Y is present in the ith component only. The error in the calculation obviously depends on the error associated with the elemental analysis. The weight fraction of nitrogen in MDI was calculated from the chemical structure to be 0.112 and that of fluorine in BA-L fractions was given in Table 3-2.

Due to financial limitations, the elemental analysis for each SMM was only performed once; therefore, it is difficult to estimate the error associated with the experimental methods. For the purpose of discussion, it will be assumed that the results were representative of the samples, and that the error associated with the experimental methods was the same for all SMMs.

3.5 Membrane experiments

The developmental work on SMMs would lack validation without a presentation of some membrane pervaporation experiments. To know the effect(s) of SMMs on pervaporation, a fixed set of membrane pervaporation experiment(s) was conducted. This section was carried out by Mr. Yi Fang of the Industrial Membrane Research Institute, Department of Chemical Engineering, University of Ottawa as a part of his Ph.D. thesis.

3.5.1 Material preparation

Prior to use, PES was dried in an air-circulating oven for 4 hours at 150°C to remove absorbed moisture. PVP was used as a non-solvent additive (Fang et al., 1994). Chloroform and DMAC of reagent grade were supplied by BDH and were used without further treatment.

3.5.2 Membrane preparation

A phase inversion method was used to cast the membranes. PES and PVP concentrations in the casting solution were maintained at 25 wt.% and 6 wt.% respectively, whereas the SMM concentration was changed from 0 to 2.5 wt.%; the balance was DMAC solvent. Membranes were cast on a glass plate to a nominal thickness of 2.5×10^{-4} m. Immediately after casting, the film was transferred into an air circulating oven preheated at 95°C and kept there for 7 minutes, then it was gelled by immersing the glass plate into ice cold water. The membrane was kept in the gelation medium overnight. They were then dried using a solvent exchange procedure as described in section 3.4.4 and ethanol was air-evaporated to yield the final dried membranes.

3.5.3 Pervaporation experiments

The pervaporation of chloroform and water mixtures was studied with various membranes. The cells used in pervaporation experiments were identical to those used in reverse osmosis experiments (Sourirajan and Matsuura, 1985). The experimental procedure was described in detail elsewhere (Deng et al., 1990). Briefly, 0.250 kg of feed liquid was loaded in the feed chamber, then a vacuum was applied at the downstream side of the membrane. The permeant sample was condensed and collected in a cold trap cooled in liquid nitrogen. The amount of the sample removed by membrane permeation was kept below 2% of the initial feed volume. Composition of chloroform in the mixture was analyzed by Liquid Chromatography (LC). A Waters liquid chromatograph model 501 fitted with a differential refractometer (Waters R401) was used. Distilled water was used as the mobile phase at a flow rate of 2.0 mL/min, and the sample size was 10 μL for each injection. The permeation rate was determined by weighing the sample collected during a predetermined period. The chloroform feed concentration was maintained at 1000 ± 10 ppm. The effective membrane area was 9.6×10^{-4} m^2. The temperature was maintained at 23 ± 1°C, and the downstream pressure was maintained at 3 ± 1 mmHg throughout the experiment. A new membrane coupon was used for each experiment unless stated otherwise.

3.6 Data evaluation (Sachs, 1984)

There are a number of techniques available to systematically analyze the experimental data. For the total factorial design of the SMM synthesis data as well as other experiments such as those for the characterization of PES/SMM blends and membrane pervaporation data, the methods used include (i) mean effect determination, (ii) analysis of goodness (ANOG), (iii) regression analysis and (iv) graphical analysis. The methods were used singularly and in combination with each other.

The mean effect determination is summarized by Equation 3.16, which represents the effect of a specific variable, with all others being constant at given values.

$$Mean\ Effect\ of\ a\ variable = \frac{\sum Responses}{number\ of\ experiments} \tag{3.16}$$

The analysis of goodness is a simple method to qualitatively determine the most significant variable(s) and to detect outlying data point(s). It is used in combination with other methods of analysis. The application is straight forward: (i) obtain the results of a factorial design, (ii) list the results in ascending or descending order, (iii) write the treatment combinations beside each experiment, then (iv) examine the best two, four or eight experiments for pattern(s) of similar sign. Such a pattern identifies the significant variable. An anomalous point can be identified if its result does not seem to follow an overall trend detected after such analysis.

Regression analysis is more effective in determining the relationship between the experimental variables and the response, compared to the two previous methods. In a multi-linear equation of the type

$$y = k_a + \beta'_a x_A + \beta'_b x_B + \beta'_c x_C + ... + \beta'_n x_N \tag{3.17}$$

with regressor variables x_A to x_N, the relationship between a variable and the observed response y is given by the regression coefficients, β'_a to β'_N with k_a representing the response average. The multi-linear regression coefficients can be estimated using a standard least squares procedure (Montgomery and Peck, 1982). Indications of the significance of the variables, such as the correlation coefficient, R^2, an overall F-test (ANOVA) and a series of individual F-tests can be performed to evaluate the importance of each variable. The factorial analysis of *mean effects* and regression analysis in this work was carried out using STAT-GRAPHICS, a statistical software package from Statistical Graphics Corporation (©1985-91, ver. 5.0).

Chapter 4

RESULTS AND DISCUSSION

The results and discussion for this work are presented in three separate sections. The first part is the synthesis and characterization of SMM. It deals with the synthesis parameters and the SMM's bulk characteristics such as relative molecular weight, polydispersity, weight fraction of the components, overall structure and glass transition temperature (T_g). The aim is to identify synthesis formula which can generate reproducible SMMs and to see which material properties can be used in to correlate the characteristics of PES/SMM blends with the observed pervaporation performance of SMM modified PES membranes. In the second part, SMM/PES blends are characterized to study the effects of SMMs on the PES bulk and surface properties. The focus is to determine whether there is any variation in surface and bulk property changes with respect to variation in SMM molecular variables. The surface and bulk property change(s) will then be studied in relation to the pervaporation performance of the modified membrane. Finally, the third part deals with the effects of SMMs on pervaporation.

4.1 SMM Synthesis and Characterization

As presented in Figure 1-3, the synthesis of an SMM polymer was carried out in two steps. First the main chains of the macromolecules were produced by a step-growth reaction between diisocyanate molecules and polymeric diol molecules (the prepolymer stage). The diisocyanate was used in excess to produce isocyanate end-capped products at the end of this first step. Following this, a monofunctional polyfluoroalcohol (BA-L) was introduced to react with the isocyanate ends to form the final surface modifying macromolecules (the end-capping stage). The chemical structure of the main chain can be changed by using different combinations of diisocyanates and/or polymeric diols, and the polyfluoro-ends can be changed by using different types of polyfluoroalcohols (i.e. a

different type of Zonyl intermediate). However, SMM will always share the same generic structure of main chains and polyfluoro-ends. As discussed previously in section 1.5, it is reasonable to assume that the functional nature of the SMM depends on their polyfluoro-end-groups, and that these end-groups will be less important if the main chain is comparatively much larger. Since the size of a polyfluoroalcohol molecule is relatively fixed in this study, a high molecular weight SMM will have a larger main chain in comparison to a low molecular weight SMM. It is well known that a step growth polymerization is a random process (Cowie, 1991), and all synthesized polymers will consist of many molecules with a distribution of chain lengths. Therefore, it is important to know how the chain length and the distribution can be controlled.

The preliminary synthesis of SMMs suggested that these polymers were not uniformly reproducible. For certain combinations of experimental variables (the reactant mole ratio, the fraction of BA-L (i.e. the type of polyfluoroalcohol) and the concentration of the prepolymer reactants), the polymer state at room temperature varied from batch to batch, yielding in some cases a hard material and in others a rubbery like substance. To effectively study the importance of these variables on the character of the final product, a factorial study was carried out. As explained in section 3.3.2, the factorial experiments were conducted by introducing step changes from an arbitrary low level to a higher one for each variable. The conditions that were held constant included the temperature range for the polymerization reaction, the reaction solvent and the stirring rate.

Overall, there were eight SMM formulations, representing eight combinations of the three experimental variables. Each formulation was carried out in triplicate to provide a total of 24 SMMs. The effect of the reactant mole ratio, the prepolymer reactant concentration and the type of polyfluoroalcohol on the final SMM products was assessed using the following molecular variables: the average molecular weight (weight (M_w) and number average (M_n)), the weight fraction of each reactant component in the final SMM and the polydispersity. The average molecular weights and the polydispersity determined in this work were relative values with respect to polystyrene standards. These values were used on a comparative basis for SMMs and have no meaning in absolute terms. M_w,

M_n and polydispersity of each of the 24 SMMs as well as the average of the triplicate synthesis can be found in Appendix A, Table A-1.

Since fluorine (F) was only associated with the polyfluoroalcohol and nitrogen (N) only with MDI, the weight fractions of MDI (f_m) and polyfluoroalcohol (f_z) components in the final polymer were calculated directly from the weight fraction of (N) and (F) in SMM, as determined by elemental analysis. The weight fraction of PPO was then determined by difference. The weight fraction of polyfluoroalcohol (f_z) has to be understood as the weight fraction of either BA-L High or BA-L Low in the SMM; hence, for the same value of f_z the SMMs will have different molecular distribution of polyfluoroalcohol if BA-L types differ. The elemental composition data, as received from Guelph Chemical Laboratories and the calculated f_m, f_p and f_z for all 24 SMMs and their averages were tabulated in Appendix B, Table B-1.

The synthesis procedure used was based on the assumption that the chain growth reaction between MDI and PPO was essentially completed before the addition of BA-L. Hence, the final molecular weight difference between MDI/PPO/BA-L High and MDI/PPO/BA-L Low for a given reactant mole ratio should be due to the difference in the molecular weight between the two fractions of BA-L, independent of the chemical reactivity or other characteristics of each BA-L fraction. This assumption also anticipates that the reproducibility of the SMM should be good, since MDI was used in excess to limit the chain growth reaction with PPO, and BA-L is monofunctional.

The extended Carothers' equation (2.24) (c.f. section 2.3.3) shows that the number average degree of polymerization x_n should be low when conditions such as an excess of one reactant and/or a monofunctional additive are present (Figure 2-7). It also predicts that a higher excess of one reactant will produce a lower molecular weight product. This prediction assumes equal reactivity of all functional groups, whether they are in a monomer or in an intermediate species. Moreover, Equation 2.24 also assumed that the kinetics of the reaction is independent of the chain length. Using computer models, Peebles (1974, 1976) has shown that both assumptions are incorrect when a two step

process of prepolymer and chain extension is employed for the synthesis of polyurethanes (c.f. section 2.3.3). The studies predicted that the chain growth reaction for a polyurethane depended on the ratios of reactivity for the various isocyanate terminated intermediate species, and that not all isocyanate terminated intermediates would react to form highly polymerized isocyanate end-capped product at the end of the prepolymer step. These results have been verified experimentally by Wang and Lyman (1992). They analyzed the intermediate products of the reaction between MDI and two different polymeric diols: polypropylene oxide (PPO, M_w = 1000) and polytetramethylene oxide (PTMO, M_w = 1000) for a 2:1 stoichiometric ratio of diisocyanate to polymeric diol. PPO has one primary hydroxyl group on one end and a secondary hydroxyl group on the other, whereas PTMO has primary hydroxyl groups on both ends (see Figure 2-9). They also investigated the effect of solvent and temperature on this reaction and fixed the reaction time at three hours. They concluded that there were more unreacted diisocyanate and polymeric diol dimer (i.e. MDI-polymeric diol-MDI-polymeric diol-MDI species) at the end of the reaction when both ends of the polymeric diol contained primary hydroxyl groups (i.e. PTMO). It was proposed that the differences were due to the higher reactivity of primary hydroxyl groups compared to that of secondary hydroxyl groups. The type of solvent used had little effect on the reaction, and reaction carried out at high temperature (100-105° C) had more unreacted diisocyanate for the MDI/PTMO system, whereas no distinct difference was observed for the MDI/PPO system, within the temperature range studied (85-105 ° C).

In order to use the Peebles model quantitatively for the prediction of product formation in the SMM prepolymer synthesis, actual kinetic rate data for the PPO used is needed. While this is beyond the scope of the current work, Peebles's results along with its verification by Wang and Lyman (1992) for the case of a 2:1 stoichiometric ratio does suggest that unreacted diisocyanates and several diisocyanate end-capped species should be present at the end of an SMM prepolymer synthesis. Wang and Lyman (1992) have shown that there were no diol monomers left at the end of a three hour period, but experiments were not available for a 3:2 ratio of MDI:PPO. Peebles (1974b) has

indicated that the length of the isocyanate terminated chains is more difficult to control for high concentrations of diisocyanate and for low ratios of isocyanate/diol groups. Therefore, the variation in molecular weight is associated with both the selected stoichiometry of the prepolymer reaction and/or with the chain terminating reaction. In the latter scenario, the BA-L hydroxyl function must compete with hydroxyl ends remaining after the prepolymer step. If the chain termination reaction between BA-L and the free isocyanate groups is fast, then the final SMM should have a low molecular weight.

Based on the above theoretical analysis of the SMM synthesis the following would be expected: (i) SMM synthesized with a MDI:PPO ratio of 3:2 should have higher molecular weight than those synthesized with a ratio of 2:1 due to a smaller excess of MDI; (ii) the difference in the molecular weight of an SMM for a given MDI:PPO ratio should be due to the differences between the different BA-L, but only when it can be assumed that at the time of BA-L addition, there will be several isocyanate terminated species and very few hydroxyl terminated ones; (iii) The reproducibility of SMM should be better for the 2:1 ratio than for the 3:2 ratio.

The average molecular characteristics and the average thermal characteristics along with their respective percent standard errors relative to the averages for each SMM synthesized are presented in Table 4-1. The average overall error of the measured characteristics is given in the final column of Table 4-1. A small standard error indicates confidence in the reproducibility of an SMM. Since the experimental error associated with the GPC method itself was only 2-3% (see Table A-2 in Appendix A), it becomes clear from the standard error that the reproducibility of some of the SMMs was better than others. In general, the standard error for the molecular weights were all near 10%, and that of the polydispersity values was even lower. The differences in standard errors did not appear to be strictly correlated to any of the three experimental variables , although a reduction in the concentration of prepolymer reactant seemed to minimize the error associated with M_w and M_n. This will be further analyzed in the discussion following Table 4-3.

Table 4 - 1: Average SMM characteristics and their percent standard errors (standard error = Percent standard error x Average) as well as the average percent error of all characteristics.

SMM	Characteristics											
	M_w		M_n		*Polydispersity*		f_z		f_m		f_p	
	Average	%Std. Err.	Average	%Std. Err.	Average	%Std. Err.	Average	%Std. Err.	Average	%Std. Err.	Average	%Std. Err.
MPB322HN	26667	10%	16273	6%	1.6	5%	0.20	6%	0.36	10%	0.43	6%
MPB322HR	22333	7%	14264	4%	1.6	2%	0.17	39%	0.42	4%	0.41	12%
MPB212HN	16333	11%	10599	6%	1.5	6%	0.30	16%	0.37	5%	0.33	9%
MPB212HR	18000	9%	11407	6%	1.6	7%	0.18	12%	0.43	10%	0.39	6%
MPB322LN	25333	15%	15373	11%	1.6	4%	0.11	35%	0.51	18%	0.39	16%
MPB322LR	19333	5%	13175	3%	1.5	2%	0.14	10%	0.41	6%	0.45	4%
MPB212LN	12667	9%	9231	5%	1.4	5%	0.31	3%	0.39	2%	0.30	5%
MPB212LR	15333	13%	10196	2%	1.5	8%	0.21	12%	0.49	2%	0.30	5%
Means:	19500	10%	12565	5%	1.5	5%	0.20	16%	0.42	7%	0.37	8%

Table 4 - 1 (Cont'd) : Average SMM characteristics and their percent standard errors (standard error = Percent standard error x Average) as well as the average percent error of all characteristics.

SMM	Characteristics								Average overall % error
	Onset T_g (°C)		*T_g width (°C)*		*Mid-point T_g (°C)*		*Δ Cp at T_g (J/g.°C)*		
	Average	%Std. Err.	Average	%Std. Err.	Average	%Std. Err.	Average	%Std. Err.	
MPB322HN	19	17%	16	5%	29	8%	0.37	9%	8%
MPB322HR	14	30%	13	5%	20	13%	0.37	8%	13%
MPB212HN	27	15%	13	21%	34	5%	0.27	22%	12%
MPB212HR	21	16%	13	13%	29	5%	0.30	7%	9%
MPB322LN	12	54%	14	0%	19	20%	0.38	7%	18%
MPB322LR	16	6%	15	2%	24	5%	0.40	3%	5%
MPB212LN	21	10%	14	2%	28	5%	0.36	5%	5%
MPB212LR	19	17%	14	4%	27	7%	0.30	3%	8%
Averages:	19	21%	14	7%	26	9%	0.34	8%	

Table 4-1 also presents data for the weight fractions of each of the three components in the SMM. These values were calculated from elemental analysis results as described in section 3.4.5. For the purpose of comparison, the theoretical weight fractions of the components were calculated, assuming a 100% conversion of the three reactants. These values are reported in Table 4-2.

Table 4 - 2: Theoretical weight fractions of BA-L (f_z), MDI (f_m) and PPO (f_p) in SMMs, assuming 100% conversion.

Reactant mole ratio, BA-L fraction	f_z	f_m	f_p	$f_m + f_p$
3:2:2, High	0.42	0.27	0.31	0.58
3:2:2, Low	0.36	0.30	0.34	0.64
2:1:2, High	0.56	0.24	0.2	0.44
2:1:2, Low	0.49	0.28	0.23	0.51

The actual f_z values reported in Table 4-1 are significantly lower than the theoretical values in Table 4-2. Another immediate observation was that these values varied widely for some SMMs (specifically for MPB322HR and MPB322LN). Based on the information available at this time, it is not possible to associate stoichiometry, reaction concentration or BA-L type with the elevated standard errors observed for MPB322HR and MPB322LN. There is also the possibility that other variables which were not studied are responsible for the non-reproducibility of the f_z characteristic. These may be specifically related to reaction kinetics, and possibly related to the relative reactivity of the hydroxyl group on the polyfluoroalcohol as compared to the hydroxyl groups on the PPO.

With the exception of MPB322LN the percent standard error for f_m and f_p values were maintained close to 10% standard error. This would indicate that the prepolymer step for most of the synthesis work was maintained relatively constant and that significant variations in material composition were more likely dependent on the kinetics of the end-capping step. This hypothesis is supported by the wide variation in some f_z values (in

Table 4-1) and the lower fluorine content incorporated relative to the theoretical predictions (in Table 4-2).

The average T_g values for the SMMs are reported in Table 4.1 and were obtained for each SMM of the triplicate synthesis (Appendix C, Table C-1). In this work, the SMMs were heated at constant rate (20° C/min.) to a much higher temperature than their T_g (260° C), where the samples were allowed to relax. This procedure allows the polymers to be as close as possible to a state of arrangement, independent of the history of sample processing. In general, there were no crystallizing endotherms detected for any of the SMMs from -50° C up to 260° C, which indicates that the polymers are amorphous within this temperature range. The lack of symmetrical chain structure (see Figure 3-2) and the possible destabilizing effect of the two polyfluoro ends may not provide enough thermodynamic stability for crystallite formation to yield a semi-crystalline structure (Rosen, 1982). Even if the SMMs possessed favorable thermodynamic conditions for crystallite formation to occur, kinetic factors may not facilitate its study, since crystallite formations could take months (Rosen, 1982).

Based on the data for the onset T_g in Table 4-1, it was observed that an SMM with a reactant mole ratio of 2:1:2 generally had less variation for T_g values, whereas the reactant concentration and the type of BA-L did not show any obvious relation with the variation in T_g for a given SMM. Similar observations applied for the mid-point T_g values.

The T_g width has been associated with the heterogeneity of a polymer sample (Turi, 1981). The heterogeneity is understood to be related to either the distribution of polymer chains and/or a difference in monomer composition (Turi, 1981). Here, the variation in a given SMM T_g width can be associated with the variation of its inherent heterogeneity. It was noted that this variation was low for systems containing BA-L Low, and that the effect of the reactant mole ratio and the reactant concentration were insignificant. Similar observations for the variation of ΔCp were also noted.

Also provided in Table 4-1 was the average overall percent error of all measured characteristics for each SMM, assuming equal importance for all characteristics. The increasing overall order of the overall error for the eight SMMs was MPB322LR = MPB212LN < MPB212LR = MPB322HN < MPB212HR < MPB212HN < MPB322HR < MPB322LN. Based on this classification, the effects of the reactant mole ratio and the prepolymer reactant concentration showed no trends (i.e. equally appear on both low and high side); however, SMMs synthesized with BA-L Low had lower overall variation in characteristics for three of the four polymers synthesized with this monomer.

It can be concluded that the most reproducible SMMs were MPB322LR and MPB212LN (least overall error). In general, there were few obvious direct relations between the variability in molecular characteristics and experimental variables studied. Except for the polydispersity, which showed a higher variability for the 2:1:2 reactant mole ratio. In regards to the variation in material thermal characteristics, it was clear that using BA-L Low reduced the variation in T_g width and ΔCp, whereas the 2:1:2 reactant mole ratio seemed to do the same for the onset T_g and the mid-point T_g, but not consistently with all materials.

The effects of the three experimental variables on the measured values for the SMM's M_w, M_n, polydispersity, f_m, f_p, f_z , f_m+f_p, onset T_g, T_g width, mid-point T_g and ΔCp are given in Table 4-3 and were assessed by means of a factorial analysis. The variables included the reactant mole ratio (RMR), the prepolymer reactant concentration (RC) and the type of polyfluoroalcohol (FB). Physically, the change in the RMR represents a move toward less excess of MDI over PPO; the change in the RC means an increase in the density of MDI and PPO molecules and therefore an increased proximity of the reactants. The number of BA-L (High or Low) molecules were kept stoichiometrically constant and therefore a change from BA-L Low to BA-L High means that a polyfluoroalcohol with a longer ($-CF_2-$) tail is incorporated into the SMM. The SMM molecular variables such as M_w, M_n, polydispersity, f_m, f_p, f_z , f_m+f_p and its thermal properties are collectively referred to as responses. Table 4-3 lists the average effect from the response averages (last row of Table 4-1), as produced by a step change in RMR, RC or FB. The effect

Table 4 - 3 : Effects on various responses due to changes in the reactant mole ratio (RMR) from 2:1:2 to 3:2:2, the prepolymer reactant concentration (RC) from 0.23:0.15 M (MDI:PPO) to 0.3:0.2 M (at RMR = 3:2:2) or from 0.15:0.075 M to 0.2:0.1 M (at RMR = 2:1:2)†; or the type of polyfluoroalcohol (FB) from BA-L Low to BA-L High.

Response	Variable	Mean Effect	Standard* error	P-value
Weight Average Molecular Weight (M_w)	**Reactant mole ratio (RMR)**	**7.8E+03**	**1.4E+03**	**0.00**
	Prepolymer reactant concentration (RC)	1.5E+03	1.4E+03	0.31
	Type of polyfluoroalcohol (FB)	2.7E+03	1.4E+03	0.08
	RMR·RC	**3.7E+03**	**1.4E+03**	**0.02**
	RMR·FB	-5.0E+02	1.4E+03	0.73
	RC·FB	-1.7E+02	1.4E+03	0.91
Number average Molecular Weight (M_n)	**RMR**	**4.4E+03**	**5.7E+02**	**0.00**
	RC	6.1E+02	5.7E+02	0.30
	FB	1.1E+03	5.7E+02	0.06
	RMR·RC	**1.5E+03**	**5.7E+02**	**0.02**
	RMR·FB	-1.4E+02	5.7E+02	0.80
	RC·FB	8.3E+00	5.7E+02	0.99
Polydispersity	RMR	8.3E-02	5.6E-02	0.16
	RC	1.7E-02	5.6E-02	0.77
	FB	8.3E-02	5.6E-02	0.16
	RMR·RC	1.0E-01	5.6E-02	0.10
	RMR·FB	-3.3E-02	5.6E-02	0.57
	RC·FB	0.0E+00	5.6E-02	1.00
Weight fraction of MDI in SMM (f_m)	RMR	8.3E-03	3.2E-02	0.80
	RC	-3.3E-02	3.2E-02	0.31
	FB	-5.7E-02	3.2E-02	0.09
	RMR·RC	5.0E-02	3.2E-02	0.14
	RMR·FB	-1.0E-02	3.2E-02	0.76
	RC·FB	-2.8E-02	3.2E-02	0.39
Weight fraction of PPO in SMM (f_p)	**RMR**	**8.3E-02**	**2.9E-02**	**0.01**
	RC	-2.5E-02	2.9E-02	0.42
	FB	-4.5E-02	2.9E-02	0.15
	RMR·RC	3.3E-03	2.9E-02	0.91
	RMR·FB	-1.3E-02	2.9E-02	0.66
	RC·FB	-1.7E-03	2.9E-02	0.96
Weight fraction of BA-L in SMM (f_z)	**RMR**	**-8.9E-02**	**2.8E-02**	**0.01**
	RC	5.6E-02	2.8E-02	0.07
	FB	**9.8E-02**	**2.8E-02**	**0.01**
	RMR·RC	-5.4E-02	2.8E-02	0.07
	RMR·FB	2.4E-02	2.8E-02	0.41
	RC·FB	3.3E-02	2.8E-02	0.27

† The reaction concentration only affect the prepolymer reactant, since this is a two steps procedure. The value for BA-L was listed for completeness (see section 3.3.3).

‡ Variables which had a significant effect on a response are bold-faced.

* The standard error was calculated with respect to the 3 x 8 frequency of variables and is constant for all variables of a particular response.

Table 4 - 3 (Cont'd) : Effects on various responses due to changes in the reactant mole ratio (RMR) from 2:1:2 to 3:2:2, the prepolymer reactant concentration (RC) from 0.23:0.15 M (MDI:PPO) to 0.3:0.2 M (at RMR = 3:2:2) or from 0.15:0.075 M to 0.2:0.1 M (at RMR = 2:1:2)†; or the type of polyfluoroalcohol (FB) from BA-L Low to BA-L High.

Response	Variable	Mean Effect	Standard* Error	P-value
Weight fraction of MDI+PPO in SMM ($f_m + f_p$)	**Reactant mole ratio (RMR)**	**9.7E-02**	**2.5E-02**	**0.00**
	Prepolymer reactant concentration (RC)	**-5.2E-02**	**2.5E-02**	**0.05**
	Type of polyfluoroalcohol (FB)	-2.2E-02	2.5E-02	0.40
	RMR·RC	**5.5E-02**	**2.5E-02**	**0.04**
	RMR·FB	-4.2E-02	2.5E-02	0.11
	RC·FB	-2.0E-02	2.5E-02	0.44
Onset T_g (°C)	**RMR**	**-5.0E+00**	**1.8E+00**	**0.02**
	RC	8.0E-01	1.8E+00	0.66
	FB	1.5E+00	1.8E+00	0.44
	RMR·RC	2.0E-01	1.8E+00	0.93
	RMR·FB	8.0E-01	1.8E+00	0.67
	RC·FB	2.0E+00	1.8E+00	0.30
T_g width (°C)	RMR	-1.8E+00	2.8E+00	0.50
	RC	3.3E+00	2.8E+00	0.26
	FB	2.8E+00	2.8E+00	0.35
	RMR·RC	-2.5E+00	2.8E+00	0.40
	RMR·FB	-2.7E+00	2.8E+00	0.37
	RC·FB	4.2E+00	2.8E+00	0.16
Mid-point T_g (°C)	**RMR**	**-6.4E+00**	**1.5E+00**	**0.00**
	RC	2.6E+00	1.5E+00	0.10
	FB	**3.3E+00**	**1.5E+00**	**0.04**
	RMR·RC	-9.0E-01	1.5E+00	0.54
	RMR·FB	-6.0E-01	1.5E+00	0.70
	RC·FB	**4.4E+00**	**1.5E+00**	**0.01**
Apparent ΔCp at T_g (J/g.°C)	**RMR**	**7.0E-02**	**1.3E-02**	**0.00**
	RC	-8.3E-04	1.3E-02	0.95
	FB	**-3.4E-02**	**1.3E-02**	**0.02**
	RMR·RC	-1.1E-02	1.3E-02	0.44
	RMR·FB	1.3E-02	1.3E-02	0.37
	RC·FB	-1.8E-02	1.3E-02	0.21

† The reaction concentration only affect the prepolymer reactant, since this is a two steps procedure. The value for BA-L was listed for completeness (see section 3.3.3).

‡ Variables which had a significant effect on a response are bold-faced.

* The standard error was calculated with respect to the 3 x 8 frequency of variables and is constant for all variables of a particular response.

produced by a combination of two variables was also reported. The standard error of each response was estimated using all SMMs and is also reported. The fifth column in Table 4-3 contains the probability value (P-value) that the observed effect of a variable on a response was not caused by the increase in the variable as estimated by the analysis of variance. In Table 4-3, the significance level was set to be 95% or a P-value of 0.05 or less for the null hypothesis.

The weight average molecular weight (M_w) increased significantly (by 7.8E+3), when the reactant mole ratio (MDI/PPO/BA-L) was changed from 2:1:2 to 3:2:2. It also increased by 1.5E+3 with higher reactant concentration although not significantly. A significant change of 3.7E+3 in the M_w was observed when both RMR and RC were changed, signifying that the effect of RC was dependent on the value of RMR. The combined changes of RMR and FB; RC and FB decreased M_w by 5E+2 and 1.7E+2 respectively although not significantly.

For the number average molecular weight (M_n) the significance of the changes was similar to that for M_w. Changing the RMR significantly increased M_n by 4.4E+3. RC did not significantly affect M_n. Changing FB also increased M_n by 1.1E+3 but it was not significant. M_n increased by 1.5E+3 due to the combined effect of RMR and RC, and the dependency of the effect of RC on the value of RMR is again observed, whereas it was not significantly affected by RMR and FB. Combining the changes of RC and FB also did not significantly affect M_n.

The ratio of M_w/M_n or the polydispersity was not affected significantly by any of the experimental variables. This result agreed with that found from Table 4-1. Since most polymers including SMMs consist of a distribution of chain lengths, and the breadth of the distribution is reflected in the polydispersity (Rosen, 1982), it can be concluded that the SMMs synthesized for this study have a similar distribution. This result was predicted by Peebles (1974).

In summary, only the effect of the reactant mole ratio and the combined effect of the latter and the reactant concentration on the average molecular weights (M_w and M_n) are

significant (>95% of the time). The effect of the reactant mole ratio on the average molecular weight was predicted by theoretical analysis as discussed earlier in this section. Moreover, for the polymerization between MDI and PPO, Peebles's (1974b) models suggested that an increase in concentration of the reactant would increase the molecular weight. Therefore, one would expect that the combined effect of positively changing these two variables would yield a higher increase in molecular weight than either of the increases due to the individual variables. However, the increase in average molecular weight was smaller for the combined changes of RMR and RC than for that of RMR. In addition, the effect of the RC was shown to be insignificant by itself. These observations suggest that for the system under study, the effect of increasing the prepolymer reactant concentration limited the increase in average molecular weight introduced by the change in the reactant mole ratio. The reason for this effect is not clear at this time. In the mean time, the results in Table 4-3 suggested that the effect of RC was dependent on the value of RMR. The interaction of solvent can be ruled out as a possible factor in justifying the limiting effect of prepolymer reactant concentration since Wang and Lyman (1992) found that DMAC did not influence the reactivity of MDI/PPO.

The experimental variables studied in this work were anticipated to have an affect on the composition of a given SMM. From Table 4-3, it can be seen that the reactant mole ratio (RMR), the prepolymer reactant concentration (RC) and the type of polyfluoroalcohol (FB) and the combined variables had no significant effect on the weight fraction of incorporated MDI in an SMM (f_m) (i.e. all P-values >0.05). The theoretical prediction for f_m in Table 4-2 indicated that f_m would show relatively small changes compared to f_p. Considering that the changes reported in Table 4-2 would be approximately 0.03 while the standard error associated with this response (see Table 4-3) is 0.029, the insignificance of step changes for f_m come as no surprise. For the weight fraction of PPO incorporated in an SMM (f_p), only the RMR had a significant effect, whereas the RC, FB and all combinations of variables did not change f_p significantly (i.e. P-values > 0.05). The change in f_p produced by changing the RMR was 8.3E-2. The

theoretical prediction of the change of this value at constant RC and FB, was given in Table 4-2 to be 1.1E-1 and confirms the observed change.

For the weight fraction of BA-L in an SMM only the RMR and FB had significant effects, whereas RC and the combinations of variables showed no significant effects (i.e. P-value > 0.05). It was observed that f_z decreased by 8.9E-2 as the RMR was changed from 2:1:2 to 3:2:2, and it increased by 9.8E-2 as the FB was changed from BA-L Low to High. The effect of the RMR on f_z was expected since an increase in RMR would increase the prepolymer molecular weight and hence reduce f_z as shown in Table 4-2. The experimental value of 8.9E-2 compares moderately well with the predicted value of 1.35E-1 (about 66% of the expected value). Compared with the theoretical average increase due to a change from BA-L Low to High, the average change of f_z was 51% higher than anticipated (theoretical increase in f_z = 6.5E-2, Table 4-2). The change in f_z was expected due to the difference in weight fraction of the pure fluoroalcohol reactants, but the fact that it was higher than the anticipated value suggested that the main chain of the SMMs synthesized with BA-L High was on average shorter than those synthesized with BA-L Low. The exact reason for this can not be explained at this time.

The combined weight fraction of MDI and PPO components (f_m+f_p) is closely related to f_z. Interestingly, the combined weight fraction was affected by both RMR and RC, as well as the combination of these two factors. Changing the RMR augmented the sum f_m+f_p by 9.7E-2 which was 78% of the value calculated and given in Table 4-2. On the other hand, a higher RC significantly decreased f_m+f_p by 5.2E-2, and the combined change of RMR and RC significantly increased (f_m+f_p) by 5.5E-2. Since (f_m+f_p) is closely related to M_w and M_n, it was no surprise that the effect and dependency of RC on RMR were again seen here. Although it would be of interest to investigate the relation of these significant effects on (f_m+f_p) and f_z, the errors on these values are not known to certify if a close relationship indeed existed. In this regard, further discussion is not possible or even significant.

As to the decrease in f_z for a change from 2:1:2 to 3:2:2 at a higher reactant concentration, it is now unclear whether the change can be associated solely with the increase in the average molecular weights, as related to an increase in prepolymer size or was it due to the influences of other factors.

Table 4-3 shows the effect of the three experimental variables on the thermal properties of the SMMs. The onset T_g, T_g width, mid-point T_g and ΔCp, as described previously, are material properties; therefore, the effects observed will be related to the associated molecular variables. Only the reactant mole ratio (RMR) significantly affected the onset T_g, whereas other variables or combinations of variables had no significant effect. The change in the onset T_g of the material was -5.0°C with a change from 2:1:2 stoichiometry to a 3:2:2 stoichiometry. The significant variables on the mid-point T_g were the RMR, the type of polyfluoroalcohol (FB), and the combination of RC and FB, which produced average changes of -6.4, 3.3 and 4.4°C respectively. One can see here that the effect of RC was dependent on FB (significant only at FB = High). The effect of RMR on the onset and mid-point T_g values was expected, since the RMR increased both the molecular weight of the SMM and the corresponding weight fraction of PPO component (f_p). PPO is the soft-segment in the SMM and acts as an internal plasticizer to reduce T_g values (Turi, 1981). The effect of PPO is further supported by the fact that the combination of RMR and RC did not decrease the T_g values even with an increase in the average molecular weight, since it did not significantly affect the f_p (Table 4-3). The effect of FB on the mid-point T_g could be associated with the decrease in f_p, but this is unlikely since FB did not have a significant effect on f_p. However, it could be associated with an increase in f_z. The effect of RC and FB produced a significant increase of 4.2° C in mid-point T_g. If f_z is a significant determinant for increasing the mid-point T_g then increasing RC, which is related with an increase in f_z, will be expected to show an increase in T_g as well.

Table 4-3 showed that ΔCp significantly increased by 0.07 J/g.° C on changing the RMR from 2:1:2 to 3:2:2, and by -0.034 J/g.° C on changing the FB from BA-L Low to

BA-L High. Other variables and combinations did not significantly affect ΔCp. Finally, T_g width was not significantly changed by any of the variables studied.

In general, T_g has been documented to decrease with a decreasing molecular weight and has a closer linear relationship with M_n than with M_w (Turi, 1981). The relationship between the SMM mid-point T_g values and their relative number average molecular weight (M_n) is shown in Figure 4-1. Without the anomalous points which did not follow the general trend, it was observed that T_g decreased with increasing M_n. In this work, the heterogeneous nature of the components contributes to the decrease in T_g with increasing molecular weights. This occurs as a result of the increase in the internal plasticizing effect associated with the incorporation of more PPO segment (Turi, 1981).

Linear regression analysis (without anomalous point) showed that SMMs with the BA-L High had a steeper decrease in mid-point T_g with respect to M_n (slope = -2.9E-3, slope @ lower 95% confidence = -4.2E-3, slope @ upper 95% confidence = -1.59E-3, P-value = 6.1E-4) than those synthesized with BA-L Low(slope = -1.5E-3, slope @ lower 95% confidence = -2.1E-3, slope @ upper 95% confidence = -9.1E-4, P-value = 1.67E-4)). This suggested that the length of the polyfluoroalcohol had a negative effect on the cohesiveness of the system similarly to what has been found in other systems (Danusso et al., 1993). This result was expected since the longer polyfluoroalcohol ends would induce more mobility. However, more data in future studies are needed to see whether the anomalous points have been justifiably removed, and whether the above conclusion remains valid.

4.2 Characteristics of SMMs in PES/SMM mixtures

In order to gain an understanding of how the SMM affects the material properties of PES, a series of characterization experiments were carried out which include the effect of the SMM on the bulk material property, T_g, and the surface chemistry/energetics of the blend material using XPS and sessile drop contact angle methods. As well, a qualitative analysis of PES/SMM solution behaviour and film formation is provided.

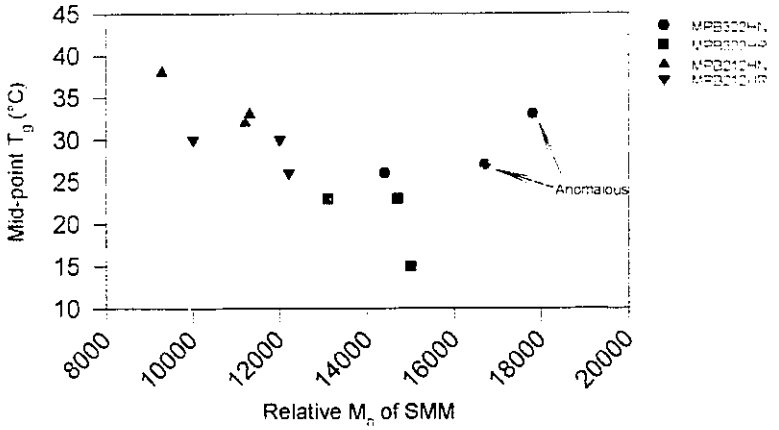

(a)

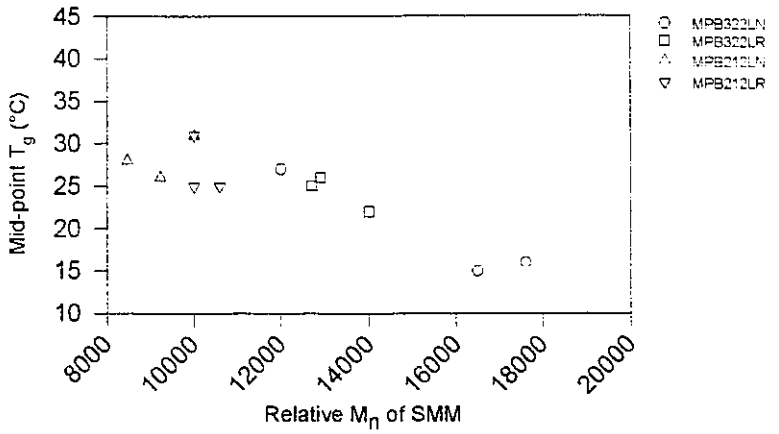

(b)

Figure 4 - 1 : Effect of relative number average molecular weight (M_n) on the mid-point T_g of SMMs synthesized with (a) BA-L High and (b) BA-L Low.

4.2.1 PES/SMM solution behaviour

Before an SMM can be tested in a pervaporation membrane, its behaviour with respect to membrane processing methods must be studied. The miscibility of one polymer into another has been shown to be rare (see general discussion in section 2.2). Even when a common solvent is added (one that is indefinitely soluble with each of the polymeric constituents alone), two polymers usually cannot coexist in a homogenous solution beyond a few percent concentration. A schematic phase diagram for such a system is shown in Figure 4-2 (Rosen, 1982). Beyond a few percent of polymer (the exact value depends on the chemical nature of the polymers and solvent and the molecular weight of polymers), two phases in equilibrium are formed, each phase containing nearly pure polymer (Rosen, 1982). In the case of pervaporation membrane formation, a homogenous phase in solution is crucial, since various membrane making techniques require this criterion in the casting of thin films (Kesting, 1971).

It was beyond the scope of this work to generate complete phase diagrams for PES and all of the SMMs. Instead, a fixed concentration of PES at 25 wt.% was used to study solution effects, since this was the intended concentration to be used in the preliminary performance testing of the pervaporation membranes (Fang et al., 1994). The solvent used for preparing the solutions was DMAC, and two distinct batches of SMM for each formulation were prepared for the work. The selected polymers included the SMM with the lowest and highest measured average molecular weight for a particular formulation.

The solution appearance for various PES/SMM/DMAC mixtures are listed in Table 4-4. An SMM was referred to by its formula name (see Table 4-1), and by the batch synthesis number in brackets (e.g. MPB322HN(1)). The solution appearance was recorded after the solution mixtures were allowed to stand for two days at controlled temperature (25° C). There were three observable states: clear solution, cloudy but only one phase and two phases. Phase separation was identified as either cloudy or observed two phases.

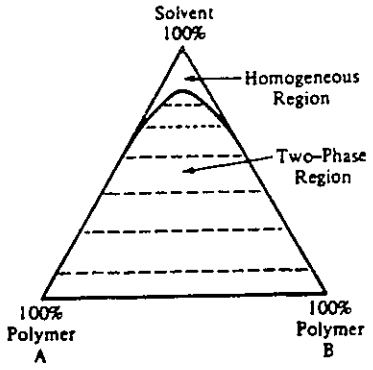

Figure 4 - 2 : Typical phase diagram of polymer/polymer/solvent. Adapted from Rosen(1982)

For practical purposes, it is desired that the homogenous region (Figure 4-2) of a given PES/SMM/DMAC system be as large as possible. On average, the order of phase behaviour from bad to good for the range of concentrations studied was MPB322HN < MPB322LN < MPB212HN < MPB322LR < MPB322HR = MPB212HR = MPB212LN = MPB212LR. This trend was consistent for both batches of the eight formulations. As the results suggest, it was inconclusive as to which of the experimental variables studied in the synthesis of these SMMs had an effect on solution phase behaviour. In general, the SMMs synthesized with the 2:1:2 mole ratio seemed to have better phase behaviour than those synthesized with the 3:2:2 ratio (75% of the times). It can be concluded then that the reactant mole ratio (RMR) had some effect on the phase behaviour of SMMs. Evidently, more experiments will be needed to confirm this at a better confidence level.

As discussed before, the RMR significantly affected the average molecular weight, the weight fraction of PPO (f_p) and the weight fraction of BA-L in the SMM (f_z). All of these properties can influence solution behaviour. However, it was seen that the type of BA-L did not have any clear effect on the phase behaviour within this SMM concentration range. Since the weight fraction of MDI in SMM (f_m) was not significantly affected by the RMR, it could be concluded that the effect of the RMR on phase behaviour was due mainly to the weight fraction of PPO in the SMM.

Table 4 - 4 : Solution appearance of PES/ SMM blends at various concentration of SMM in solution. The wt.% of PES was kept at 25, and the solvent was DMAC. Legend: 0 = clear solution; 1 = cloudy, one phase; 2 = two phases.

SMM	Solution apprearance when mixed with PES		
	Concentration of SMM (wt.%)		
	0.5	1.0	2.0
MPB322HN(1)	0	1	1
MPB322HN(3)	1	1	2
MPB322HR(2)	0	0	0
MPB322HR(3)	0	0	0
MPB212HN(2)	0	0	1
MPB212HN(3)	0	0	1
MPB212HR(1)	0	0	0
MPB212HR(2)	0	0	0
MPB322LN(2)	0	1	2
MPB322LN(3)	0	1	1
MPB322LR(1)	0	0	0
MPB322LR(2)	0	0	1
MPB212LN(2)	0	0	0
MPB212LN(3)	0	0	0
MPB212LR(2)	0	0	0
MPB212LR(3)	0	0	0

4.2.2 The thermal properties of cast PES/SMM films and the miscibility film components

For solutions which did not separate into two distinct phases, films were prepared and characterized by differential scanning calorimetry (onset T_g, T_g width, mid-point T_g and change in specific heat capacity at T_g). To simulate as much as possible the conditions at which solutions would be used in the preliminary membrane testing (Fang et al., 1994), the solutions were cast on glass slides, followed by solvent evaporation in a dry air circulating oven at 110°C for 15 min, at which time solid surfaces were formed. After further drying as described in section 3.4.2, the appearance of these films was recorded. The results are presented in Table 4-5. The films obtained were qualified according to optical characteristics (opaque or transparent), surface patterns and differences in morphology. The classification for the films were (i) uniform if the surface was smooth and had no distinguishable feature; (ii) as somewhat uniform if it was smooth, but had some kind of pattern; and (iii) phase separated if distinct phases were visually observed.

As has been indicated by Krause (1978) and Paul (1993), the transition of apparently miscible polymer-polymer mixtures from a ternary state with solvent to a binary one with only polymers can be unpredictable. The solvent type can mislead the results, since binary polymer mixtures can be immiscible, although their ternary compositions showed otherwise (Krause, 1978). Miscible polymer pairs are usually optically transparent and show only one intermediate T_g for all compositions (Krause, 1982). Exceptions arise when the refractive indexes or the T_g values of the two polymers are close (Krause, 1982). The results in Table 4-5 showed that all PES/SMM mixtures were immiscible, at least by the optical criterion. Similarly to the situation with the ternary solution, the ability of a given SMM to yield a single macroscopic phase across the concentration was of interest, since films with distinct morphological regions would not be practical for pervaporation membrane applications. Therefore, a good SMM would have a slow morphological change with increasing concentration. Based on this criterion, the order of the degree of phase separation of SMMs was classified from bad to good as MPB322HN = MPB212HN < MPB212LN < MPB212HR = MPB212LR < MPB322LN < MPB322LR

Table 4 - 5 : Film appearance of PES/ SMM blends at various concentration of SMM in casting solution. The concentration of PES in solution was fixed at 25 wt.%, and the solvent was DMAC. Legend: 00 ≡ Transparent; 0 ≡ Opaque, white and uniform; 1 ≡ Opaque, white and somewhat uniform; 2 ≡ Phase separated; N/A ≡ not applicable due to phase separation of solution.

SMM	Film apprearance when mixed with PES		
	Concentration of SMM (wt.%) in casting solution		
	0.5	1.0	2.0
MPB322HN(1)	0	1	2
MPB322HN(3)	1	1	N/A
MPB322HR(2)	0	0	0
MPB322HR(3)	0	0	0
MPB212HN(2)	1	1	2
MPB212HN(3)	1	1	2
MPB212HR(1)	0	0	0
MPB212HR(2)	0	1	1
MPB322LN(2)	0	0	N/A
MPB322LN(3)	0	0	0
MPB322LR(1)	0	0	2
MPB322LR(2)	0	0	0
MPB212LN(2)	0	1	1
MPB212LN(3)	0	1	1
MPB212LR(2)	0	0	0
MPB212LR(3)	0	0	0

< MPB322HR. A similar behaviour between the two batches for a given SMM formulation was again observed. However, it must be emphasized that these results are only based on qualitative visual inspection and should not be used to draw definite conclusions.

The general morphology of immiscible and partially miscible systems has been noted as being spherical domains of one material within the rich phase of the other material (Piirma, 1992). The spherical shape is due to the interfacial phenomena between the two materials (Andrade, 1985; Gibbs, 1928). The size and number of these domains depend on the specific surface energies of the materials and also on the molecular weights (Piirma, 1992; Andrade, 1985; Burns and Kim, 1988). Although there is a lack of pictorial support at the micron level, the opaqueness and surface patterns associated with the films can be somewhat proof to the existence of these domains.

From the results, it was inconclusive as to which experimental variable and its associated molecular characteristics determined the degree of phase separation in the binary polymers. However, there were trends associated with the reactant mole ratio (RMR), the type of polyfluoroalcohol (FB) and the prepolymer reactant concentration (RC). It was interesting to note that in general a RMR of 2:1:2 yielded less phase separation. This observation was directly opposite to the observed trend for the solution phase. SMMs synthesized with BA-L Low also seemed to reduce the phase separation, and those synthesized with a reduced reactant concentration also seemed to have a similar effect. It was impossible to detect a combination of effects based on available results; therefore, only single variables were considered.

From the previous discussion (section 4.1), it was found that the RMR affected the average molecular weight, the weight fraction of PPO and BA-L in SMM (f_p and $f_=$), and that the FB only affected $f_=$, whereas the RC by itself did not have any significant effect on any of the studied molecular variables. Since the weight fraction of MDI was not affected significantly by any of the three experimental variables, it can be concluded that

the observed trends relating RMR to phase separation are due mainly to the PPO portion of the SMM.

With the current results, it can be suggested that the observed trends relating FB to phase separation were due to both a reduction in f_z (contributing to a change in overall average molecular weight) and a change in the type of the hydrophobic polyfluoroalcohol. The trend associated with the reactant concentration, cannot be rationalized with the current data.

As discussed previously in section 2.2, polymers phase-separate as a rule rather than an exception. According to Paul (1993), increased miscibility results from a specific interaction between polymer strains (species) to lower the energy of mixing. Some of these interactions include hydrogen bonding, electron donor-acceptor groups and primary bonding between reactive groups of the two polymers (Paul, 1993). According to the theoretical structure of the SMM (Figure 3-1a) and that of PES (Figure 3-1b), pseudo-hydrogen bonds between strong donor groups of PES such as ether and sulfonyl and the SMM hydrogens can contribute to this specific interaction.

The negative influence of the PPO groups of the SMM on the formation of a homogenous solution phase was discussed in section 4.2.1. When the solvent phase has been removed, the opposite trend is observed. This opposite effect on phase separation behaviour could be explained through the lower cohesiveness of molecules associated with high molecular weight SMM material (i.e. polymers synthesized with a 3:2:2 have a higher molecular weight than those with a 2:1:2 stoichiometry, see Table 4-1). Since phase formation depends on the magnitude of the tendency for each material to be with each other, a lowering of this tendency (i.e. lower cohesiveness) may produce a smaller phase for the SMM material (Rosen, 1982, Krause, 1978) and therefore yielding a reduction in the size of the separated domain associated with phase separation. However, the hypothesis of lower cohesiveness alone is insufficient, since SMM synthesized with BA-L High have also been associated with a decrease in the cohesiveness (see the discussion on T_g and molecular weight in section 4.1), yet less phase separation was

observed with SMMs synthesized using BA-L Low. Further investigations directed towards evaluating the distribution of SMM within the PES material will be required to pursue this discussion much further.

The miscibility of polymer systems can be detected by measuring its T_g (see section 2.2). A single T_g value for the blend is an indication of miscibility (section 2.2.1). To study the miscibility of SMMs and PES, the thermal analysis of random samples cut from uniform and somewhat-uniform films were performed. The mid-point T_g, the T_g width and change in specific heat capacity at the T_g (ΔCp) of the blends were recorded. These data are tabulated in Table C-2, Appendix C. The results for the mid-point T_g are illustrated in Figure 4-3 with a deviation due to instrumentation of $\pm 1°C$. Since the observations recorded in Table 4-5 indicated that none of the films were transparent, it was expected to find two T_g values. However, only one T_g was observed for the blends. Apparently, the transitions for the SMMs were not readily detected due to the sensitivity of the instrument. This difficulty in measuring the second transition at low concentrations was also reported by Burns and Kim (1988). The mid-point T_g values for the blends were those of a PES rich phase but were lower than that of the pure PES which was recorded at 220°C (this T_g value for pure PES was also reported by Xu et al., 1991). There were no statistical differences among the behaviour of PES/SMM blends for the three concentrations of SMM, indicating the DSC's lack of sensitivity to quantity and distribution of SMM in the polymer.

The width of the transition region has previously been associated with microheterogeneity of the material (Cortázar et. al., 1987). The normal T_g width of a pure material is due to its heterogeneity index (Turi, 1981). As Figure 4-4 indicated, the PES/SMM blends have higher heterogeneity than the pure PES material (almost double). This was expected due to the effect of phase separation. There was no distinguishable trends among the blends therefore suggesting a similar behaviour.

The study of phase behaviour within the solid phase is much more difficult than in dilute solution (Krause, 1982). Nevertheless, a study of the PES-rich state of blends is of

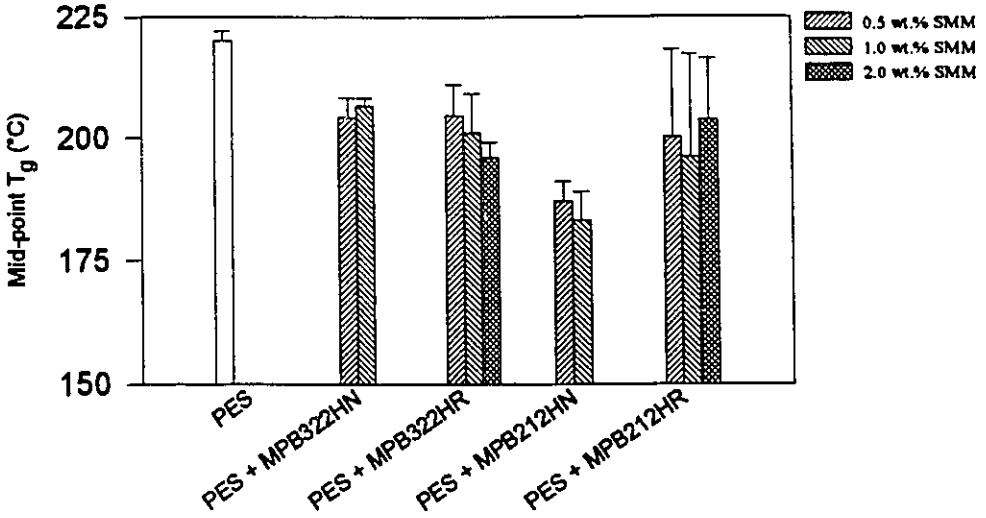

(a)

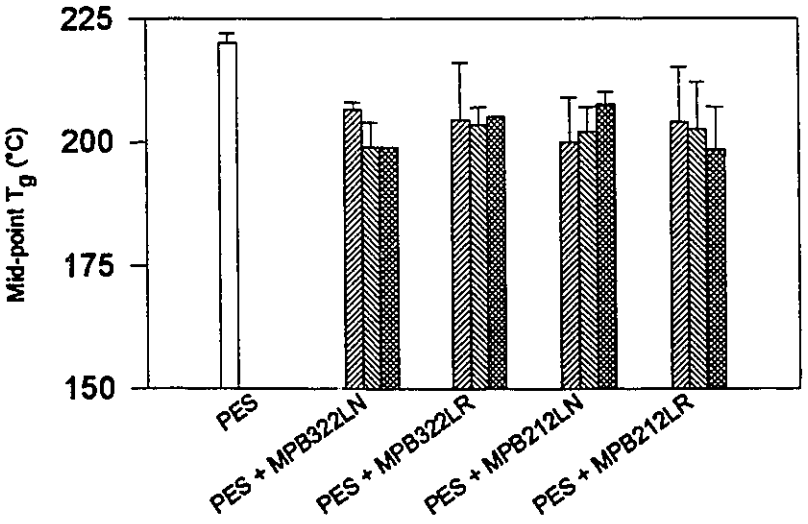

(b)

Figure 4 - 3 : Average mid-point T_g of PES and PES/SMM blends (with standard error) for SMMs synthesized with (a) BA-L High and (b) BA-L Low.

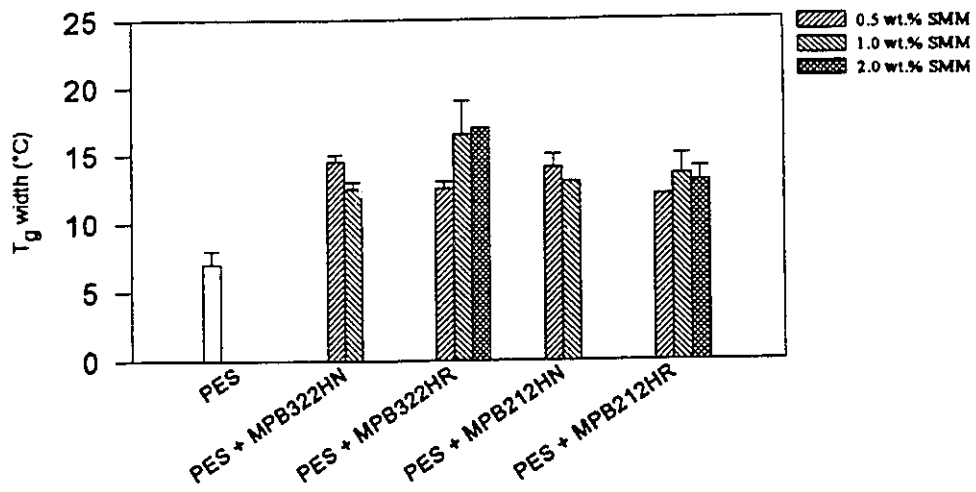

(a)

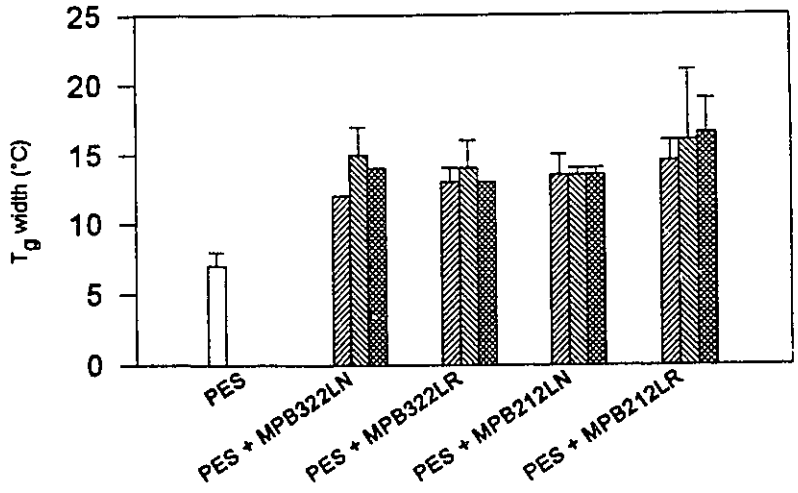

(b)

Figure 4 - 4 : Average T_g width of PES and PES/ SMM blends(with standard error) for SMMs synthesized with (a) BA-L High and (b) BA-L Low.

primary interest to this work, since the SMM was intended to be used as an additive and therefore requiring only small amounts of material to be blended with PES (< 10 w/w). Hence a blend with clear phase distinction was not a criteria for these membranes. Burns and Kim (1988) had suggested after a series of studies that a decrease in the change of specific heat capacity at T_g for the rich phase polymer component with an increase in the concentration of the poorer phase component was an indication of partial miscibility. As illustrated in Figure 4-5, only PES/MPB212HR, PES/MPB322LR exhibited degrees of partial miscibility with some confidence (with the given standard errors), whereas a clear immiscibility was observed with the rest of the blends. How this apparent partial miscibility influences solution behaviour and solid phase behaviour was not readily known due to the lack of complete phase diagrams.

In summary, only trends could be reported on the solution and solid phase behaviour of blends. This limit of certainty was due to three factors: (i) the qualitative nature of the results, (ii) the concentration range chosen which was large (i.e. 0.5 - 2 wt.%) and (iii) the level of the step change chosen which possibly was not sufficient to create 95% or more level of confidence. More detailed studies with dilute solution would yield additional information allowing the differentiation and confirmation of the general trends. As for the thermal data of the blends, the low concentration of SMMs made the determination of an SMM rich phase impossible. However, the change in specific heat capacity at the T_g for the blends indicated that most of the SMM systems were immiscible with PES, while a few were partially miscible. The statistical similarity of behaviour for the blends suggests that all the SMMs behave in a similar manner in terms of influencing the mid-point T_g of the PES-rich phase and the width of the transition.

4.2.3 PES/SMM surface characterization by XPS

As discussed before in section 2.1, the effect of the surface active additive on interfacial phenomena will most likely lead the SMM materials to concentrate at the top most layer of the membrane surface. X-rays photoelectron spectroscopy (XPS) (method summarized in section 3.4.4) is a popular tool for the study of chemical composition and structure within the top 100 Å of the surface. In this work, the surfaces of PES/SMM

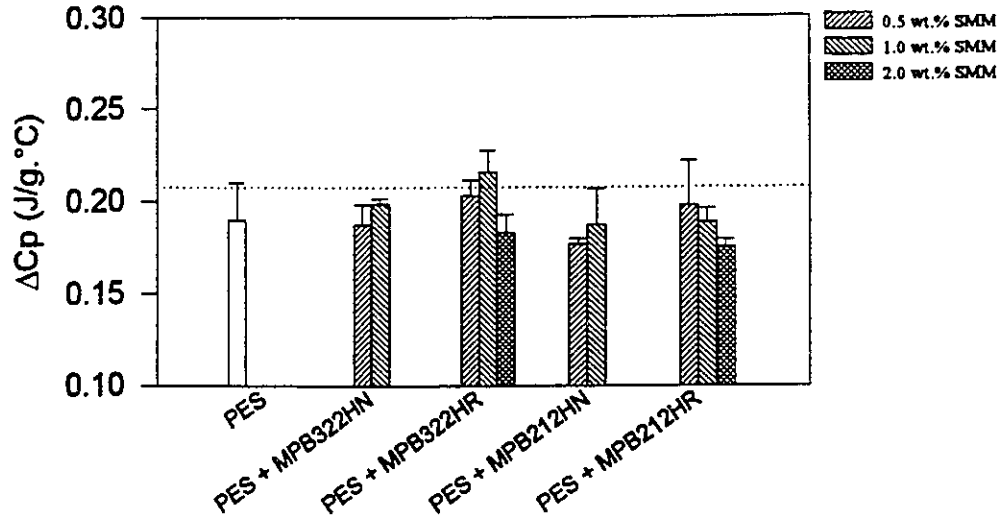

(a)

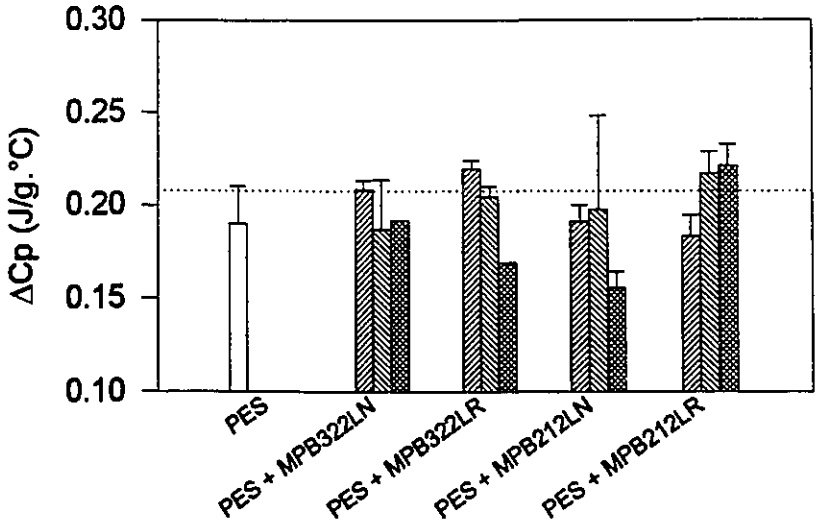

(b)

Figure 4 - 5 : Change in specific heat capacity at T_g (ΔCp) for blends of PES and SMM (with standard error) for blends with SMMs synthesized with (a) BA-L High and (b) BA-L Low.

films prepared with PES and MPB322HN, MPB322LN, MPB212HN and MPB212LN were studied using films from solutions of 0.5, 1.0 and 2.0 wt.% SMM. The sample selection was limited to these four formulations due to the high cost of sample analysis. In the case of MPB322HN and MPB212HN the films at 2.0 wt.% SMM were phase separated samples. The purpose of using the latter samples was to determine if there would be a difference in surface composition when the phase separation phenomenon occurred. As mentioned in section 3.4.4, the spatial resolution of XPS is very limited, which means that there can be large uncertainties associated with extending the results obtained for a particular 'spot' studied by XPS to another area. In the case of homogeneous polymers or high molecular weight copolymers, a certain macroscopic homogeneity can be assumed to be valid (Clark, 1971). In this work however, this is no longer valid because of the heterogeneous nature of the system. Therefore, a certain confidence level was assured by using two separately cast films for each synthesis batch of a given SMM, at a given concentration. The errors obtained will be associated with error due to film casting as well as variation due to the differences in polymer batch synthesis for a given SMM. Two random XPS 'spots' were analyzed on each film surface. In total, four XPS 'spots' were carried out at each concentration of SMM, and these values were used to represent the average observations for each SMM. The XPS sampling was performed at two take-off angles: 15° and 90°. The technique to achieve these angles has been illustrated in section 3.4.4. Briefly, the data obtained at 15° represent the chemical composition of approximately the top 2 nm of the surface, whereas the information collected at 90° is associated with approximately the material top 10 nm (Andrade, 1985).

The elements fluorine and nitrogen are only associated with the SMMs while the element S is only found in PES. The ratio F/C is indicative of the SMM's polyfluoro-segment, whereas the ratio N/C is indicative of the main SMM's chain. The quantity S/C is indicative of PES. The high resolution data from XPS provided information on PES/SMM composition through five ratios: C-O-C/C-C (number of ether group, from SMM and PES), N-COO/C-C (number of amide group, from SMM), $-CF_2-$/C-C,

$-CF_3$/C-C (from SMM's polyfluoro-segment) and $-CF_2-/-CF_3$ (a degree of orientation of the polyfluoro-segment). The C-O-C/C-C ratio was not quantitatively useful due to the fact that C-O-C bonds were present in both the SMM and the PES polymers. Therefore, it was omitted from the following discussion. It must be noted that the association of binding energy shift to identify chemical bonds is highly subjective because there could be several shifts which identify the same chemical group (Feast and Munro, 1987; Robinson, 1991). Tabulated average results of low and high resolution data, a typical high resolution spectrogram of a sample from this work and a list of associated identifications and references can be found in Appendix D.

From the results obtained (Figures 4-6 to 4-12), it was difficult to detect significant differences among the surface of blends of PES and each of the four SMMs. The increase in SMM concentration increased the degree of variation and offered no new information. This suggests either that the blends' surfaces were heterogeneous or the thickness of the SMM layers were non homogeneous. While there was no significant differences observed between the chemistry of the various PES/SMM mixtures and between the 90° and 15° XPS layers, the data did show trends of differences in composition between the XPS layers studied. For the case of the S/C ratio, there were decreases from the 10 nm to the 2 nm layer, suggesting a decrease in PES presence at the surface (Figure 4-6). Moreover, the theoretical S/C ratio calculated based on the chemical structure of the PES repeating unit was 0.08, which was significantly larger than the values measured for both take off angles.

The decrease in the presence of PES was accompanied by an enrichment of SMM toward the surfaces and particularly the polyfluoro-ends as shown by Figure (4-7) and supported by the trends of the high resolution data shown in Figures 4-8 to 4-10. The average F/C ratios determined by elemental analysis for the pure SMM (Guelph Chemical Laboratories for MPB322HN, MPB212HN, MPB322LN and MPB212LN) were 0.24, 0.38, 0.10 and 0.3 respectively (Table B-1, Appendix B). Figure 4-7 shows that the average values obtained by XPS were comparable suggesting that the surface is

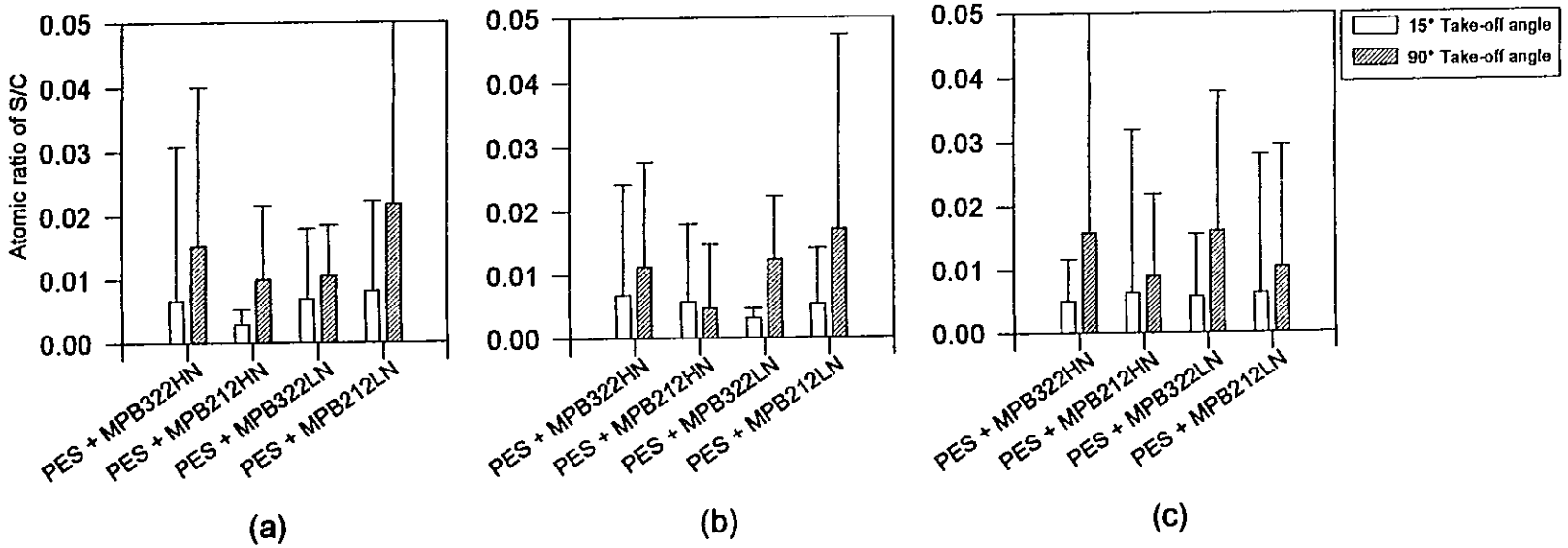

Figure 4 - 6: XPS composition of atomic sulfur with respect to atomic carbon for (a) 0.5, (b) 1.0 and (c) 2.0 wt.% of SMM in casting solution at two take off angles.

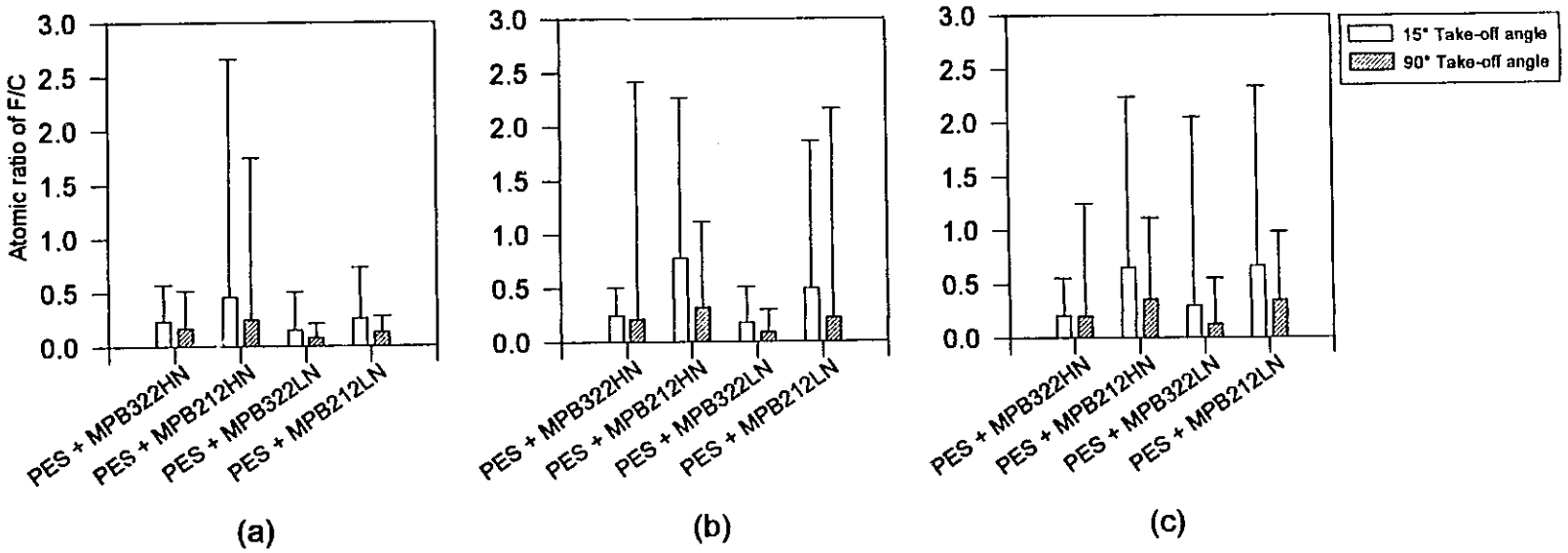

Figure 4 - 7: XPS composition of atomic fluorine with respect to atomic carbon for (a) 0.5, (b) 1.0 and (c) 2.0 wt.% of SMM in casting solution at two take off angles.

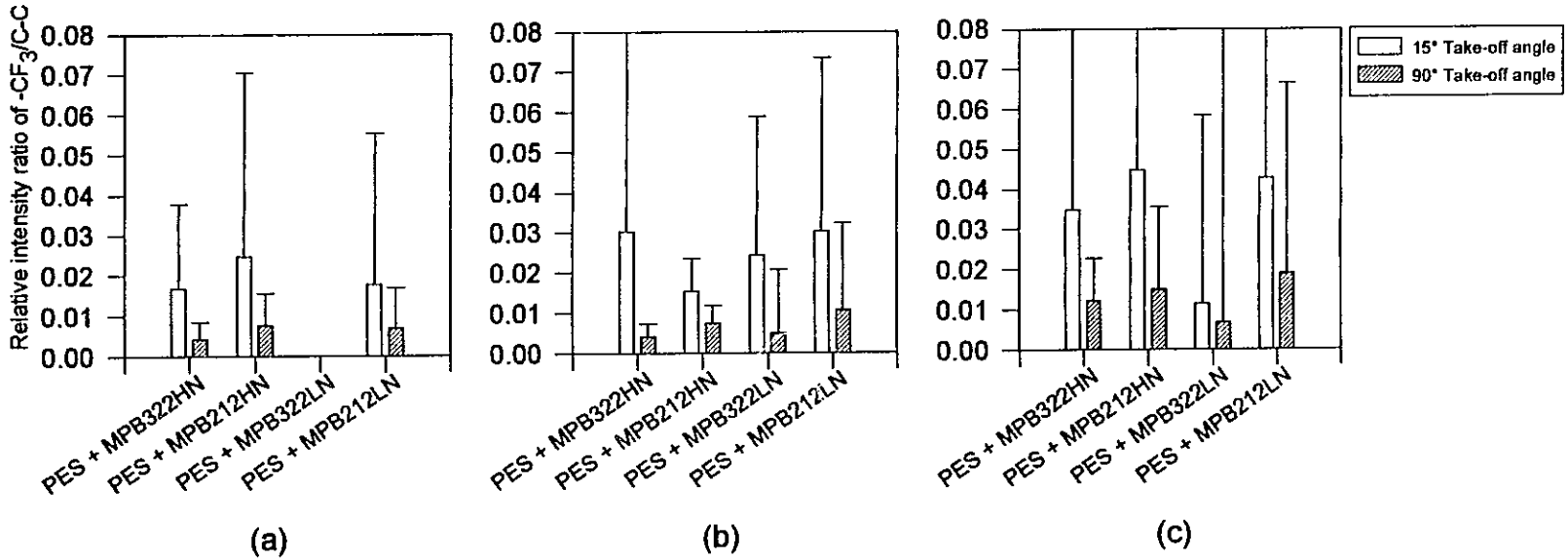

Figure 4 - 8: XPS composition of -CF_3 group with respect to C-C for (a) 0.5, (b) 1.0 and (c) 2.0 wt.% of SMM in casting solution at two take off angles.

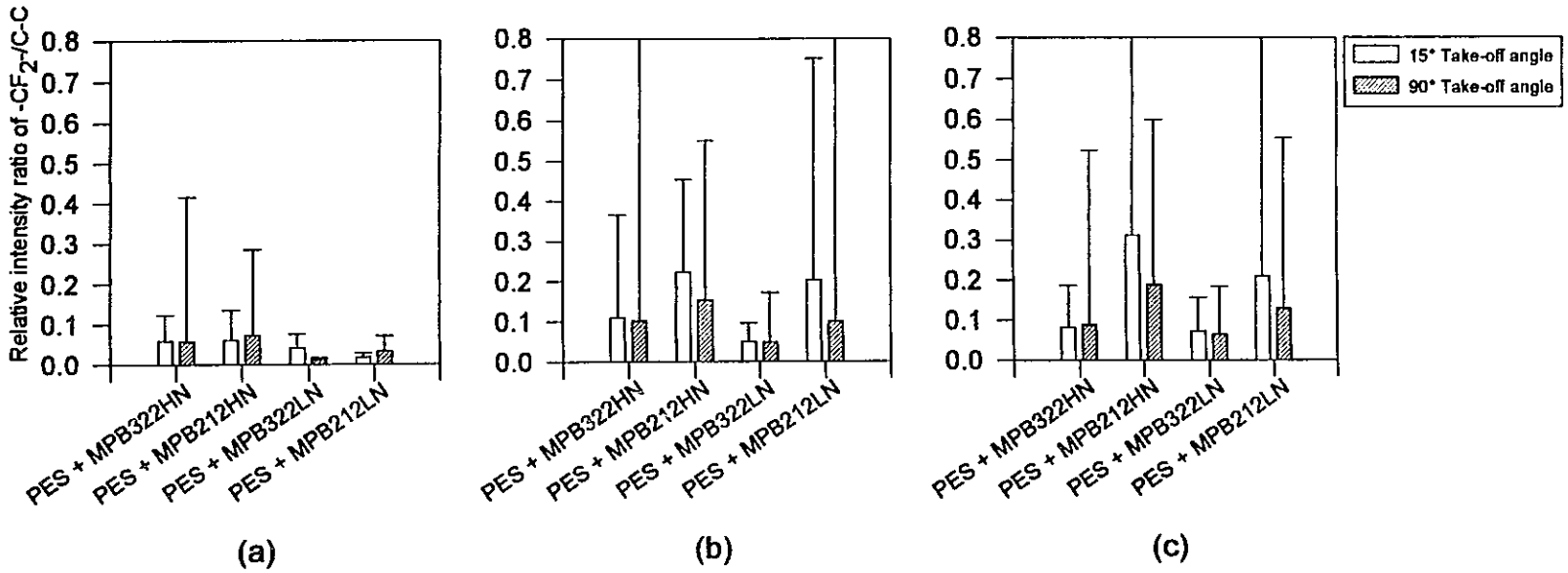

Figure 4 - 9: XPS composition of $-CF_2-$ group with respect to C-C for (a) 0.5, (b) 1.0 and (c) 2.0 wt.% of SMM in casting solution at two take-off angles.

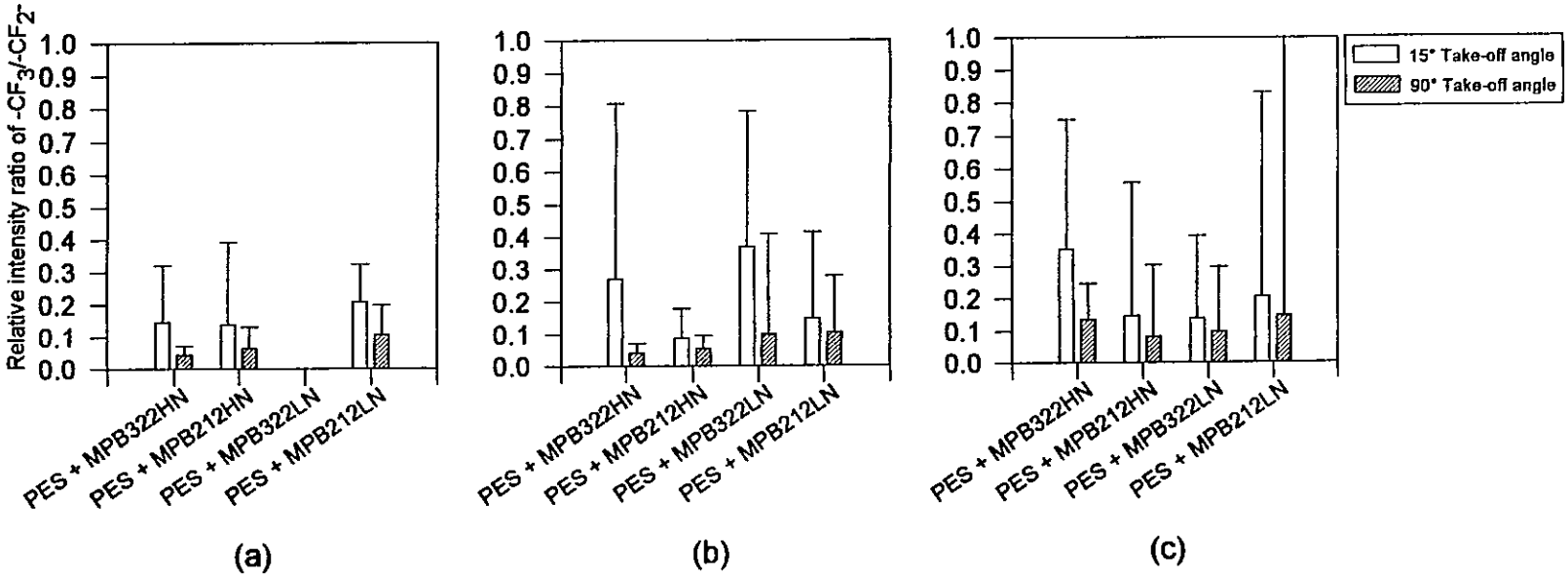

Figure 4 - 10: XPS composition of $-CF_3$ group with respect to $-CF_2-$ for (a) 0.5, (b) 1.0 and (c) 2.0 wt.% of SMM in casting solution at two take off angles.

composed of almost 100% SMM. The data in Figure 4-7 also show that there are trend of increases of the F/C ratio from 10 to 2 nm layer (i.e. from 90° to 15° take-off angle). Furthermore, the number of $-CF_3$ and $-CF_2-$ groups (Figure 4-8 and 4-9) as well as the ratio $-CF_3/-CF_2-$ (Figure 4-10) also indicate similar trends of increasing fluoro-segment content toward the surface.

The results in Figures 4-8 and 4-9 imply that the orientation of these polyfluoro-ends is predominantly toward the surface while the main chain(s) of the SMMs is (are) located relatively deeper away from it. This is supported by the trends in Figures 4-9 to 4-12. Figure 4-10 showed a relative decrease of $-CF_2-$ groups at the upper surface as compared to $-CF_3$ group, while Figure 4-11 indicates that the N/C ratios were higher at 90° as compared to 15°. Similarly, the number of amide bonds associated with SMM also correspondingly decreased toward the surface (Figure 4-12). The observed orientation of the polyfluoro-segment rationalizes the values for the F/C ratio which were larger than those of the pure SMM itself (Figure 4-7). It should be noted that the N/C ratios for the pure SMMs (determined by Guelph Chemical Laboratories) are 0.07, 0.08, 0.09 and 0.08 for MPB322HN, MPB212HN, MPB322LN and MPB212LN, respectively. Hence, the average values reported in Figure 4-11 were representative of pure SMM. The results illustrated in Figure 4-11 again confirm that the SMM chemistry dominated the surface's composition. Together, these results clearly show that the SMM materials have successfully migrated to the PES surface.

The fact that there were no significant differences among the SMMs and the layers studied is perhaps no surprise. Ward et al. (1984) have stated without proof that it would take little surface active material to saturate a surface. This was shown experimentally in the works of Kasemura et al. (1993) for modified epoxy resins. The results in Table 4-4 and 4-5 for PES/MPB322HN and PES/MPB322LN surfaces (at 2.0 wt.% of SMM in casting solution) for which phase separation was observed indicates the limitation of XPS in this type of system. In this case, the XPS technique could not differentiate between the surface of a visually homogeneous film and that of a completely phase separated film. It

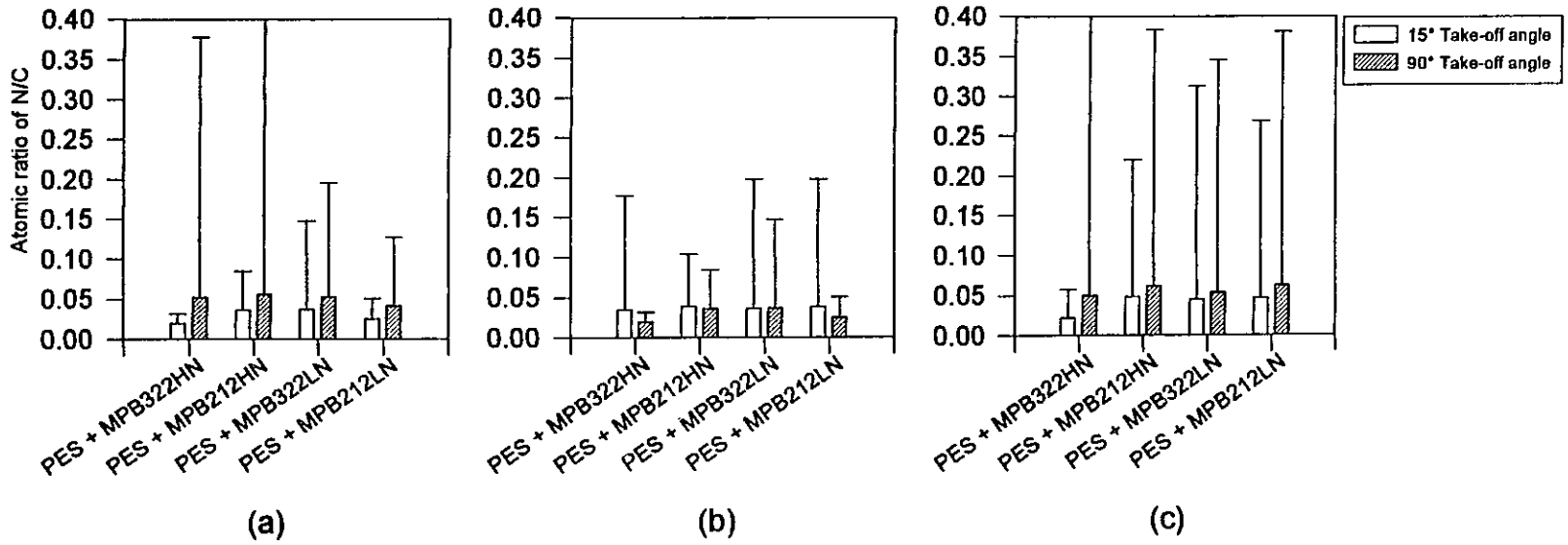

Figure 4 - 11: XPS composition of atomic nitrogen with respect to atomic carbon for (a) 0.5, (b) 1.0 and (c) 2.0 wt.% of SMM in casting solution at two take-off angles.

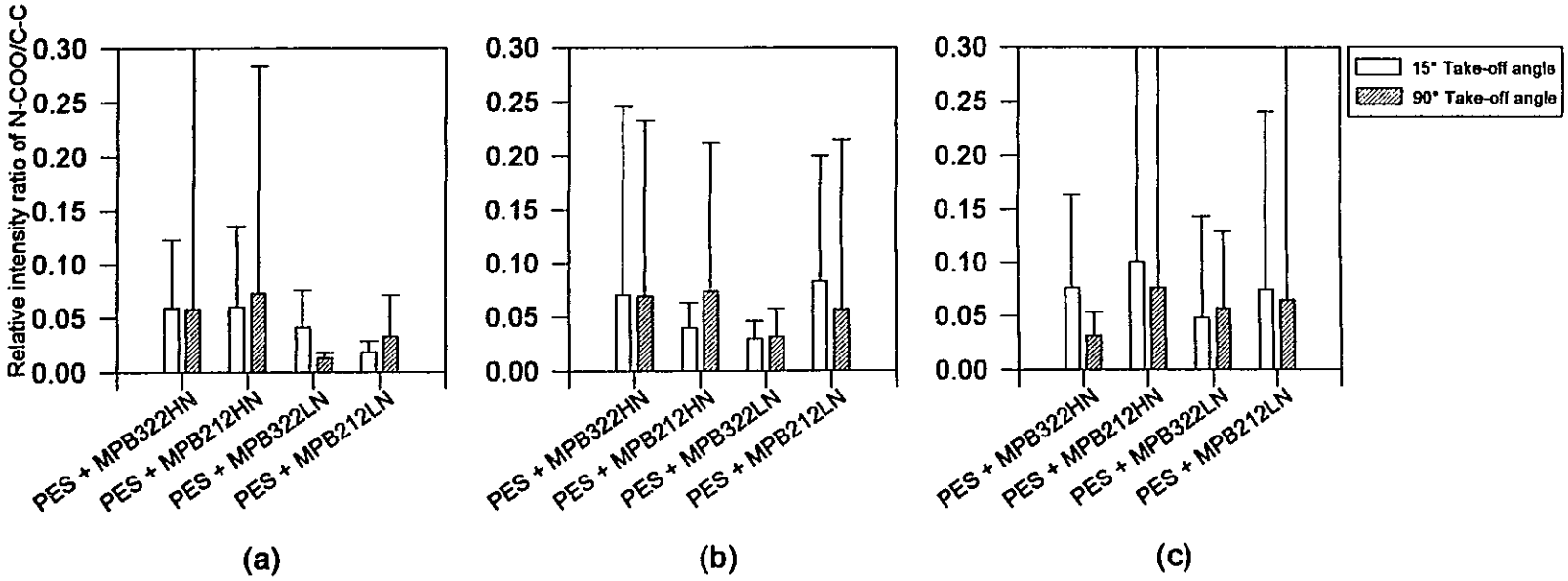

Figure 4 - 12: XPS composition of N-COO group with respect to C-C for (a) 0.5, (b) 1.0 and (c) 2.0 wt.% of SMM in casting solution at two take-off angles.

can be hypothesized that the composition of the XPS characterized layer and the phenomena which lead to its formation occurred before a bulk phenomenon such as phase-separation. This would imply that a very thin layer can exist throughout the film, eventhough phase separation is observed.

4.2.4 Surface energetics of PES/SMM materials

The hypothesis of this thesis is that the SMM can enhance membrane pervaporation separation performance by modifying the surface energetics of the material in which it is dispersed (i.e. to make the surface of the resulting material hydrophobic). The concentration of the SMM at the polymer-air interface has been provided by XPS results. However, XPS has limited lateral resolution (~200 μm, Clark, 1971); therefore, a measure of the contact angles for the modified surface would provide further evidence that this surface accumulation has occurred and the spatial extent of this modification is sufficiently large (through random sampling of the surface). The contact angle is a common measure of wettability. Correctly applied, it provides information regarding the surface energetics, surface roughness, surface heterogeneity and surface dynamics.

A surface is highly wettable by a given liquid if the contact angles are low. In this work, water was used as tested liquid to provide a direct measure of hydrophobicity. The average advancing contact angle (θ_{adv}) for the PES/SMM surfaces with the eight SMMs are shown in Figure 4-13, whereas their average receding angle (θ_{rec}) are plotted in Figure 4-14. In general, the contact angles increase with increasing concentration of SMM as expected (except for PES/MPB322HN's θ_{adv}, where a saturation is observed at 0.5 wt.% SMM). The surface of PES containing SMM synthesized with BA-L High had generally higher contact angles (θ_{adv} and θ_{rec}) values than those containing SMM synthesized with BA-L Low. The polymer systems which have achieved θ_{adv} values close to that of poly(tetrafluoroethylene) (PTFE, Teflon™) were PES/MPB322HN, PES/MPB212HN, PES/MPB212HR and PES/MPB212LN (the water θ_{adv} of Teflon is 116°, (Brandrup and Immergut, 1982)). On the other hand, the highest average values of receding angles of these same systems was not as close to the value of pure Teflon™, which is 92° (Brandrup and Immergut, 1982). The desired characteristics for the PES/SMM mixture

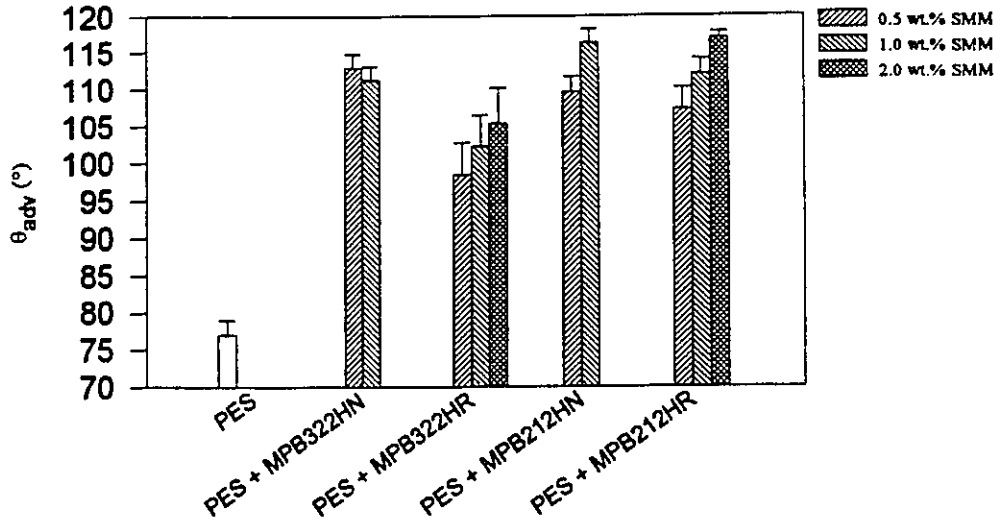

(a)

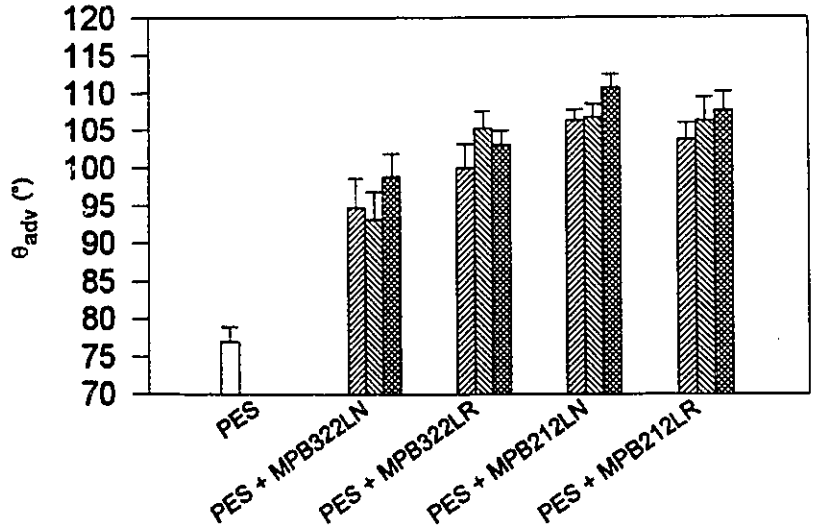

(b)

Figure 4 - 13: Advancing contact angle (θ_{adv}) of surfaces of PES/ SMM blends containing SMMs synthesized with (a) BA-L High and (b) BA-L Low. Note: Data for 2.0 wt.% of MPB322HN and MPB212HN were not provided because films could not be cast due to severe phase separation.

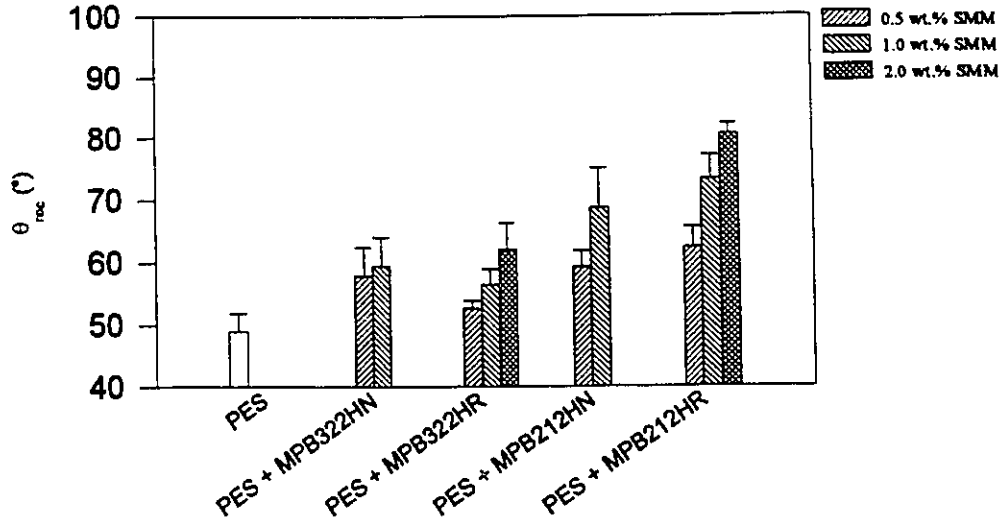

(a)

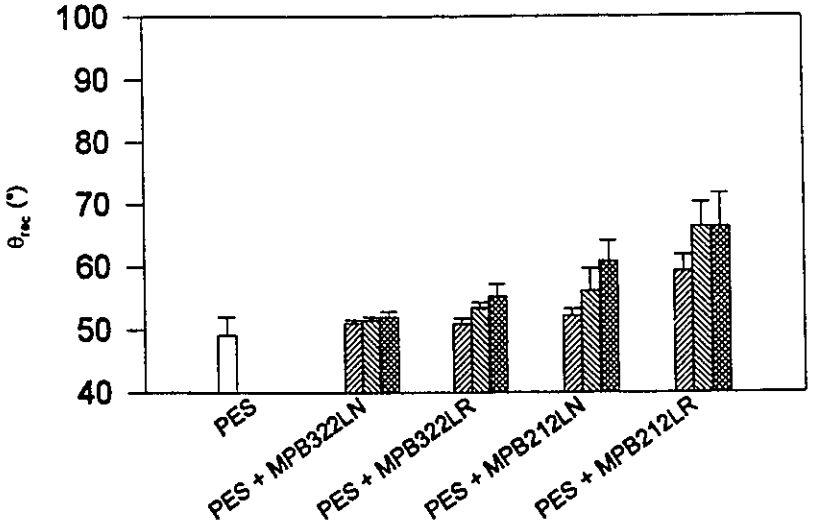

(b)

Figure 4 - 14: Receding contact angle (θ_{rec}) of surfaces of PES/ SMM blends containing SMMs synthesized with (a) BA-L High and (b) BA-L Low. Note: Data for 2.0 wt.% of MPB322HN and MPB212HN were not provided because films could not be cast due to severe phase separation.

surfaces were high water contact angles (θ_{adv} and θ_{rec}) and small hysteresis. There was no trend correlating θ_{adv} values with the experimental variables (i.e. reactant mole ratio, prepolymer reactant concentration); however, for SMMs synthesized with BA-L Low there was a small trend correlating increasing θ_{adv} with the reactant mole ratio (Figure 4-13b). These results suggests a combination effect of the reactant mole ratio and the type of polyfluoroalcohol. A much clearer trend of increasing θ_{rec} was observed, for both BA-L High and Low, as the reactant mole ratio of SMM synthesis was changed from 3:2:2 to 2:1:2 (Figure 4-14). From these results, it seems that the surface characteristics of PES/SMM blends were sufficiently distinct for SMM with a specific type of BA-L used in the synthesis.

The surfaces studied in this work are not ideal; hence, hysteresis of contact angles exists. Section 3.4.3 had presented some of the causes of hysteresis. By studying the hysteresis results obtained in this work in light of the background literature, additional information on the surface such as surface roughness, heterogeneity and dynamics can be obtained. In the following discussion, emphasis will be on the thermodynamic hysteresis which is due to surface roughness and/or heterogeneity. The time constraints in this research thesis did not permit a comprehensive study of dynamic hysteresis which was assumed to be small, due to reasons discussed in section 3.4.3.

The surfaces studied in this work were in general optically smooth (Table 4-3); hence, it can be assumed that hysteresis due to surface roughness was negligible. Hysteresis due to compositional heterogeneity of the surface is only significant when the domains (see Figure 3-6) of different material are larger than 0.1 μm in size (Andrade et al., 1985). The lateral resolution of XPS is approximately 200 μm (Clark, 1984) and surface characterization by XPS (section 4.2.3) pointed toward a model of a pure SMM layer (assume that the results also extend to the PES/SMM blend surfaces which were not studied with XPS); hence the effect of heterogeneity due to surface composition of mixed PES and SMM is negligible. If heterogeneity exists, it would be due to the difference in the SMM make-up (i.e. due to the copolymer structure). However, the information about surface energetics of pure SMMs is not available due to insufficient mechanical

properties of the SMMs to form thin film necessary for the measurements. Hence, it is difficult to distinguish the surface energetics of blends from that of pure SMM.

Assuming that the surface energetics of a copolymer (such as an SMM) behave similarly to a model heterogeneous surface, the general conclusions from the studies of Johnson and Dettre model can be applied (Johnson and Dettre, 1969; Andrade et al., 1985). The first conclusion of Johnson and Dettre (1964) model states that the advancing angle is more reproducible on a predominantly low energy surface, while the receding angle is more reproducible on a predominantly high energy surface. From the results obtained in Figures 4-13 and 4-14, the reproducibility of the two angles were roughly the same. Hence, it was theoretically difficult to conclude as to which of the types of surface was dominant. Johnson and Dettre (1964) also concluded that on a heterogeneous surface, the advancing angle is characteristic of the low energy region, whereas the receding angle is characteristic of the high energy regions of the surface. Figures 4.13 and 4.14 infer that both low and high energy regions of PES surface were modified by SMMs. For θ_{adv} data, it was seen that the surface energy of the low-surface-energy regions have become much lower by the addition of SMMs (Figure 4-13), whereas that of the high-surface-energy regions of PES were exchanged for lower energy domains with all but one of the SMMs, namely MPB322LN (see Figure 4-14).

The observed hysteresis is significant and cannot be completely explained by its thermodynamic components and therefore a kinetic component such as a molecular rearrangement of the material's molecules at the interface must be considered (see section 3.4.3). Unfortunately, this study could not be carried out due to time limitations and the defined scope of the thesis. For the hysteresis results presented in Figure 4-15, it has been assumed that molecular rearrangement already occurs during the three measurement cycle. However, future studies are needed to confirm this. The data in Figure 4-15 show no determining factor that could alter hysteresis except for the trend observed by increasing the SMM concentration, for some of the SMM. The lower hysteresis values seemed to be dominantly associated with SMMs synthesized using the 2:1:2 ratio in combination with BA-L High (Figure 4-15a). Recall that the reduction of hysteresis is a

desirable character of the SMM. Based on this, MPB212HR would generate the most stable interface.

In summary, all SMMs modified the surface energetics of PES. However, the SMMs synthesized with BA-L High modified both low and high surface energy regions of PES, whereas those synthesized with BA-L Low seemed to modify only the low energy parts. Since the polymer surfaces were found to be heterogeneous due to the copolymeric nature of the SMM, hysteresis was considered to be due in part to heterogeneity and probably to a component related to molecular rearrangement between PES and SMM molecules at the interfaces. Furthermore, it was not clear whether the modified surfaces were predominantly low-energy or high energy. This strongly suggests the occurrence of molecular rearrangement.

It was not possible to associate the contact angle data with the factors affecting the synthesis of a given SMM and consequently hysteresis. Although a combination of High BA-L and 2:1:2 chemistry would be the preferred option. At the present time the mechanism of SMM separation from PES and the SMM saturation process of the surface is still not known, other than the qualitative and thermodynamic assessment of the phenomenon that has been provided (c.f. section 2.1). A conceptual model combining results of bulk and XPS analysis, and contact angles measurements of a typical PES/SMM surface is illustrated in Figure 4-16. The DSC thermal analysis data indicated that there are phases of SMM dispersed in PES. The size of these dispersed phases in some cases must be less than 20 μm (limit of visual detection). The shape of these phases would likely to be spherical in order to minimize interfacial tensions (Andrade, 1985; Gibbs, 1928). The XPS results showed that for the top 10 nm surface layer, there were mixed domains of pure SMM and PES with SMM dominating the upper surface.

As a hypothesis, the mechanism of surface modification probably involves two steps: (i) phase separation from PES and (ii) migration of SMM toward the polymer solution-air interface during film formation. DSC and XPS results indicated that phase separation not

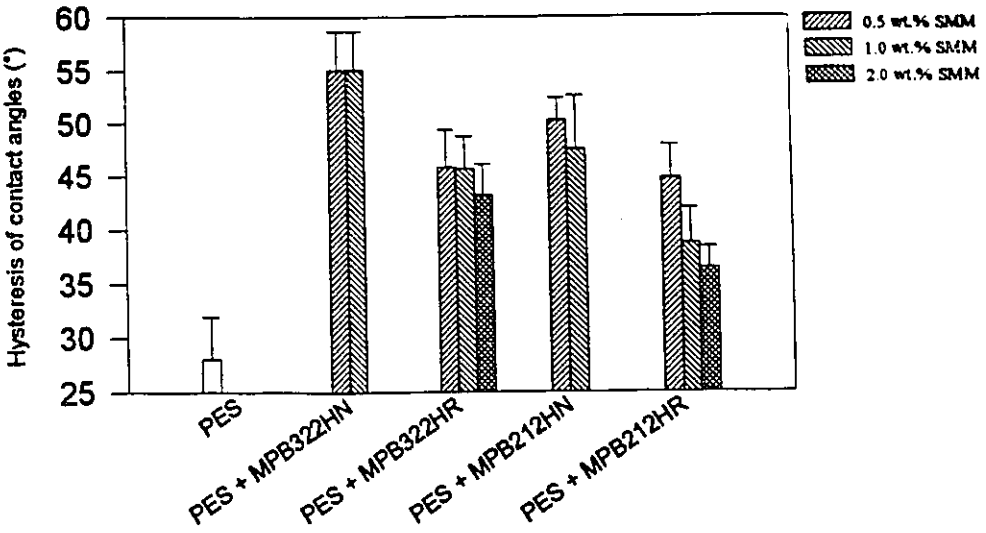

(a)

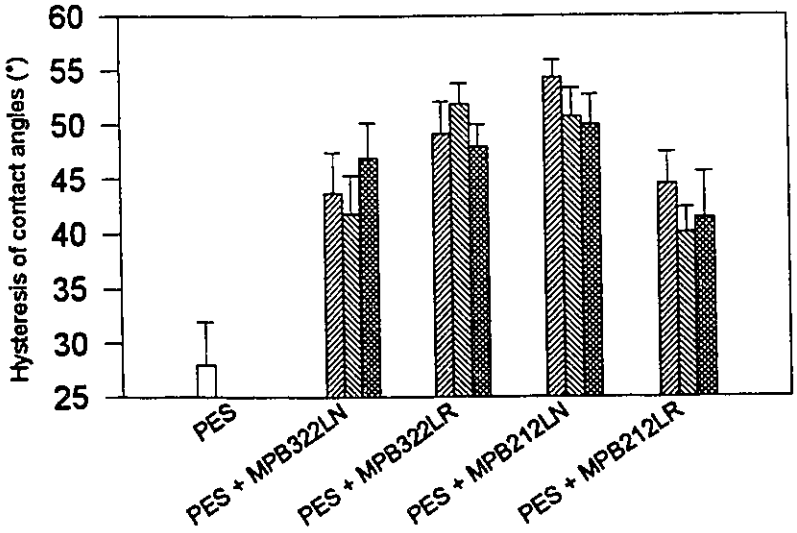

(b)

Figure 4 - 15: Hysteresis of contact angles of surfaces of blends of PES and SMM containing (a) BA-L High and (b) BA-L Low.

only created a layer of SMM on top of PES, but it also led to the formation of SMM phase domains that were dispersed within PES.

Phase separation is a thermodynamic phenomenon and depends on the chemical structure of the materials and their molecular weights (Rosen, 1982); it also has a kinetic component of one polymer diffusing out of the other (Rosen, 1982). The migration mechanism would depend on the molecular weight of the SMM, the magnitude of the driving force, whether or not interactions between polymers, between polymer and solvent are present (based on general descriptions of Rosen (1982)). SMM density and stability at the interface would also need to be known to sort out its resulting effects on surface energetics. The SMMs in this work were different in terms of the type of polyfluoro-ends,. the distribution of the SMM components and the average molecular weights. However, to be able to relate these variables to their behaviour in modifying the surface energetics, step-wise analysis on phase separation and migration will be necessary.

4.2.5 Thermal analysis and surface energetics of PES/SMM/PVP materials

In the preparation of pervaporation membranes, as described in section 3.5.2, 6 wt.% of Polyvinylpyrrolidone (PVP) was added as a non-solvent additive to increase the viscosity of the casting solution and to improve the pore characteristics (Lafrenière et al., 1987). Because of this additive, it was possible to prepare homogeneous solutions and cast continuous films, for pervaporation experiments, at SMM concentrations beyond 2.0 wt.%. The nature of this additive on solution properties has yet to be studied for the PES/SMM system, but it is reasonable to suggest that it will play a role as a compatibilizer to improve the miscibility between PES and the SMMs. As shown before, the PES was either immiscible or partially miscible with a given SMM (c.f. discussion on Figure 4-5); therefore, the dispersed SMM phase in a PES matrix would be finer in size, if a compatibilizer was used. The reduction in domain size of one polymer inside the other using a polymeric compatibilizer for an immiscible polymer pair has been reviewed by Piirma (1992). Compatibilizers reduce the interfacial tension between phases by being partially miscible with both of the immiscible polymers (Piirma, 1992).

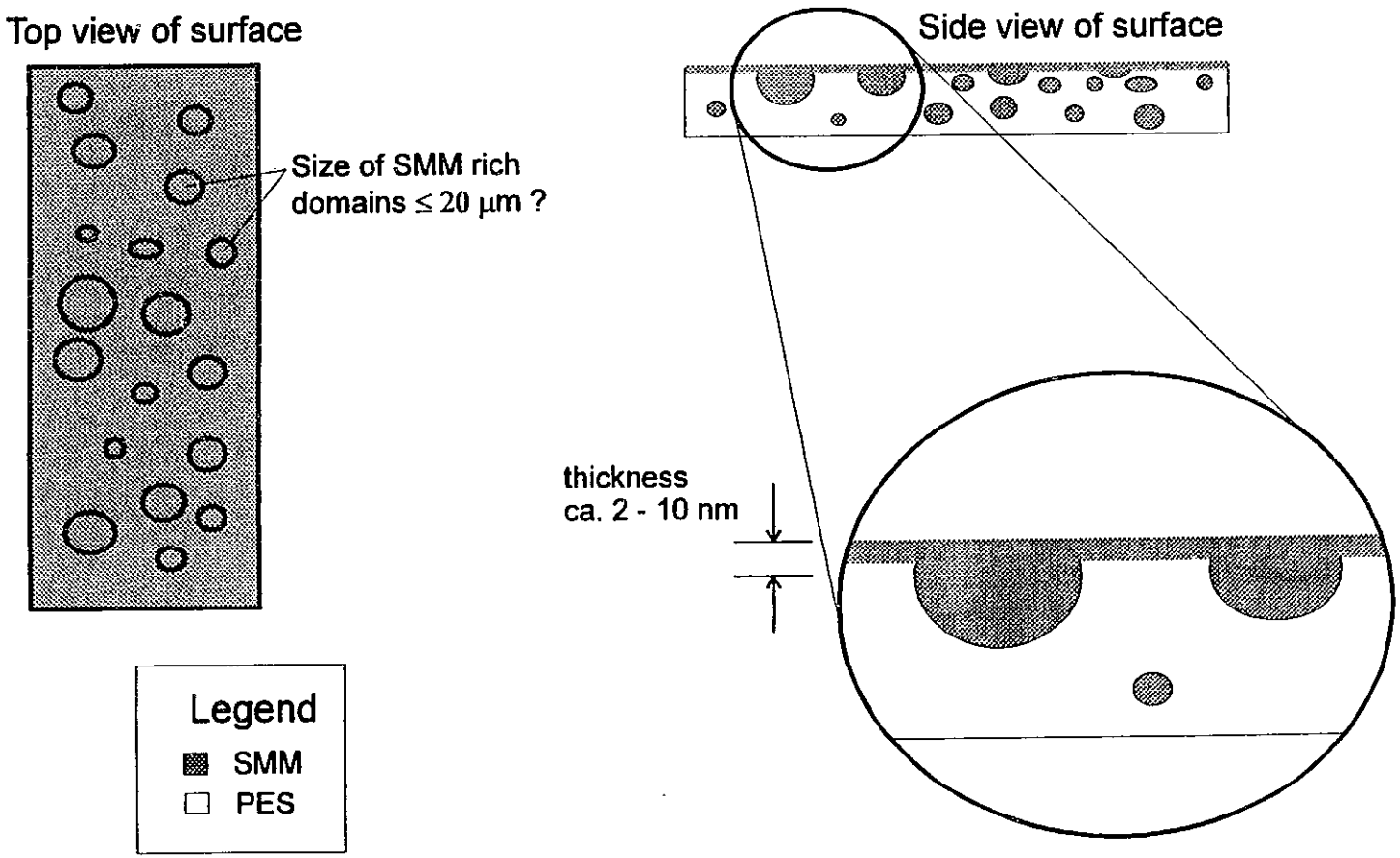

Figure 4 - 16: Conceptual model of a typical cast PES/SMM surface produced in this work. Note: the exploded view from side view is not to scale.

In order to assess the possible impact of PVP on the function of the SMMs in PES. studies of PES/SMM blends containing PVP were carried out using DSC and contact angle experiments. For DSC studies, films were cast from solutions containing PVP, gelled and dried using the protocol described in section 3.5.2. Although previous studies have shown that there is very little PVP left in the films after gellation and drying for binary mixtures of PES and PVP (Lafrenière et al., 1987), a similar confirmation was not available with the PES/SMM/PVP system. For the study of surface energetics in the presence of PVP, films were prepared using the protocol described in section 3.4.3.

The PES/SMM films cast for DSC from solution containing PVP had significantly lower T_g values than those of the PES membrane as shown in Figure 4-17. These values represent those of the PES rich phase as discussed previously in section 4.2.2. The mid-point T_g of PES without SMMs (211° C) was less than that of pure PES (220° C), indicating a plasticizing effect that was related to PVP still present in the film after the preparation procedure. Hence, an assumption of minimal involvement of PVP in the phase behaviour PES/SMM materials cast from solutions containing PVP is not possible. The microheterogeneity of the materials containing low SMM concentration (phase domain size) was seen to be reduced by the presence of PVP in casting solutions, as shown by the reduction of T_g width in Figure 4-18. Recall from Figure 4-4 that the average T_g width for all SMMs was approximately twice as large as that of pure PES, even at low concentration of SMMs. However, the effect of PVP on T_g width is lost at SMM concentrations greater than 2 wt.%. It is also interesting to note that the T_g width of PES/PVP films was the same as that of pure PES (7° C). This was expected since PES and PVP are miscible in all proportions (Lafrenière et al., 1987).

Based on contact angle data, the PES/SMM/PVP film surfaces were more hydrophobic than the PES/PVP surfaces as shown in Figure 4-19. The advancing contact angle increased and leveled off for films cast from solution of 1 - 2 wt.% SMMs. The advancing angle value for membranes without any SMM was about 11° lower than for that of pure PES (c.f. Figure 4-13). This decrease reflects the presence of PVP at the

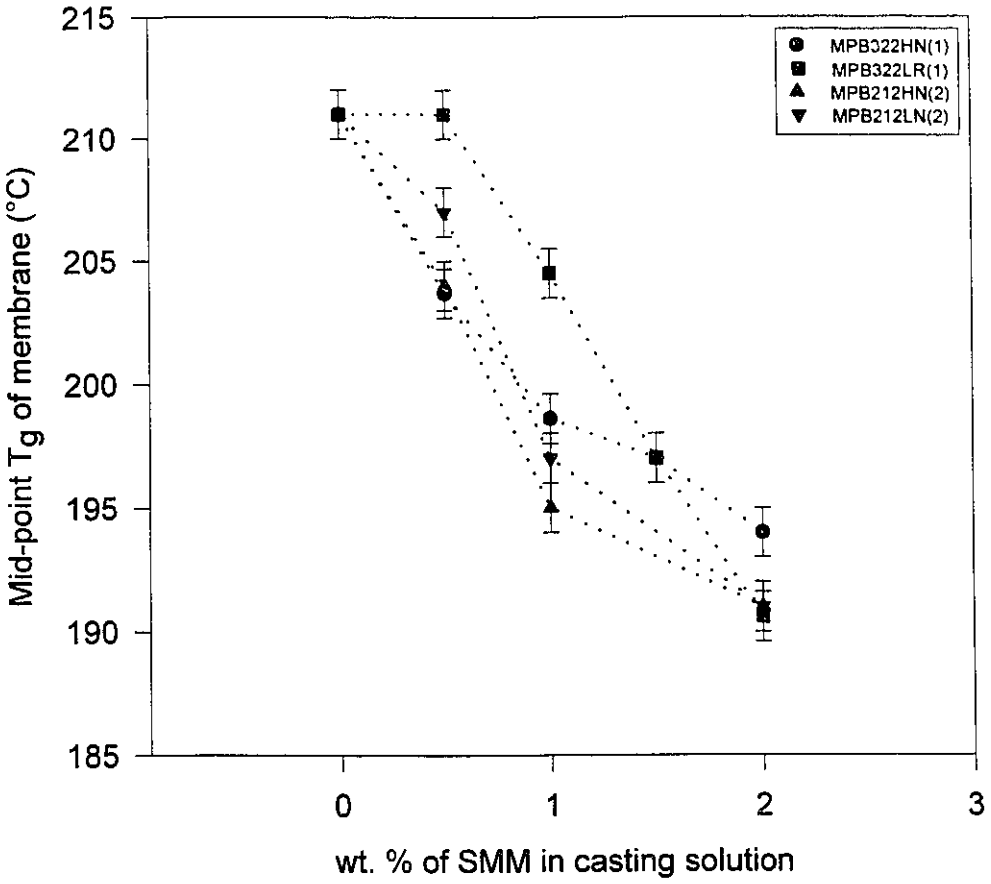

Figure 4 - 17: Effect of SMM concentration in casting solution (containing 6 wt.% PVP, 25 wt.% of PES and balancing wt.% of DMAC) on mid-point T_g of PES/SMM membranes.

surface, since it is hydrophilic (Lafrenière et al., 1987). The average change in advancing contact angle achieved with MPB322HN(1) and MPB212HN(2) was 50° whereas that achieved with MPB322LR(1) and MPB212LN(2) was 40°. SMMs synthesized with BA-L High yielded higher advancing contact angles than those synthesized with BA-L Low, even in the presence of PVP as shown in Figure 4-19. Recall that higher contact angles were also achieved with BA-L High in the absence of PVP (see Figure 4-13). As for the water receding contact angles for the surfaces cast from solution with PVP, a saturation was also observed, and the values were lower than those cast from solution without PVP (c.f. Figure 4-14). Recall that the receding angles are more characteristic of the high energy component of the surface; hence, a decrease of this angle signifies an increase in the high energy part of the surface, which is reflected by the hydrophilic nature of PVP. In summary, SMMs still enhanced the low surface energy regions of the surface and reduced the high surface energy component. PVP, on the other hand enhanced the high-surface-energy regions and reduced the overall effect of SMMs. This clearly indicates that the use of PVP needs to be well characterized, because changes in surface phenomena are affected by the presence of PVP.

The reproducibility for both advancing and receding angles were better than those with the film surfaces prepared from solutions without PVP. This again was possibly due to a compatibilizing effect of the PVP. The reproducibility of receding angles was not as good with MPB212HN(2) as with the other SMMs (see Figure 4-19). The reproducibility of the advancing angles were generally good. As with the case for films cast without PVP, these similarities in reproducibility made it difficult to assess theoretically which of the low-energy or high-energy regions of the surface were dominant.

The hysteresis of water contact angles for the surfaces prepared with PES/SMM/PVP are given in Figure 4-20. The assumption that hysteresis due to surface roughness was negligible was applicable with these systems as well, since the films were optically smooth. The hysteresis of the surfaces in these systems was due partly to surface heterogeneity. On average, they were higher than those without PVP in the casting

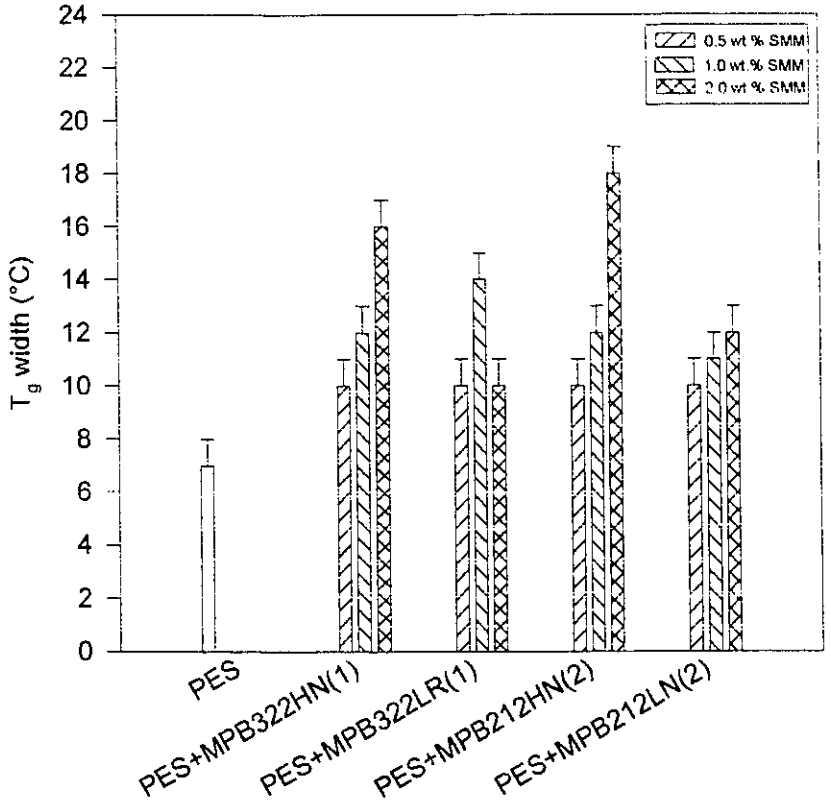

Figure 4 - 18: T_g width of PES/SMM membranes cast from solution containing 6 wt.% PVP, 25 wt.% PES, varying wt.% of SMM and balancing wt.% of DMAC.

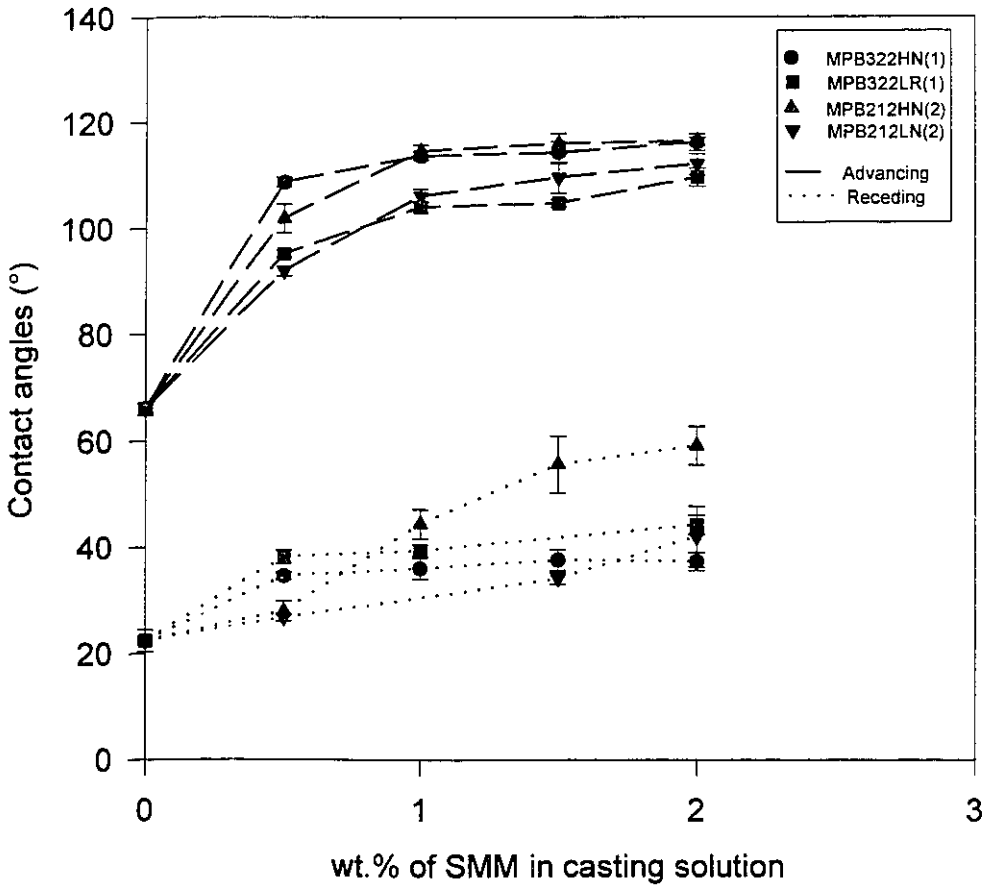

Figure 4 - 19: Contact angles of PES/SMM films prepared from membrane casting solution containing 6 wt.% PVP, 25 wt. % PES, varying wt.% of SMM and with balancing wt.% of DMAC.

solution (c.f. Figure 4-20), suggesting a higher wettability by water. There was a transitional concentration with the four SMMs studied, beyond which hysteresis started to decrease to value closer to those of PES/SMM (no PVP) surfaces (c.f. Figure 4-20). This indicates an increasing SMM dominance at the surface relative to PVP. Previous discussions on the contributing factors to heterogeneity and resulting hysteresis is also applicable here (c.f. section 4.2.4).

4.3 Pervaporation results for dilute chloroform water mixture

Fairly to well reproducible SMMs were tested in pervaporation experiments to assess any enhancement in terms of selectivity and permeate rate. An aqueous chloroform mixture was used as the test feed solution and the details of the experiments were described section 3.5. In the following discussion, the effect of SMMs on the chloroform enrichment factor, total permeation flux and net recovery of chloroform will be presented. The pervaporation experiments were performed by Mr. Y. Fang, a Ph.D. candidate in the Department of Chemical Engineering, University of Ottawa. However, the discussion describing the relationship between the pervaporation data and the characteristics of the PES/SMM and PES/SMM/PVP are the original ideas of this thesis.

4.3.1 Effect of adding SMM on chloroform enrichment

The enrichment factor (β) is defined as the ratio of concentration of chloroform in the permeate to that in the feed and was determined for various PES/SMM membranes prepared from casting solutions with different SMM concentrations. The method of membrane preparation was described in section 3.5.2. The PVP left in the membrane was assumed to be negligible as in previous works (Lafrenière et al., 1987). For these results and others in section 4.3, the error reported with the pervaporation experiment was small (<1 % standard error) as obtained by using a given membrane coupon three times.

The effect(s) of SMMs on the membrane enrichment factor for chloroform are shown in Figure 4-21. The selectivity of membranes toward chloroform was clearly enhanced by the addition of SMMs into the casting solution. A maximum in β value of about 16 was obtained for membranes containing SMM MPB322HN(1). The β value for MPB322LR(1) was approximately 15, while values for MPB212LN(2) and

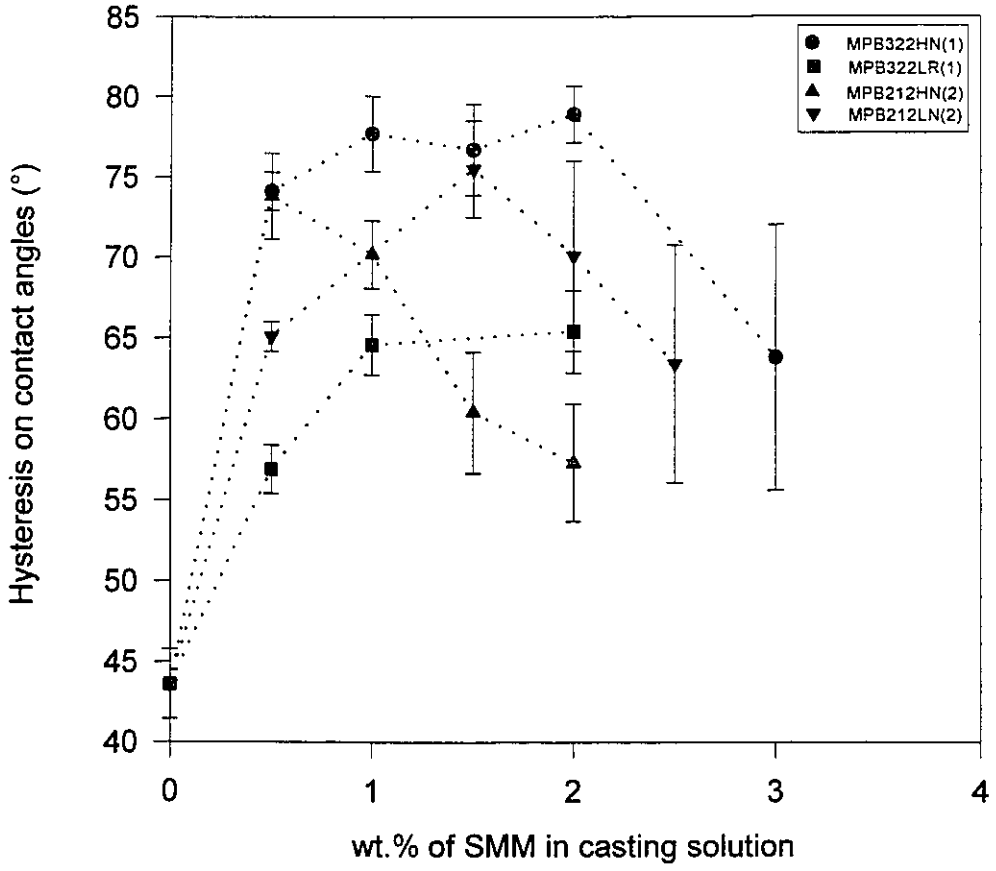

Figure 4 - 20: Hysteresis of contact angles of PES/SMM film surfaces prepared from membrane casting solution containing 6 wt.% PVP, 25 wt.% PES, varying SMM wt.% and balancing wt.% of DMAC.

MPB212HN(2) were approximately 14 and 11 respectively. It seems that the concentration at which the maximum occurred was characteristic of the type of SMM, under identical membrane preparation conditions. The addition of 1 wt.% MPB322HN(1) in the casting solution enhanced the chloroform enrichment by 232% compared to PES; adding MPB322LR(1) at 2 wt.% enhanced the enrichment by more than 240%. Adding MPB212LN(2) at 1.5 wt.% enhanced the enrichment by 200%, and adding MPB212HN(2) at 2 wt.% enhanced it by more than 150%.

4.3.2 Effects of SMM on total permeation flux

The permeation rate was measured for various PES/SMM membranes, and the results are illustrated in Figure 4-22. Two types of behaviour were observed: (i) flux initially increased slightly and then decreased to a minimum with increasing SMM concentration (MPB322HN(1) and MPB212LN(2), minima were equal at 0.02g/h), or (ii) flux increased with increasing SMM concentration to a maximum and then decreased (MPB322LR(1) and MPB212HN(2), maxima were also approximately equal near 0.07g/h). It should be noted that in case (i) the minimum permeate rate is lower than the permeation rate without SMM.

In comparing the results from Figures 4-20 and 4-21, it was interesting to note that the SMM concentration at which minima and maxima in permeation behaviour occur for both selectivity and flux are very similar. It is generally believed that an increase in selectivity is achieved at the expense of a decrease in permeation rate (Huang and Rhim, 1991). This was observed for membranes of PES/MPB322HN(1) and PES/MPB212LN(2) but not for PES/MPB322LR(1) and PES/MPB212HN(2). Apparently, the SMM addition can improve simultaneously both selectivity and permeation rate properties of PES membranes.

It is often useful to compare the overall performance of the membrane in terms of the net recovery of the permeant. The net recovery of chloroform is defined as the product of the permeation rate (g/h) and the chloroform mass concentration in the permeate. The net recovery for the membranes containing SMMs at different concentration is plotted in Figure 4-23. From this figure, one can see that MPB212LN(2) did not offer any

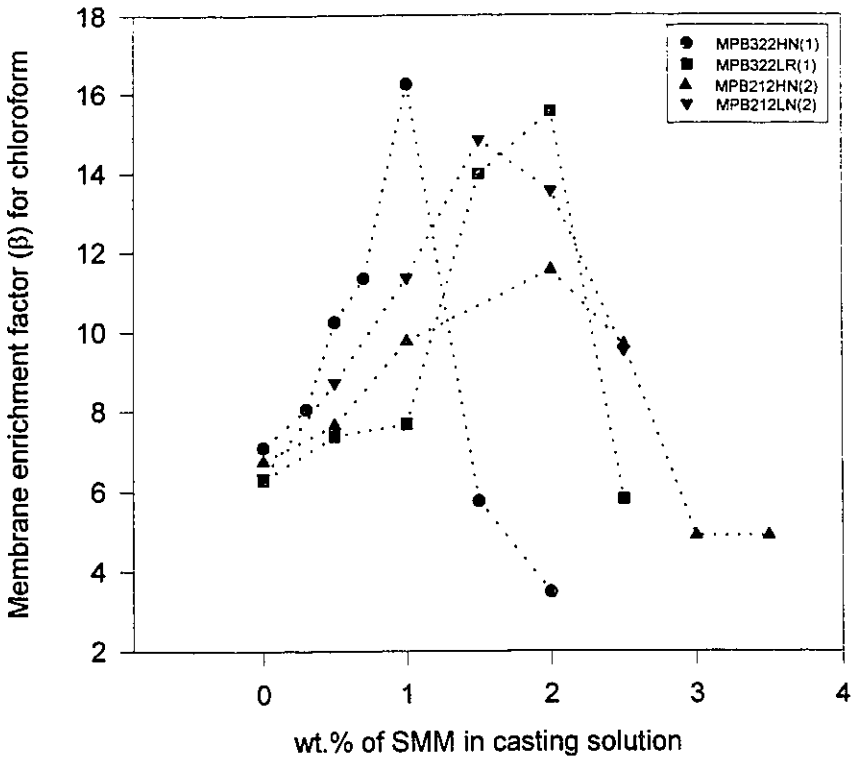

Figure 4 - 21: Effect of SMMs on PES/SMM membrane enrichment factor for chloroform. PES and PVP were kept constant in the casting solution at 25 and 6 wt.% respectively.

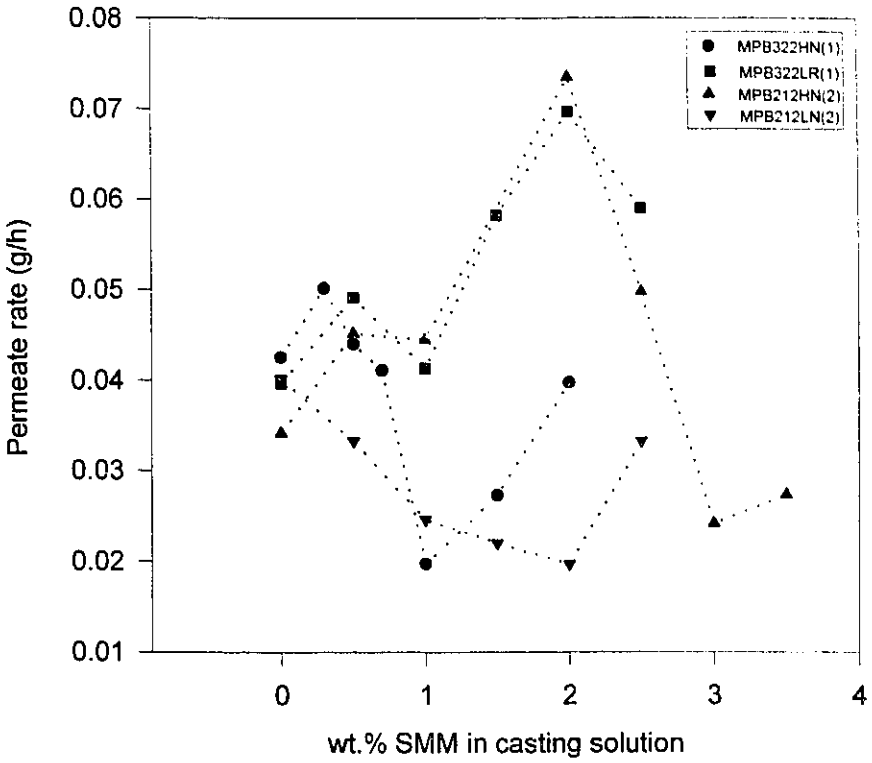

Figure 4 - 22: Effect of SMMs on the permeation rate. PES and PVP in casting solution were kept constant at 25 and 6 wt.% respectively.

significant improvement, whereas each of the remaining SMMs showed a net positive effect for chloroform recovery.

It would be of interest to identify the SMMs' molecular characteristics that could be related to the changes in membrane performance, and particularly how this change happens. Unfortunately, the data in this thesis are insufficient to answer these questions. However, some preliminary observations can be obtained by looking at Figure 4-24. This figure is a comparison of normalized (against averages) responses such as selectivity, permeation flux, mid-point T_g, T_g width, contact angles, and contact angle hysteresis versus the wt.% of SMM in casting solution for MPB322LR(1). Other similar plots for MPB322HN(1), MPB212HN(2) and MPB212LN(2) can be found in Appendix E. The surface energetics of membrane in Figure 4-24 are assumed to be between those measured with and without PVP (for other plots in Appendix E only surface energetics with PVP are shown for simplicity). Two trends were observed from Figure 4-24 and those in Appendix E: (i) a lagging effect between surface modification and performance enhancement and (ii) bulk properties changes as represented by mid-point T_g and T_g width are likely the causes for loss of enhancement effect. The second observation is supported by the continuing bulk properties changes as compared to saturation in surface behaviours. How the bulk change and that of surface chemistry produces the enhancement, and which bulk property change(s) is(are) the determinant factor(s) in the decline of enhancement effect are certainly of great interest in future works.

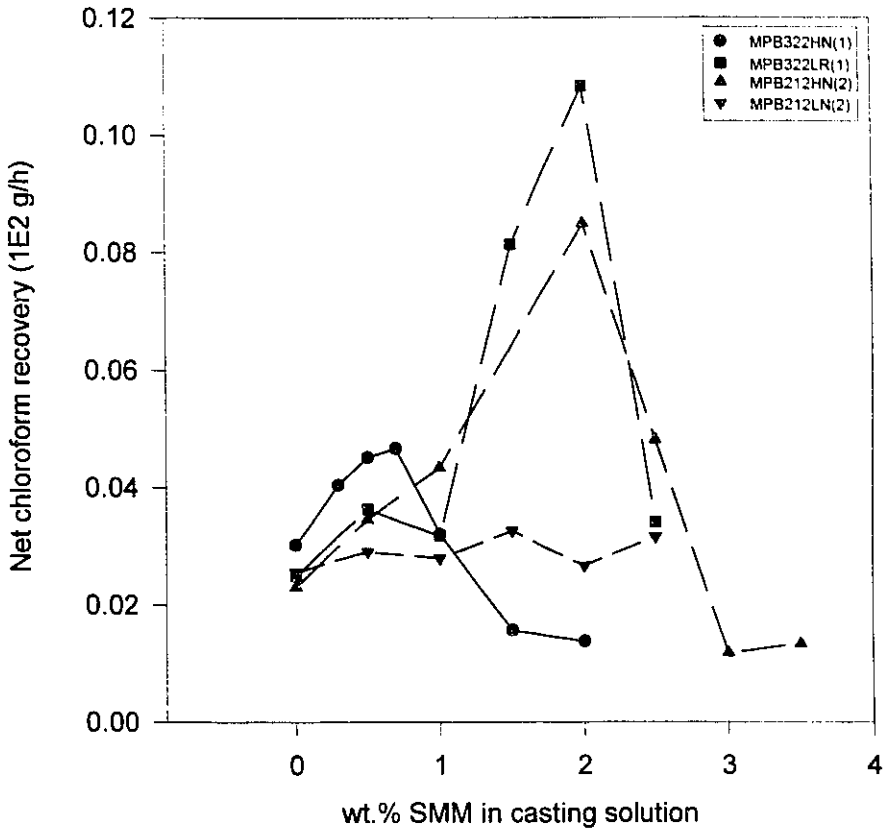

Figure 4 - 23: Effect of SMMs on the net chloroform recovery. PES and PVP in casting solution were kept constant at 25 and 6 wt.% respectively.

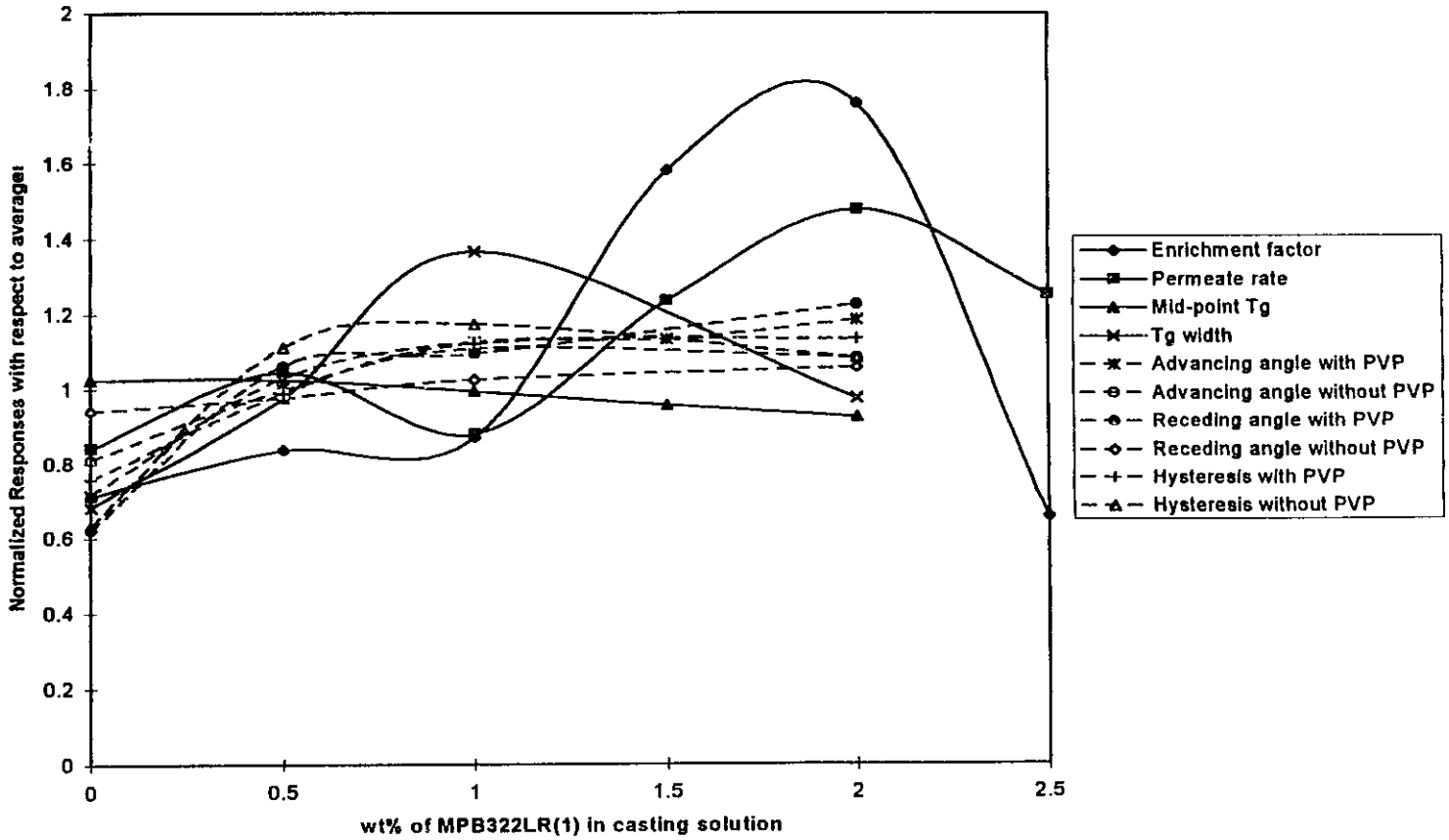

Figure 4 - 24: Comparisons of normalized response curves of various membrane bulk and surface characteristics (shown in dashed lines) and membrane selectivity and permeation flux behaviour for MPB322LR(1). PES and PVP in casting solution were kept constant at 25 and 6 wt.% respectively. The curves were artificially smoothed to improve visibility.

Chapter 5

CONCLUSIONS

Surface modifying macromolecules (SMMs) have been successfully synthesized using eight formulations composing of varying amounts of MDI, PPO and two types of BA-L. Based on available results the following conclusions were drawn:

1. It was found that the stoichiometry, the prepolymer reactant concentration and the type of BA-L contributed significantly to the control of SMM properties.

2. The most reproducible formulations were those using a 3:2:2 stoichiometry, BA-L Low and reduced prepolymer reactant concentration, and those using a 2:1:2 stoichiometry, BA-L Low and normal prepolymer reactant concentration. There were few direct relations between the variability in molecular characteristics and experimental variables studied, although SMMs synthesized with BA-L Low and the 2:1:2 stoichiometry seemed to offer better reproducibility.

3. It was found that SMMs were amorphous from -50 to 260° C. Their mid-point T_g decreased with increasing average molecular weight due to the internal plasticizing effect of the PPO component in the materials.

4. The increasing weight fraction of PPO in the SMM increased phase separation in the ternary PES/SMM/DMAC system (75% of the time), where the composition of PES was fixed at 25 wt.%. However, the increasing weight fraction of PPO in the SMM decreased the phase separation in the binary PES/SMM system (75% of the time).

5. MPB212HR, MPB322LR exhibited degrees of partial miscibility with PES, while SMMs synthesized by other formulations were immiscible with PES.

6. XPS studies indicated a similar surface chemistry for all materials containing MPB322HN, MPB322LN, MPB212HN and MPB212LN, in the 2 to 10 nm surface

range. Also, the XPS results showed that for these surface layers there were mixed domains of pure SMM and PES with SMM on top.

7. All SMMs influenced the surface energetics of PES. The polymer systems which achieved θ_{adv} values close to that of poly(tetrafluoroethylene) (PTFE, Teflon™) were PES/MPB322HN, PES/MPB212HN, PES/MPB212HR and PES/MPB212LN. However, the highest average values of receding angles of these systems were not as close to that of Teflon™. The SMMs synthesized with BA-L High modified both low and high surface energy regions of PES, whereas those synthesized with BA-L Low seemed to modify only the low energy parts. Furthermore, it was not clear whether the modified surfaces were predominantly low or high energy.

8. SMMs were found to be successful in creating a better membrane: the addition of 1 wt.% MPB322HN(1) in the casting solution enhanced the chloroform enrichment by 232% , and the addition of MPB322LR(1) at 2 wt.% enhanced the enrichment by more than 240%. Adding MPB212LN(2) at 1.5 wt.% enhanced the enrichment by 200%, and adding MPB212HN(2) at 2 wt.% enhanced it by more than 150%.

9. In the presence of SMMs: (i) permeation flux initially increased slightly and then decreased to a minimum with increasing SMM concentration (MPB322HN(1) and MPB212LN(2), where the minima were equal and were 0.02g/h), or (ii) permeation flux increased with increasing SMM concentration to a maximum and then decreased (MPB322LR(1) and MPB212HN(2), where the maxima were approximately equal and were near 0.07g/h).

10. MPB322HN(1), MPB322LR(1) and MPB212HN(2) had positive effects in terms of net chloroform recovery.

11. A preliminary comparison of changes in membrane surface and bulk characteristics indicated that surface chemistry may have an important role in inducing the changes in pervaporation performance. However, it is not the only factor because of a lag effect observed between surface changes and performance enhancement. As well, DSC data implied that bulk phenomena changes are important.

Chapter 6

RECOMMENDATIONS

In summary, 8 SMMs were successfully synthesized and characterized in this work. Furthermore, enhanced pervaporation performance was demonstrated by the addition of selected SMMs. However, the synthesis of these SMMs is not yet fully understood, and it was observed that surface changes in chemistry alone were not the sole factors which determined the enhancement effects. Moreover, several key areas of the research have not been pursued due to the set objectives and time limitations. To address these issues partially, the following recommendations are suggested:

1. For the synthesis of SMM, it is crucial to determine why the variability in bulk properties occurs. Analysis of the intermediate products of the synthesis using established analytical chemistry methods is recommended.

2. A numerical model of the synthesis can be developed based on the work of Peebles (1974). This model can be built along with the chemical analysis studies outlined in the previous recommendation. The usefulness of the model is evident when multiple reactant changes are involved.

3. Solution behaviour of PES/SMM/Solvent is crucial in membrane manufacturing. Therefore, it is recommended that a complete phase diagram of the SMM of interest be constructed. The choice of solvent is important, and it is necessary that phase behaviour be studied with a variety of solvents.

4. Since the phase behaviour, both in solution (PES/SMM/DMAC) and in solid phase (PES/SMM) was found to be influenced adversely by the PPO segments of the SMM, it is recommended to replace these segments or to reduce their effects. The list of

possible solutions can be extensive since there is a limited amount of data available on SMM technology in the membrane area.

5. To fully characterize the PES/SMM blends, studies of different polymer ratios are required. It is recommended that the best SMMs be properly studied to yield a complete picture of phase domains and phase formation.

6. An investigation of the kinetic hysteresis is recommended to understand the possible molecular rearrangement and other kinetic related surface phenomena. Thermodynamic hysteresis also needs to be restudied, once kinetic hysteresis is properly accounted for.

7. Appropriate method(s) have to be devised to study the surface energetics after the PVP has been leached out from the membranes. With the current method, this is not possible due to wrinkle formation on the film surface after the drying procedure.

8. As Figure 6-1 illustrates, the mechanism of SMM effect on pervaporation can be studied only when the events in Box A are kept constant or their effects are well understood. Therefore, a sensitivity study for these events is recommended.

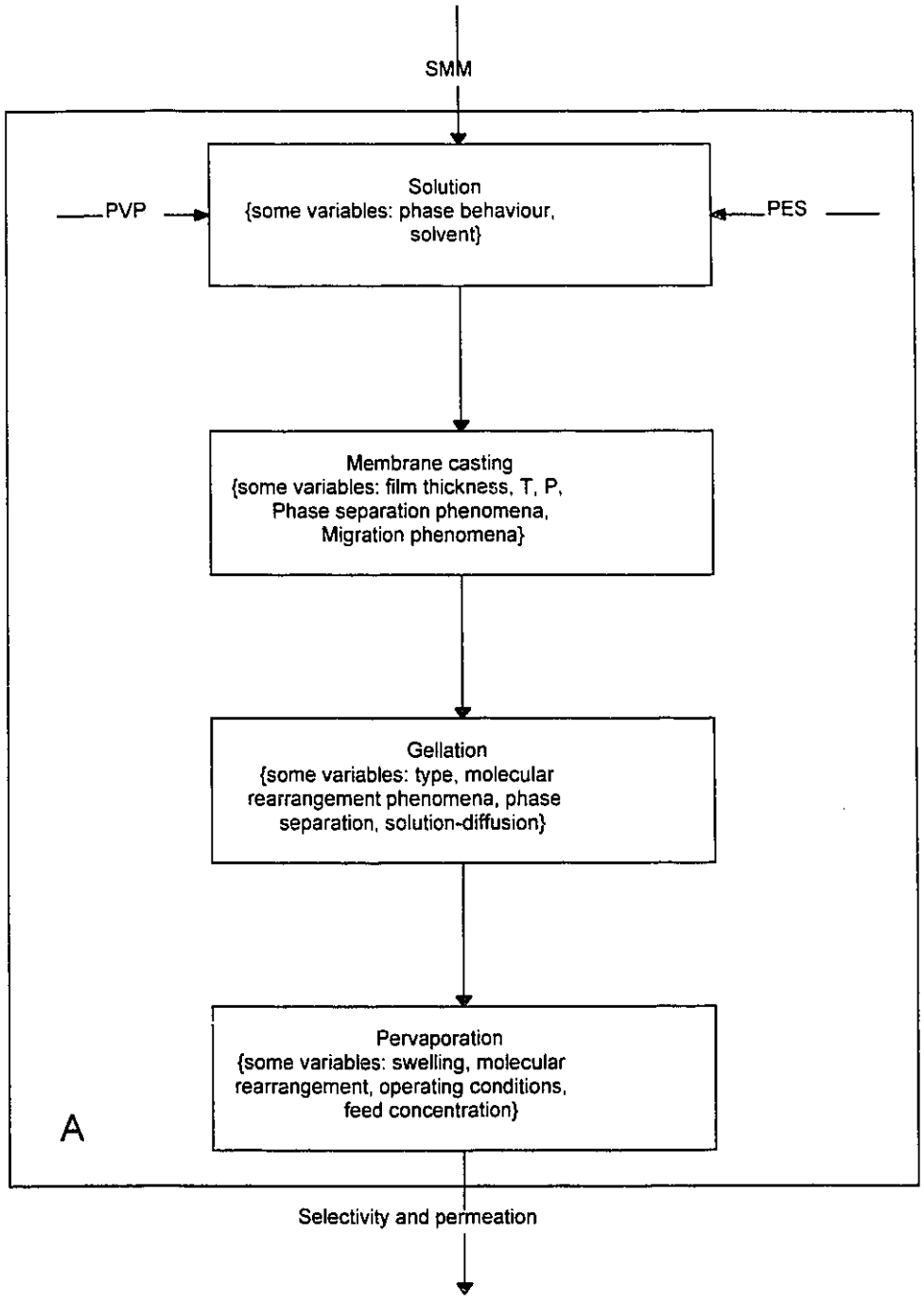

Figure 6 - 1: Processes involved in SMM effects on pervaporation.

NOMENCLATURE

A	area (m^2)
a	activity
B	Mobility coefficient
C	Concentration
c	Mass concentration (g/cm^3)
Cp	Specific heat capacity (J/g·°C)
D	Diffusivity (cm^2/s)
E	Internal surface energy (mJ)
e_s	Specific internal surface energy (mJ/m^2)
F	Surface Helmholtz free energy (mJ)
f	Weight fraction of component in material
f_s	Specific surface Helmholtz free energy (mJ/m^2)
G	Surface Gibbs free energy (mJ)
g_s	Specific surface Gibbs free energy (mJ/m^2)
H	Enthalpy (mJ)
J^*	Permeation flux ($g/s \cdot m^2$)
J_i	Permeation rate of component *i* ($g/s \cdot m^2$)
k	Proportionality constant
k_a	Response average

L	Membrane thickness (m)
M_i	Molecular weight of polymer in *i*th volume increment
M_n	Number average molecular weight
M_w	Weight average molecular weight
N	Number of molecules
n_i	number of mole in a volume increment *i*
N_o	Initial number of molecules
N_{si}	Number of segment containing *i* pair
N_{st}	Total number of segments
N_t	Number of molecules after time *t*
P	Pressure (Pa)
P_e	Extent of reaction
P^o	Saturated vapor pressure
PSI	Pervaporation performance index
Q	detector read-out (arbitrary unit)
Q_p	Permeability (g/cm·s)
r	Ratio of N limiting reactant to that of excess reactant
R	Universal gas constant (J/mol•K)
S	Entropy (mJ/K)
S^*	Henry's law constant
T	Temperature (K)
T_g	Glass transition temperature (°C)

T_m	Melting temperature (°C)
v	Elution volume (cm^3)
V	Volume (m^3)
V'	Molar volume (cm^3/mol)
w	Work (J)
w'	Weight fraction of an element in material
x_n	Number average degree of polymerization
x	Distance variable
$x_{i,}$, x_j	Mole fraction of component *i,j* in liquid phase
y	Observed response
y_i, y_j	Mole fraction of component *i,j* in gas phase

GREEK LETTERS

α	A function of total conversion
$\alpha_{i/j}$	Selectivity
β	Enrichment factor
β'	regression coefficient
χ	Interaction parameter
δ	Solubility parameter ($J^{1/2}\cdot cm^{2/3}\cdot mol^{-1}$)
ϕ	Volume fraction
γ	reversible work to create a unit area at constant T, V and μ (J)
Γ	Surface excess

μ	Chemical potential
θ	Contact angle (°)
θ_r'	Tailing contact angle on inclined surface
θ_a'	Forward contact angle on inclined surface
θ''	Take-off angle (°)
σ	Standard deviation (sample)
τ	Plasticizing coefficient

SUBSCRIPTS

A, B	Polymer A, B
CR	Critical
adv	Advancing
i	*i*th Component
ip	Penetrant polymer
lg	Liquid-gas interface
rec	Receding
sg	Solid-gas interface
sl	Solid liquid interface
1,2	Component 1,2

REFERENCES

Andrade, J.D., "Surface and interfacial aspects of biomaterial polymers", Plenum Press, New York (1985).

Andrade, J.D., L.M. Smith, and D.E. Gregonis, "The Contact Angle and Interface Energetics", in "Surface and interfacial aspects of biomaterial polymers", J.D. Andrade, Ed., Plenum Press, New York (1985), pp. 249-292.

Amy, G.L., R.M. Narbaitz and W.J. Cooper, "Removing VOCs from groundwater containing humic substances by means of coupled air stripping and adsorption", J. Amer. Waters Works Assoc., **79** (8), 49-54 (1987).

Aptel, P., N. Challard, J. Cuny, and J. Néel, "Application of pervaporation process to separate azeotropic mixtures", J. Membrane Sci., **1**, 271-287 (1976).

Aubin, M. and R.E. Prud'homme, "Analysis of the Glass Transition Temperature of Miscible Polymer Blends", Macromolecules, **21**, 2945-2949 (1988).

Aveyard, R. and D.A. Haydon, "Introduction to Principles of Surface Chemistry", Cambridge University Press, London (1973).

Baker, J.W. and J.B. Holdsworth, "The mechanism of aromatic side-chain reactions with special reference to the polar effect of substituents. XIII. Kinetic examination of the reaction of aryl isocyanates with methyl alcohol", J.Chem.Soc., **7**, 713-726 (1947).

Baker, J.W. and J. Gaunt, "The mechanism of the reaction of aryl isocyanates with alcohols and amines. II. The base catalyzed reaction of phenyl-isocyanate with alcohols", J.Chem.Soc., **9**, 18-27 (1949).

Ballard, D.G.H., M.G. Rayner, and J. Schelten, "Configuration of low molecular weight polystyrene in deuterated cyclohexane", Polymer, **17**(4), 349-351 (1976).

Barton, A.F.M., "Handbook of Solubility Parameters and Other Cohesion Parameters", CRC Press, Boca Raton (1983).

Bayer, O., "Polyurethanes", Modern Plastics, **24** (10), 149-152, 250, 252, 256, 260, 262 (1947).

Bayer O., H. Rinke, W. Siefken, L. Orthner, and H. Schild, German Patent 728,981 (1942).

Bengston, G. and K.W. Boddeler, "Pervaporation of low volatiles from water", in "Proceedings of Third International Conference on Pervaporation Processes in the Chemical Industry", R.A. Bakish, Ed., Englewood, NJ (1988), pp. 439-448.

Bikerman, J.J., "Physical Surfaces", Academic Press, New York (1970).

Binning R.C., R.J. Lee. J.F. Jennings and E.C. Martin, "Separation of liquid mixtures by permeation", Am. Chem. Soc., Div. Petrol. Chem., Gen. Papers, Preprints **3** (1), 131-142 (1958).

Blume, I. and R.W. Baker, "Separation and concentration of Organic Solvents from Water Using Pervaporation", in "Proceedings of Second International Conference on Pervaporation Processes in the Chemical Industry", R.A. Bakish, Ed., Englewood, NJ (1987), pp. 111-125.

Brady, J.M. and D. Narinesingh, "Bifunctional catalysis by amides and ureas in the reaction of amines with phenyl-isocyanate", Tetrahedron Lett., 4143 (1971).

Brandrup, J. and E.H. Immergut, Eds., "Polymer Handbook", 3rd Ed., John Wiley & Sons (1989).

Brewer, J., "Literature reviews and research scoping study on the treatment of volatile organic carbon compound in the off-gas from contaminated groundwater and soil remedial technologies, National Groundwater and Soil Remediation Program", Environment Canada, Ottawa (1991).

Brun J.P., C. Larchet, M. Melet, and G. Bulvestre, "Modelling of the pervaporation of binary mixtures through moderately swelling, non-reacting membrane", J. Membrane Sci., **23**, 257-283 (1985).

Burns, C.M. and W.N. Kim, "Solution blending of Polystyrene and Poly(Methyl Methacrylate)", Polym. Eng. & Sci., **28** (21), 1362-1372 (1988).

Charsley, E.L. and Warrington S.B., Eds., "Thermal analysis - Techniques & Applications", Royal Society of Chemistry, Cambridge (1992), pp. 156-179.

Chow, T.S., "Molecular interpretation of glass transition temperature of polymer-diluent systems", Macromolecules, **13**, 362-364 (1980).

Clark, D.T., "The investigation of Polymer Surfaces by Means of ESCA", in "Polymer Surface", D.T. Clark and W.J. Feast, Eds., Wiley (1978), pp. 309-351.

Cortázar M., J.I. Eguiazábal, C. Uriarte, and J.J. Iruin, "Glass transition temperatures of plasticized poly(acrylate)", Polymer Bulletin, **18**, 149-157 (1987).

Couchman, P.R., "Compositional variation of glass transition temperatures 2-Application of the thermodynamic theory to compatible polymer blends", Macromolecules, **11**, 1156-1161 (1978).

Couchman, P.R. and F.E. Karasz, "A classical thermodynamic discussion of the effect of composition on glass transition temperatures", Macromolecules, **11**, 117-119 (1978).

Cowie, J.M.G., "Polymers: Chemistry & Physics of Modern Materials", 2nd edition, Chapman & Hall, New York (1991).

Davies, J.J. and E.K. Rideal, "Interfacial Phenomena", 2nd Ed., Academic Press, New York (1963).

Danusso, F., M. Levi, G. Gianotti and S. Turri, "End unit effect on the glass transition temperature of low-molecular-weight polymers and copolymers", Polymer, **34**(17), 3687-3693 (1993).

Deng, S., Shiyao B., Sourirajan S. and Matsuura T., "A study on the Pervaporation of Isopropyl Alcohol/Water Mixtures by Cellulose Acetate Membranes", J. Colloid and Interface Sci., **136,** 283-291 (1990).

Dibenedetto, A. T., J. Membr. Sci., **A, 1**, 3459, 3477 (1963). Referenced from Huang R.Y.M. and J.W. Rhim, "Separation Characteristics of Pervaporation Membrane Separation Processes", in "Pervaporation Membrane Separation Processes", R.Y.M. Huang, Ed., Elsevier, New York (1991), pp. 111-180.

Dibenedetto, A. T. and Paul D. R., J. Membr. Sci., **A, 2**, 1001 (1964). Referenced from Huang R.Y.M. and J.W. Rhim, "Separation Characteristics of Pervaporation Membrane Separation Processes", in "Pervaporation Membrane Separation Processes", R.Y.M. Huang, Ed., Elsevier, New York (1991), pp. 111-180.

Dobkowski, Z., "Application of Elemental Analysis for the Charaterization of Polymers", in "Applied Polymer Analysis and Characterization, Vol. 2", J. Mitchell, Jr., Ed., Hanser-Oxford University Press, New York (1991), pp. 363-378.

DuPont technical data, document #H-00172, 1-24 (1988).

Escudier, J.L., M. Le Bouar, M. Moutounet, C. Jouret and J.M. Barillere, "Application and evaluation of pervaporation for the production of low alcohol wines", in "Proceedings of Third International Conference on Pervaporation Processes in the Chemical Industry", R.A. Bakish, Ed., Englewood, NJ (1988), pp. 379-386.

Eustache, H. and G. Histi, "Separation of aqueous organic mixtures by pervaporation and analysis by mass spectroscopy or a coupled Gas chromatograph-Mass spectrometer", J. Membr. Sci., **8**, 105-114 (1981).

Fang, Y., V.A. Pham, T. Matsuura, J.P. Santerre and R.M. Narbaitz, "Effect of Surface-Modifying Macromolecules and Solvent Evaporation Time on the Performance of Polyethersulfone Membranes for the Separation of Chloroform/Water Mixtures by Pervaporation", J. Appl. Polym. Sci., **54**, 1937-1943 (1994).

Feast, W.J. and Munro, H.S., Eds., "Polymer Surfaces and Interfaces", John Wiley & Sons (1987).

Fleming, H.L. and C.S. Slater, "Pervaporation-Applications and Economics" in "Membrane Handbook", W.S.W. Ho and K.K. Sirkar, Eds., Van Nostrand Reinhold, New York (1992), pp.132-159.

Flory, P.J., "Principles of Polymer Chemistry", Cornell University Press, Ithaca, New York (1953).

Fox, T.J., Bull. Am. Phys. Soc., **1**, 123 (1956), referenced from Cortázar M., J.I. Eguiazábal, C. Uriarte, and J.J. Iruin, "Glass transition temperatures of plasticized poly(acrylate)", Polymer Bulletin, **18**, 149-157 (1987).

Gibbs, J.W., "Collected Works, Vol. 1", Longmans-Green, New York, 1928.

Gogolewski S., "Leading Contribution, Selected topics in biomedical polyurethanes. A review", Coll. & Polym Sci., **267**, 757-785 (1989).

Gordon, M and Taylor, J.S., J. Appl. Polym. Sci., **2**, 493 (1952), referenced from Aubin, M. and R.E. Prud'homme, "Analysis of the Glass Transition Temperature of Miscible Polymer Blends", Macromolecules, **21**, 2945-2949 (1988).

Harrell L.L., "Segmented polyurethanes. Properties as a function of segment size and distribution", Macromolecules, **2**, 607-614 (1969).

Huang, R.Y.M., Ed., "Pervaporation Membrane Separation Processes", Elsevier, New York (1991).

Huang R.Y.M and N.R. Jarvis, "Separation of liquid mixtures by using polymer membranes. II. Permeation of aqueous alcohol solutions through cellophane and poly(vinyl alcohol)", J. Appl. Polym. Sci., **14**, 2341-2356 (1970).

Huang R.Y.M and V.J.C. Lin, "Separation of liquid mixtures by the permeation process with graft copolymer membranes", J. Appl. Polym. Sci., **12**, 2615-2631 (1968).

Huang R.Y.M. and J.W. Rhim, "Separation Characteristics of Pervaporation Membrane Separation Processes", in "Pervaporation Membrane Separation Processes", R.Y.M. Huang, Ed., Elsevier, New York (1991), pp. 111-180.

Huang R.Y.M. and Y.F. Xu, "Pervaporation separation of ethanol-water mixtures using grafted poly(acrylic acid)-nylon 6 membranes", Eur. Polym. J., **24**(10), 927-931 (1988).

Huang R.Y.M, A. Moriera, R. Notarfonzo and Y.F. Xu, "Pervaporationseparation of acetic acid-water mixtures using modified membranes", J. Appl. Polym. Sci., **35**(5), 1391-1200 (1988).

Hvid, K.B., P.S. Nielsen and F.F. Stengaard, "Preparation and characterization of a new ultrafiltration membrane", J. Membr. Sci., **50**, 189-202 (1991).

Hu, C.B. and C.S.P. Sung, "Surface chemical composition-depth profile of polyether polyurethaneureas as studied by FT-IR and ESCA", Polym. Prepr., Am. Chem. Soc., Div. Polym. Chem., **21**, 156-174 (1980).

Hunston, D.L. ., J.R. Griffith and R.C. Bowers, "Fluoro epoxies: surface properties and applications", Ind. Eng. Chem. Prod. Res. Dev., **17**(1), 10-14 (1978).

Inagaki, N., S. Tasaka and Y. Kobayashi, "Pervaporation of ethanol-water mixture by plasma films prepared from hexamethyldisiloxane", Desalination, **70**, 465-479 (1988).

Johnson Jr., R.E. and Dettre R.H., "Wettability and Contact Angles", in "Surface and Colloid Science Vol. 2", E. Matijevíc, Ed., Wiley-Interscience, New York (1969), pp. 85-153.

Kang, Y.S., S.W. Lee, U.Y. Kim and J.S. Shim, "Pervaporation of water-ethanol mixtures through cross-linked and surface-modified poly(vinyl alcohol) membrane", J. Membrane Sci., **51**, 215-226 (1990).

Kaschemekat, J., J.G. Wijmans, R.W. Baker and I. Blume, "Separation of organics from water using pervaporation", in "Proceedings of Third International Conference on

Pervaporation Processes in the Chemical Industry", R.A. Bakish, Ed., Englewood, NJ (1988), pp. 405-412,.

Kasemura, T., Y. Oshibe, H. Uozumi, S. Kawai, Y. Yamada, H. Ohmura and T. Yamamoto, "Surface modification of epoxy resin with fluorine-containing methacrylic ester copolymers", J. Appl. Polym. Sci., **47**, 2207-2216 (1993).

Kasemura, T., N. Yamashita, K. Suzuki, T. Kondo and T. Hata, Kobunshi Ronbunshu (Jpn. J. Polym. Sci. Technol.), **35**, 215 (1987). Referenced from Kasemura, T., Y. Oshibe, H. Uozumi, S. Kawai, Y. Yamada, H. Ohmura and T. Yamamoto, "Surface modification of epoxy resin with fluorine-containing methacrylic ester copolymers", J. Appl. Polym. Sci., **47**, 2207-2216 (1993).

Kasemura, T., K. Suzuki, F. Uzi, T. Kondo and T. Hata, Kobunshi Ronbunshu, **35**, 779 (1978). Referenced from Kasemura, T., Y. Oshibe, H. Uozumi, S. Kawai, Y. Yamada, H. Ohmura and T. Yamamoto, "Surface modification of epoxy resin with fluorine-containing methacrylic ester copolymers", J. Appl. Polym. Sci., **47**, 2207-2216 (1993).

Kasemura, T., T. Kondo and T. Hata, Kobunshi Ronbunshu, **36**, 815 (1979). Referenced from Kasemura, T., Y. Oshibe, H. Uozumi, S. Kawai, Y. Yamada, H. Ohmura and T. Yamamoto, "Surface modification of epoxy resin with fluorine-containing methacrylic ester copolymers", J. Appl. Polym. Sci., **47**, 2207-2216 (1993).

Kasemura, T., M. Inagaki and T. Hata, Kobunshi Ronbunshu, **44**, 131 (1987). Referenced from Kasemura, T., Y. Oshibe, H. Uozumi, S. Kawai, Y. Yamada, H. Ohmura and T. Yamamoto, "Surface modification of epoxy resin with fluorine-containing methacrylic ester copolymers", J. Appl. Polym. Sci., **47**, 2207-2216 (1993).

Kasemura, T., S. Yamaguchi and T. Hata, Kobunshi Ronbunshu, **44**, 657 (1987). Referenced from Kasemura, T., Y. Oshibe, H. Uozumi, S. Kawai, Y. Yamada, H. Ohmura and T. Yamamoto, "Surface modification of epoxy resin with fluorine-containing methacrylic ester copolymers", J. Appl. Polym. Sci., **47**, 2207-2216 (1993).

Kasemura, T., S. Yamaguchi, K. Hattori and T. Hata, Kobunshi Ronbunshu, **45**, 63 (1988). Referenced from Kasemura, T., Y. Oshibe, H. Uozumi, S. Kawai, Y. Yamada, H. Ohmura and T. Yamamoto, "Surface modification of epoxy resin with fluorine-containing methacrylic ester copolymers", J. Appl. Polym. Sci., **47**, 2207-2216 (1993).

Kesting, R.E., "Synthetic Polymeric Membranes", McGraw-Hill, New York, NY (1971).

Keszler, B., G. Kovác, A. Tóth, I. Bertóti and M. Hegyi, "Modified polyethersulfone membranes", J. Membr. Sci., **62**, 201-210 (1991).

Kirste, R. G. and B.R. Lehnen, "Determination of the chemical potential and the expansion coefficient in mixtures of poly(dimethylsiloxanes" of different molecular weights", (original citation in Ger.) Makromol. Chem. , **177**, 1137-1143 (1976).

Kober M. and B. Wesslén, "Amphiphilic segmented polyurethanes as surface modifying additives", J. Polym. Sci., Part A: Polym. Chem., **30**, 1061-1070 (1992).

Koops, G.H. and C.A. Smolders, "Estimation and evaluation of polymeric materials for pervaporation membranes", in "Pervaporation Membrane Separation Processes", R.Y.M. Huang, Ed., Elsevier, New York (1991), pp. 253-278.

Krause, S., "Polymer-Polymer Compatibility", in "Polymer blends", D.R. Paul and S. Newman, Eds., Academic Press, London (1978), pp. 16-106.

Krause, W.A., R.G. Kirste, J. Haas, B.J. Schmitt, and D.J. Stein, Makromol. Chem., **177**, 1145 (1976). Referenced from Krause, S., "Polymer-Polymer Compatibility", in "Polymer blends", D.R. Paul and S. Newman, Eds., Academic Press, London (1978), pp. 16-106.

Lafrenière, L.Y., Talbot D.F., Matsuura T. and Sourirajan S., "Effect of Polyvinylpyrrolidone Additive on the Performance of Polyethersulfone Ultrafiltration Membranes", Ind. Eng. Chem. res., **26**, 2385-2389 (1987).

Lai, J.Y. and Y.C. Chao, "Plasma-modified nylon 4 membranes for reverse osmosis desalination", J. Appl. Polym. Sci., **39**, 2293-2303 (1990).

Lee C.H., "Theory of reverse osmosis and some other membrane permeation operations", J. Appl. Polym. Sci., **19**, 83-95 (1975).

Lelah M.D. and S.L. Cooper, "Polyurethanes in Medicine", CRC Press, Boca Raton (1986).

Levenston, B.H. Assoc. et al, "Background information for an environment code of practice for dry cleaning facilities", Environment Canada, Ottawa (1991).

Li, X., Z. Li, C. Chen and W. Wu, "Plasma polymerization of hydrophilic and hydrophobic monomers for surface modification of nucle-microporous membrane", Chin. J. Polym. Sci., **8**(2), 165-169 (1990).

Long R.B., Ind. Eng. Chem. Fundamentals, **4**, 445 (1965). Referenced from Huang R.Y.M. and J.W. Rhim, "Separation Characteristics of Pervaporation Membrane Separation Processes", in "Pervaporation Membrane Separation Processes", R.Y.M. Huang, Ed., Elsevier, New York (1991), pp. 111-180.

Lonsdale H.K., U. Merten and R.L. Riley, J. Appl. Polym. Sci., **9**, 593 (1965). Referenced from Huang R.Y.M. and J.W. Rhim, "Separation Characteristics of Pervaporation Membrane Separation Processes", in "Pervaporation Membrane Separation Processes", R.Y.M. Huang, Ed., Elsevier, New York (1991), pp. 111-180.

Masnoka, T., T. Iwatubo, S. Hongyo and K. Mizoguchi, "Performance of a pervaporation membrane for separating mixtures of ethanol and water, prepared by plasma polymerization of an allylamine-hexafluoroethane system", Int. Chem. Eng., **32**(3), 552-559 (1992).

Matsuura, T., "Synthetic Membranes and Membranes Separation Processes", CRC Press, Boca Raton (1993).

Merten U. (Ed.), "Transport Properties of Osmotic Membranes", MIT Press, Cambridge, Mass. (1966).

Mohr, J.M., D.R. Paul, I. Pinnau and W.J. Koros, "Surface fluorination of polysulfone asymmetric membranes and films", J. Membr. Sci., **56**, 77-98 (1991).

Montgomery, D.C. and Peck E.A., "Introduction to Linear Regression Analysis", John Wiley & Sons, New York (1982).

Munekata, S., "Fluoropolymers as coating material", Prog. in Org. Coat., **16**, 113-134 (1988).

Mulder M.H.V. and C.A. Smolders, "On the mechanism of separation of ethanol/water mixtures by pervaporation. I. Calculations of concentration profiles", J. Membrane Sci., **17**, 289-307 (1984).

Mulder M.H.V. and C.A. Smolders, "Pervaporation, solubility aspects of the solution-diffusion model", J. Membrane Sci., **15**, 1-19 (1985).

Mulder M.H.V., T. Franken, and C.A. Smolders, "Preferential sorption versus preferential permeability in pervaporation", J. Membrane Sci., **22**, 155-173 (1985).

Néel, J., "Introduction to pervaporation", in "Pervaporation Membrane Separation Processes", R.Y.M. Huang, Ed., Elsevier, New York (1991), pp. 1-86.

Nyström, M., "Fouling of unmodified and modified polysulfone ultrafiltration membranes by ovalbumin", J. Membrane Sci., **44**, 183-196 (1989).

Patai, S., "The Chemistry of Cyanates and Their Thio Derivatives, Parts 1 and 2", in "The Chemistry of Functional Group Series", John Wiley & Sons, New York (1977).

Paul, D.R., "Background and Perspective", in "Polymer blends", D.R. Paul and S. Newman, Eds., Academic Press, London (1978), pp. 2-14.

Paul D.R., "Stategies for compatibilization of Polymer Blends", in "Advances in Polymer Blends and Alloys Technology, Vol. 4", K. Finlayson, Ed., Technomic Publishing Company, Lancaster (1993), pp. 80-86.

Paul, D.R. and A.T. Dibenedetto, J. Polym. Sci., **C**, **10**, 17 (1965). Referenced from Huang R.Y.M. and J.W. Rhim, "Separation Characteristics of Pervaporation Membrane Separation Processes", in "Pervaporation Membrane Separation Processes", R.Y.M. Huang, Ed., Elsevier, New York (1991), pp. 111-180.

Paul, D.R. and S. Newman, Eds., "Polymer blends", Academic Press, London (1978).

Peebles, L.H., Jr., "Sequence Length Distribution in Segmented Block Copolymers", Macromolecules, **7**, 872-882 (1974).

Peebles, L.H., Jr., "Hard Block Length Distribution in Segmented Block Copolymers", Macromolecules, **9**, 58-61 (1974).

Piirma, I., "Polymeric surfactants", Marcel Dekker, New York (1992), pp. 203-224.

Qipeng, G., "Miscibility of poly(n-vinyl-2-pyrrolidone) with poly(ether sulphone) and two phenolphthalein-based polymers", Eur. Polym. J., **28** (9), 1049-1051 (1992).

Rautenbach R. and R. Albrecht, "Separation of organic binary mixtures by pervaporation", J. Membrane Sci., **7**, 203-223 (1980).

Ratner, B.D. and R.W. Paynter, "Polyurethane surfaces: the importance of molecular weight distribution, bulk chemistry and casting conditions", in "Polyurethanes in Biomedical Engineering, Progress in Biomedical Engineering, Vol. 1", H. Plank, G. Egbers and I. Syre, Eds., Elsevier, Amsterdam (1984), pp. 41-68.

Ratner, B.D., S.C. Yoon, A. Kaul and R. Rahman, "Control of polyurethane surface structure by synthesis and additives: Implications for blood interactions",in "Polyurethanes in Biomedical Engineering, Progress in Biomedical Engineering, Vol. 2", H. Plank, G. Egbers and I. Syre, Eds., Elsevier, Amsterdam (1984), pp. 213-229.

Reegen, S.L. and K.C. Frisch, "Catalysis in isocyanate reactions", Adv. Urethane Sci. & Tech., **1**, 1 (1971). Referenced from Lelah M.D. and S.L. Cooper, "Polyurethanes in Medicine", CRC Press, Boca Raton (1986), pp. 21-33.

Rinke, H., H. Schild, and W. Siefken, French Patent 845,917 (1939); U.S. Patent 2,511,544 (1950).

Robinson, J.W., Ed., "Practical Handbook of Spectroscopy", CRC Press, Boca Raton (1991), pp 183-416.

Rosen, S., "Fundamental Principles of Polymeric Materials", Jonh Wiley & Sons (1982).

Sachs, L., "Applied statistics", translated by Z. Reynarowych, Springer-Verlag, New York (1984).

Schmidt, D.L., C.E. Coburn, B.M. Dekoven, G.E. Potter, G.F. Meyers and D.A. Fischer, "Water-based non-stick hydrophobic coatings", Nature, **368** (3), 39-41 (1994).

Schollenberger, C.S. and K. Dinbergs, "Thermoplastic urethane molecular weight property relations", J.Elast. Plast., **5**, 222-251 (1973).

Sedath R.H., D.R. Taylor and N.N. Li, "Reduced fouling of ultrafiltration membranes via surface fluorination", Sep. Sci. and Tech., **28**(1-3), 225-269 (1993).

Shultz, A.R. and A.L. Young, "Glass Transitions of Styrene/α-Methylstyrene Statistical Copolymers and of Their blends with PPO® Resin.", J. Appl. Polym. Sci., **28**, 1677-1684 (1983).

Shultz, A.R., A.L. Young, S. Alessi and M. Stewart, "Glass Transitions of Poly(bisphenol-A Carbonate)/Ultraviolet Light Stabilizer Blends by DSC and TOA", J. Appl. Polym. Sci., **28**, 1685-1700 (1983).

Simha R. and R.F. Boyer, J. Chem. Phys., **37**, 1003 (1962). Referenced from Cortázar M., J.I. Eguiazábal, C. Uriarte, and J.J. Iruin, "Glass transition temperatures of plasticized poly(acrylate)", Polymer Bulletin, **18**, 149-157 (1987).

Somorjai, G.A., "Chemistry in Two Dimensions: Surfaces", Cornell University Press (1981).

Sourirajan, S. and Matsuura T., "Reverse Osmosis/Ultrafiltration Process Principles", National Research Council Canada, Ottawa, Canada (1985).

Stengaard, F.F., "Characteristics and performance of new types of ultrafiltration membranes with chemically modified surfaces", Desalination, **70**, 207-224 (1988).

Stein, D.J., R.H. Jung, K.H. Illers, and H. Hendus, "Phenomenological investigation on the miscibility of polymers", (original citation in German), Angew. Makromol. Chem., **36**, 89-100 (1974).

Turi, E. A., Ed., "Thermal Characterization of Polymeric Materials", Academic Press (1981).

Vrentas J.S. and J.L. Duda, Macromolecules, **4**, 785 (1976). Referenced from Huang R.Y.M. and J.W. Rhim, "Separation Characteristics of Pervaporation Membrane Separation Processes", in "Pervaporation Membrane Separation Processes", R.Y.M. Huang, Ed., Elsevier, New York (1991), pp. 111-180.

Vrentas J.S. and J.L. Duda, J. Polym. Sci., Polym. Phys. Ed., **15**, 403, 401 (1977). Referenced from Huang R.Y.M. and J.W. Rhim, "Separation Characteristics of Pervaporation Membrane Separation Processes", in "Pervaporation Membrane Separation Processes", R.Y.M. Huang, Ed., Elsevier, New York (1991), pp. 111-180.

Ward R.S., K.A. White and C.B. Hu, "Use of surface-modifying additives in the development of a new biomedical polyurethaneurea", in "Polyurethanes in Biomedical Engineering, Progress in Biomedical Engineering, Vol. 1", H. Plank, G. Egbers and I. Syre, Eds., Elsevier, Amsterdam (1984), pp. 181-200.

Ward, R.S., "Surface Modifying Additives for Biomedical Polymers", IEEE Eng. in Med. and Bio. Magazine, 22-25 (June, 1989).

Wang, T.L. and D.J. Lyman, "The effect of reaction conditions on the urethane prepolymer formation", Polymer Bull., **27**, 549-555 (1992).

Wood, L.A., J. Polym. Sci., **28**, 319 (1958). Referenced from Cortázar M., J.I. Eguiazábal, C. Uriarte, and J.J. Iruin, "Glass transition temperatures of plasticized poly(acrylate)", Polymer Bulletin, **18**, 149-157 (1987).

Wu Y., Y. Kong, X. Lin, W. Lin and J. Xu, "Surface -modified hydrophilic membranes in membrane distillation", J. Membr. Sci., **72**, 189-196 (1992).

Xu Y.F. and R.Y.M. Huang, "Pervaporation separation of ethanol-water mixtures using ionically cross-linked blended polyacrylic acid-nylon 6 membranes", J. Appl. Polym. Sci., **36**(5), 1121-1128 (1988).

Xu, J., W. Xian and H. Zeng, "Polyethersulphone induced crystallization with liquid crystal polymer", Polym. Com., **32**(11), 336-338 (1991).

Yoshikawa M., T. Yukoshi, K. Sanui and N. Ogata, "Separation of water and ethanol by pervaporation through poly(acrylic acid-co-acrylonitrile) membrane", J. Polym. Sci.:Polym. lett. Ed., bf 22, 473-475 (1984).

Yoshikawa M., H. Yokoi, K. Sanui and N. Ogata, "Pervaporation of water-ethanol mixture through poly(maleimide-co-acrylonitrile) membrane", J. Polym. Sci.:Polym. lett. Ed., **22**, 125-127 (1984).

Young, R.J. and P.A. Lowell, "Introduction to polymers", Chapman & Hall, 1991.

Yu X.H., A.Z. Okkema and S.L. Cooper, "Synthesis and Physical Properties of Poly(fluoroalkylether) urethanes", J. Appl. Polym. Sci., **41**, 1777-1795 (1990).

Appendix A Molecular weight characterization

Table A - 1: Relative molecular weight for the eight different SMM formulations determined by gel permeation chromatography (GPC) analysis.

SMM	Synthesis#*	M_w	Ave.	Std. err.	M_n	Ave.	Std. err.	Polydispersity	Ave.	Std. err.
MPB322HN	1 (40)	23000			14375			1.6		
	2 (38)	25000	26667	2728	16667	16273	1002	1.5	1.6	0.1
	3 (36)	32000			17778			1.8		
MPB322HR	1 (51)	21000			13125			1.6		
	2 (53)	22000	22333	882	14667	14264	578	1.5	1.6	0.0
	3 (55)	24000			15000			1.6		
MPB212HN	1 (49)	17000			11333			1.5		
	2 (58)	19000	16333	1764	11176	10599	658	1.7	1.5	0.1
	3 (46)	13000			9286			1.4		
MPB212HR	1 (52)	14000			10000			1.4		
	2 (56)	22000	18000	2309	12222	11407	707	1.8	1.6	0.1
	3 (57)	18000			12000			1.5		
MPB322LN	1 (19)	28000			16471			1.7		
	2 (30)	30000	25333	3712	17647	15373	1720	1.7	1.6	0.1
	3 (43)	18000			12000			1.5		
MPB322LR	1 (41)	19000			12667			1.5		
	2 (61)	21000	19333	882	14000	13175	416	1.5	1.5	0.0
	3 (63)	18000			12857			1.4		
MPB212LN	1 (60)	12000			9231			1.3		
	2 (62)	11000	12667	1202	8462	9231	444	1.3	1.4	0.1
	3 (64)	15000			10000			1.5		
MPB212LR	1 (50	14000			10000			1.4		
	2 (54)	18000	15333	1333	10588	10196	196	1.7	1.5	0.1
	3 (59)	14000			10000			1.4		

* The numbers in bracket beside the synthesis number are internal identification number.

Table A - 2 : Percent standard error of multiple GPC runs of polystyrene standards.

Run #	Polystyrene standard #									
	1	2	3	4	5	6	7	8	9	10
1	1089464	706785	355274	189374	96055	39039	18411	9679	5422	2990
2	1085807	717555	323012	213322	89551	39749	19171	8998	5582	2959
3	1084279	714834	350883	188181	97759	38443	18349	9833	5283	3018
4	1086397	696126	357394	186371	94188	38612	18153	9295	5278	2886
5	1094371	697111	353970	192353	97720	38280	18360	9643	5441	3000
	Mean									
	1088064	706482	348107	193920	95055	38825	18489	9490	5401	2971
	% std. err.									
	0%	1%	4%	6%	4%	2%	2%	4%	2%	2%

Appendix B *Elemental analysis and weight fractions of components*

Table B - 1 : Weight fraction of BA-L (f_z), MDI (f_m), PPO (f_p) in SMM calculated from weight percentnitrogen (%N) and weight percent fluorine (%F) as determined from elemental analysis

SMM	Synthesis#	%N	%F	%C	f_z	f_m	f_p	%F/%C	Ave	Std err	%N/%C	Ave	Std err
MPB322HN	1	4.3	13.7	57.9	0.21	0.38	0.41	0.24			0.07		
	2	3.2	14.8	55.0	0.22	0.29	0.49	0.27	0.24	0.01	0.06	0.07	0.01
	3	4.7	12.2	55.9	0.18	0.42	0.40	0.22			0.08		
MPB322HR	1	4.8	10.9	57.8	0.17	0.43	0.40	0.19			0.08		
	2	4.3	19.4	57.9	0.29	0.39	0.32	0.33	0.20	0.08	0.07	0.08	0.00
	3	5.0	3.8	61.6	0.06	0.45	0.49	0.06			0.08		
MPB212HN	1	4.2	16.2	53.6	0.25	0.37	0.38	0.30			0.08		
	2	4.4	17.2	54.8	0.26	0.39	0.34	0.31	0.38	0.07	0.08	0.08	0.00
	3	3.7	25.9	50.1	0.39	0.33	0.28	0.52			0.07		
MPB212HR	1	3.8	14.5	55.4	0.22	0.34	0.44	0.26			0.07		
	2	5.5	9.6	58.1	0.15	0.49	0.36	0.17	0.21	0.03	0.09	0.08	0.01
	3	5.1	12.3	57.7	0.19	0.45	0.36	0.21			0.09		
MPB322LN	1	5.4	3.9	63.5	0.07	0.49	0.44	0.06			0.09		
	2	7.5	3.6	63.1	0.07	0.67	0.26	0.06	0.10	0.04	0.12	0.09	0.01
	3	4.1	9.8	57.2	0.18	0.36	0.46	0.17			0.07		
MPB322LR	1	5.0	7.8	59.5	0.14	0.45	0.41	0.13			0.08		
	2	4.1	9.0	57.4	0.17	0.37	0.47	0.16	0.14	0.01	0.07	0.08	0.00
	3	4.7	7.0	57.9	0.12	0.42	0.47	0.12			0.08		
MPB212LN	1	4.5	18.1	53.6	0.33	0.40	0.26	0.34			0.08		
	2	4.3	17.1	52.7	0.31	0.38	0.31	0.32	0.32	0.01	0.08	0.08	0.00
	3	4.3	16.2	54.2	0.30	0.39	0.32	0.30			0.08		
MPB212LR	1	5.8	9.1	60.4	0.17	0.52	0.32	0.15			0.10		
	2	5.4	11.9	58.4	0.22	0.48	0.30	0.20	0.20	0.03	0.09	0.09	0.00
	3	5.4	13.7	56.6	0.25	0.48	0.27	0.24			0.10		

Samples of calculation:

f_z of MPB322HN(1) = $w'_{F\text{-}SMM} / w'_{F\text{-}BA\text{-}L}$ = 0.137 / 0.658 = 0.208 ≈ 0.21

f_z for MPB322LN(1) = $w'_{F\text{-}SMM} / w'_{F\text{-}BA\text{-}L}$ = 0.039 / 0.546 = 0.071 ≈ 0.07

Note the difference in value of $w'_{F\text{-}BA\text{-}L}$ to reflect that there are two BA-L. Therefore, f_z value is a measure of the incorporation of each type of BA-L and not just the fluorine content.

f_m of MPB322HN(1) = $w'_{N\text{-}SMM} / w'_{N\text{-}MDI}$ = 0.043 / 0.112 = 0.383 ≈ 0.38

and f_p of MPB322HN(1) = 1- f_z - f_m = 1 - 0.21 - 0.38 = 0.41

Appendix C Results of thermal analysis by DSC

Table C - 1 : Thermal analysis data for the eight different SMM formulations determined from Differential Scanning Calorimetry (DSC) analysis. The reported glass transition temperature (T_g) has three components: the onset T_g is the temperature at which the transition starts, the T_g width which is the difference between the final T_g and this onset T_g, and the mid-point T_g which is taken at half way of the change in specific heat capacity. The heat flow at T_g is the specific amount of heat flow for the entire transition. The ΔCp at T_g is the apparent change in specific heat capacity between the liquid and glassy state.

SMM	Synthesis #	Onset T_g (°C)	Fin. T_g (°C)	T_g width (°C)	Mid-point T_g (°C)	Heat flow at T_g (J/g)	ΔCp at T_g (J/g.°C)	Mid-point T_g x ΔCp @ T_g (J/g)
MPB322HN	1	17	33	16	26	6.5	0.4	10.5
	2	18	33	15	27	5.3	0.4	9.5
	3	23	41	18	33	6.1	0.3	11.3
MPB322HR	1	15	29	14	23	5.6	0.4	9.2
	2	17	31	14	23	4.9	0.3	8.0
	3	9	21	12	15	4.2	0.3	5.2
MPB212HN	1	25	39	14	33	4.1	0.3	9.6
	2	24	38	14	32	4.3	0.3	9.9
	3(1)*	13	27	14	21	3.9	0.3	5.9
	3(2)	50	61	11	55	1.3	0.1	6.5
MPB212HR	1	23	33	10	30	3.2	0.3	9.7
	2	17	32	15	26	4.5	0.3	7.8
	3	22	37	15	30	4.3	0.3	8.5
MPB322LN	1	8	22	14	15	5.1	0.4	5.5
	2	9	23	14	16	5.7	0.4	6.5
	3	20	34	14	27	5.0	0.4	9.6
MPB322LR	1	16	32	16	25	6.1	0.4	9.6
	2	15	30	15	22	6.1	0.4	8.9
	3	17	32	15	26	6.0	0.4	10.5
MPB212LN	1	19	33	14	26	5.0	0.4	9.2
	2	20	34	14	28	4.8	0.3	9.6
	3	23	36	13	31	4.9	0.4	11.7
MPB212LR	1	17	32	15	25	4.6	0.3	7.6
	2	18	32	14	25	4.1	0.3	7.4
	3	23	36	13	31	4.1	0.3	9.8

* This particular material had two distinct but close to each other T_g regions. Average values was reported in Table 4-1, and the appropriate error was accounted for this variation. The reason for this peculiar behaviour is unknown at the moment.

Sample of calculation of ΔCp:

ΔCp of MPB322HN(1) = Heat flow at T_g / T_g width = 6.5 / 16 = 0.406 ≈ 0.4 J/g·°C

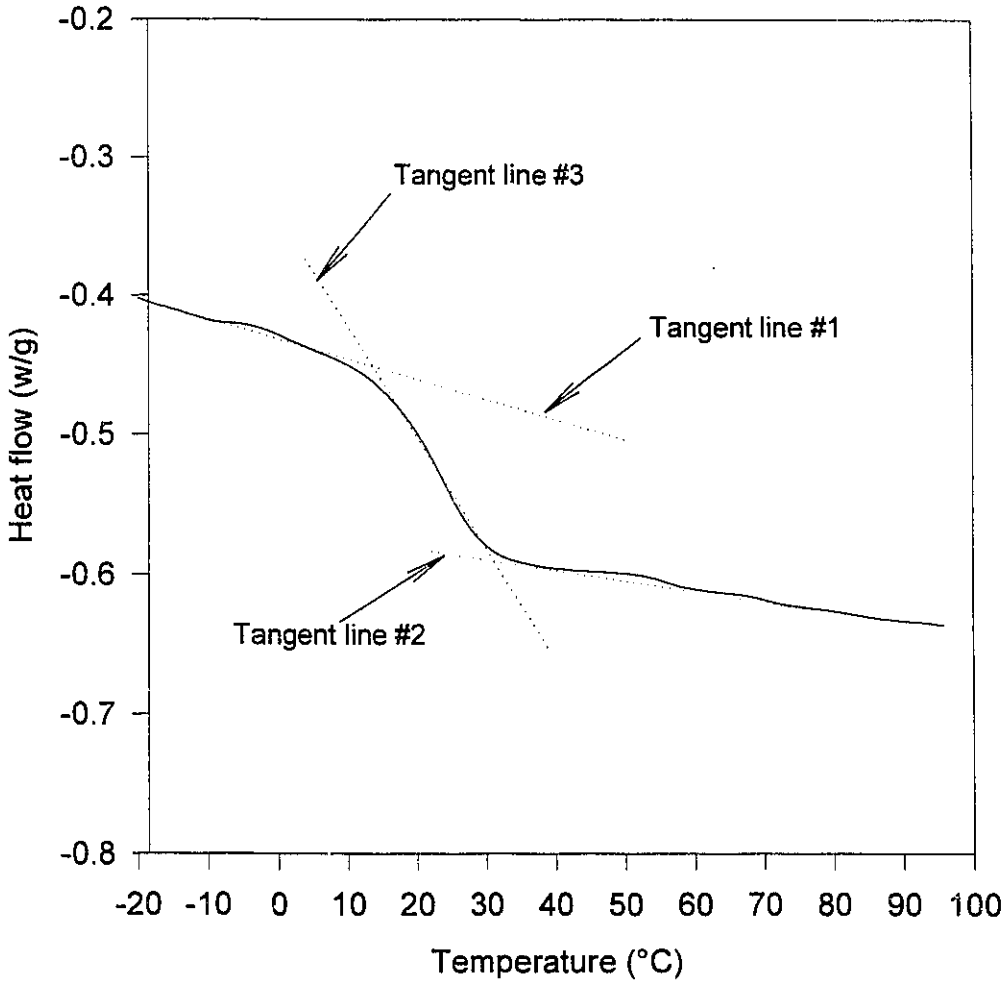

Figure C - 1: Graphical method to determine T_g. Onset T_g is determined at the intersection of tangent line #1 and #3, whereas final T_g is determined at the intersection of tangent line #3 and #2. The mid-point T_g is determined by computer software at half the ΔCp change. Tangent lines were entered directly through interactive analyzing software (see section 3.4.2).

Table C - 2: Experimental thermal analysis data for blends of PES and SMMs. The average onset T_g, T_g width, mid-point T_g and the ΔCp were included with standard error.

SMM in blends	SMM:PES 2:98 (0.5 wt.% SMM in solution)							
	Onset T_g	Std. Err.	T_g width	Std. Err.	Mid-point T_g	Std. Err.	ΔCp (J/°C.g)	Std.Err.
MPB322HN	197	4	15	0.50	204	4	0.19	0.01
MPB322HR	198	6	13	0.50	205	7	0.20	0.01
MPB212HN	181	4	14	1.00	187	4	0.18	0.00
MPB212HR	195	18	12	0.00	200	18	0.20	0.02
MPB322LN	201	1	12	0.00	207	2	0.21	0.01
MPB322LR	197	14	13	1.00	205	12	0.22	0.00
MPB212LN	194	9	14	1.50	200	9	0.19	0.01
MPB212LR	198	12	15	1.50	204	11	0.18	0.01

Table C - 2 (Cont'd): Experimental thermal analysis data for blends of PES and SMMs. The average onset T_g, T_g width, mid-point T_g and the ΔCp were included with standard error.

SMM in blends	SMM:PES 4:96 (1.0 wt.% SMM in solution)							
	Onset T_g	Std. Err.	T_g width	Std. Err.	Mid-point T_g	Std. Err.	ΔCp (J/°C.g)	Std.Err.
MPB322HN	200	2	13	0.50	207	2	0.20	0.00
MPB322HR	194	7	17	2.50	201	8	0.22	0.01
MPB212HN	177	6	13	0.00	183	6	0.19	0.02
MPB212HR	190	22	14	1.50	196	21	0.19	0.01
MPB322LN	193	6	15	2.00	199	5	0.19	0.03
MPB322LR	198	4	14	2.00	204	4	0.20	0.01
MPB212LN	195	5	14	0.50	202	5	0.20	0.05
MPB212LR	195	10	16	5.00	203	10	0.22	0.01

Table C - 2 (Cont'd): Experimental thermal analysis data for blends of PES and SMMs. The average onset T_g, T_g width, mid-point T_g and the ΔCp were included with standard error. N/D : not determined due to phase separation; N/A : not available due to insufficient data point.

SMM in blends	SMM:PES 7:93 (2.0 wt.% SMM in solution)							
	Onset T_g	Std. Err.	T_g width	Std. Err.	Mid-point T_g	Std. Err.	ΔCp (J/°C.g)	Std.Err
MPB32[illegible]HN	N/D	N/D	N/D	N/D	N/D	N/D	N/D	N/D
MPB322HR	189	2	17	0.00	196	3	0.18	0.01
MPB212HN	N/D	N/D	N/D	N/D	N/D	N/D	N/D	N/D
MPB212HR	197	13	13	1.00	204	13	0.18	0.00
MPB322LN	191	N/A	14	N/A	199	N/A	0.19	N/A
MPB322LR	198	N/A	13	N/A	205	N/A	0.17	N/A
MPB212LN	201	3	14	0.50	208	3	0.16	0.01
MPB212LR	193	10	17	2.50	199	9	0.22	0.01

Appendix D Results of surface characterization by XPS

Table D - 1: Average relative intensities of various element for selected PES-SMM surfaces determined by XPS.

SMM	[SMM] = 0.5 wt.%			1.0 wt.%		2.0 wt.%	
	Element	Relative intensity (%) at 90°	Relative intensity (%) at 15°	Relative intensity (%) at 90°	Relative intensity (%) at 15°	Relative intensity (%) at 90°	Relative intensity (%) at 15°
MPB322HN	F	11.93	17.45	14.15	19.17	13.53	16.54
	O	16.20	13.80	15.47	13.51	15.27	10.10
	N	3.51	2.07	3.69	1.59	3.31	1.68
	C	67.22	66.22	65.83	65.17	66.80	71.25
	S	1.13	0.46	0.86	0.48	1.10	0.44
MPB322LN	F	6.18	11.24	6.76	13.49	9.15	19.04
	O	17.55	15.20	17.01	14.22	17.17	14.53
	N	3.92	2.69	3.75	2.51	3.73	2.87
	C	70.96	70.30	71.03	69.34	68.63	63.15
	S	1.42	0.57	1.45	0.45	1.32	0.41
MPB212HN	F	16.22	26.74	20.99	40.21	23.28	35.77
	O	14.22	12.28	12.39	8.16	11.42	8.89
	N	3.61	2.46	3.70	2.06	3.75	2.54
	C	65.11	58.22	62.62	49.27	60.92	52.46
	S	0.84	0.30	0.31	0.30	0.64	0.34
MPB212LN	F	10.78	18.72	14.95	29.49	22.79	36.28
	O	15.69	13.28	14.61	10.49	12.12	8.12
	N	2.99	1.95	3.47	2.23	3.79	2.46
	C	68.95	65.44	65.73	57.43	60.61	52.80
	S	1.59	0.60	1.24	0.35	0.69	0.34

Table D - 1: Chemical functional groups identified by XPS through chemical binding energy shifts (eV) in this thesis. Average standard error = 10% (Robinson, 1991)

Functional group	Chemical shift (eV)	Reference
C–C	285.00	Robinson, 1991
C–O–C	286.45, 286.13, 286.75	Robinson, 1991
N–C–O ‖ O	289.60	Robinson, 1991
$-CF_2-$	290.90 291.10, 291.80	Robinson, 1991
$-CF_3$	292.65, 292.70, 292.72 292.80, 293.70, 293.0	Robinson, 1991

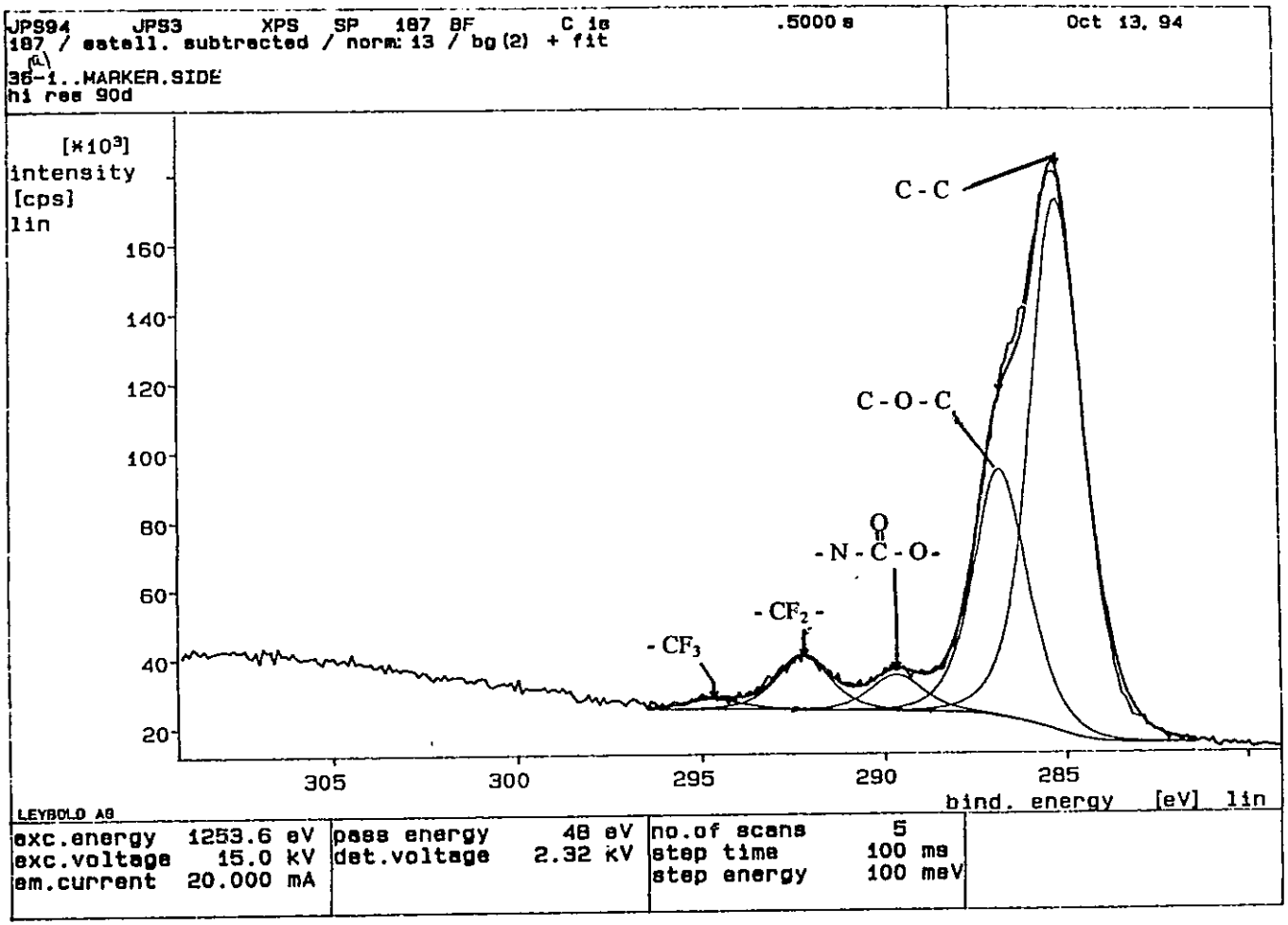

Figure D - 1: Typical high resolution XPS data with peaks identified. Data shown is that of the surface of PES/MPB322HN(2) with the wt.% of MPB322HN(2) in casting solution of 1.0. The take-off angle was 90°. Figure generated by Dr. R. Sadhi at the Centre for Biomaterials, University of Toronto.

Table D - 2: Average binding energy shift and peak's relative intensities for selected PES/SMM's surface determined by XPS. N/D: not detectable.

SMM	[SMM] = 0.5 wt.%				1.0 wt.%				2.0 wt.%			
	Binding energy shift at 90°	Relative intensity (%)	Binding energy shift at 15°	Relative intensity (%)	Binding energy shift at 90°	Relative intensity (%)	Binding energy shift at 15°	Relative intensity (%)	Binding energy shift at 90°	Relative intensity (%)	Binding energy shift at 15°	Relative intensity (%)
MPB322HN	284.88	59.48	285.00	53.97	285.01	57.15	284.98	62.82	284.85	63.16	284.73	53.31
	286.48	31.51	286.60	34.75	286.81	32.41	286.58	23.45	286.45	27.39	286.33	36.38
	289.38	3.45	289.50	3.92	289.51	4.11	289.48	4.63	289.35	3.10	286.33	4.59
	291.86	5.20	292.46	6.20	292.13	5.82	292.31	7.12	291.87	5.60	291.68	5.25
	294.80	0.36	295.08	1.33	294.80	0.52	295.11	1.99	294.83	1.06	295.03	1.85
MPB322LN	284.77	57.47	284.92	62.13	284.88	63.35	284.91	61.65	284.68	56.85	284.85	61.79
	286.37	36.54	286.52	30.16	286.68	30.51	286.51	29.62	286.28	35.24	286.45	29.70
	289.27	3.08	289.42	3.51	289.38	2.85	289.41	3.40	289.18	3.74	286.45	3.23
	291.81	2.44	291.84	4.19	291.84	3.14	291.93	4.50	291.74	3.98	291.76	5.11
	N/D	N/D	N/D	N/D	294.92	0.31	294.92	1.72	294.92	0.39	294.92	0.70
MPB212HN	284.98	58.69	284.94	58.87	285.01	56.16	284.92	57.63	284.99	57.11	284.97	51.96
	286.58	28.82	286.54	24.99	286.81	29.87	286.52	22.20	286.59	25.92	286.57	23.52
	289.48	4.42	289.44	3.95	289.51	4.45	289.42	3.79	289.49	4.43	286.57	5.31
	292.12	7.46	292.07	10.58	292.07	8.88	291.89	14.61	292.11	11.50	291.98	16.67
	294.83	0.61	294.38	1.56	294.83	0.72	294.38	1.77	294.83	1.04	294.38	2.55
MPB212LN	285.04	70.15	285.05	68.71	284.95	61.14	284.99	51.86	285.00	59.59	284.95	55.78
	286.64	22.72	286.65	23.27	286.75	28.45	286.59	30.81	286.60	27.23	286.55	25.75
	289.54	2.70	289.55	2.95	289.45	3.59	289.49	4.75	289.50	3.96	286.55	4.38
	292.28	4.14	292.06	4.59	291.99	6.11	291.89	10.80	292.19	7.91	291.87	11.65
	294.59	0.55	294.30	1.29	294.35	0.71	294.30	1.78	294.35	1.17	294.30	2.45

Appendix E Plots of comparisons of responses

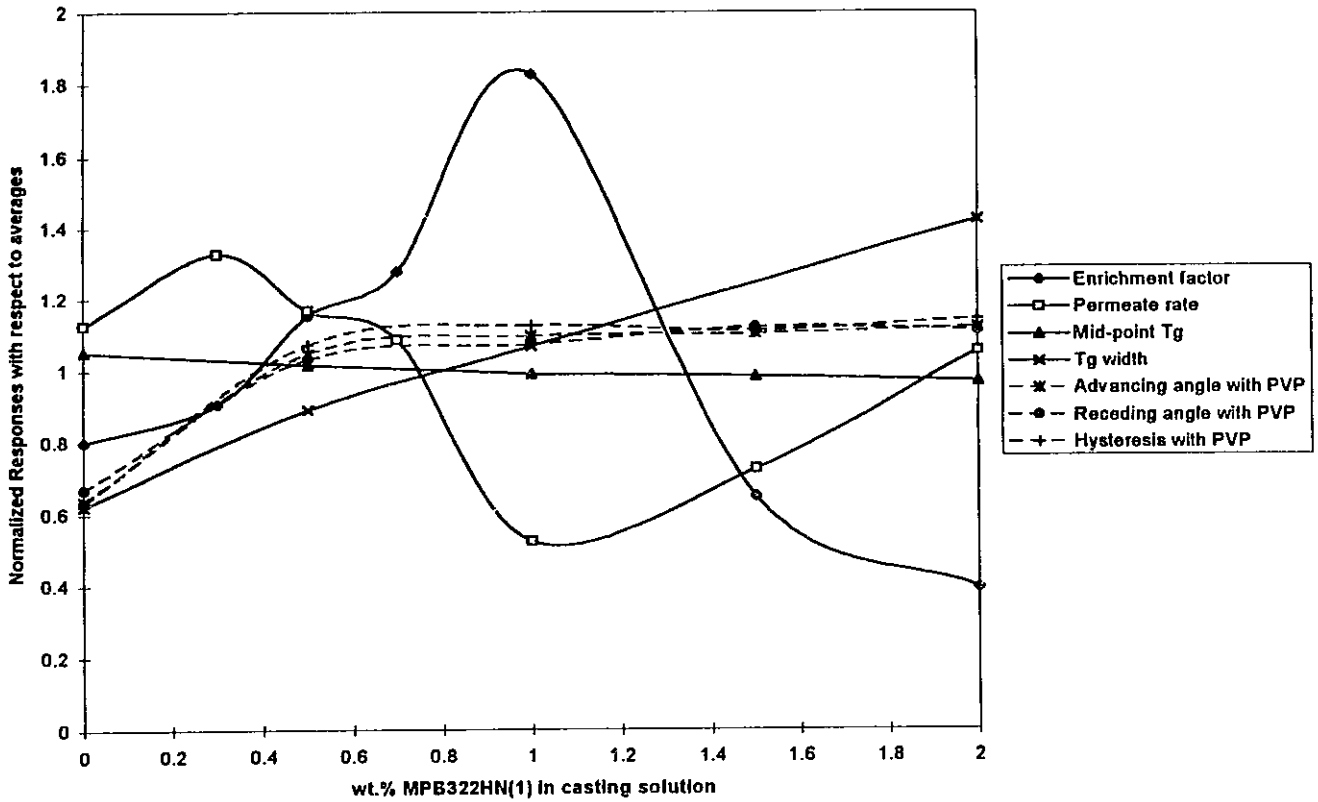

Figure E - 1: Comparisons of normalized response curves of various membrane bulk and surface characteristics (shown in dash line) and membrane selectivity and permeation flux behaviour for MPB322HN(1). PES and PVP in casting solution were kept constant at 25 and 6 wt.% respectively. The curves were artificially smoothed to improve visibility.

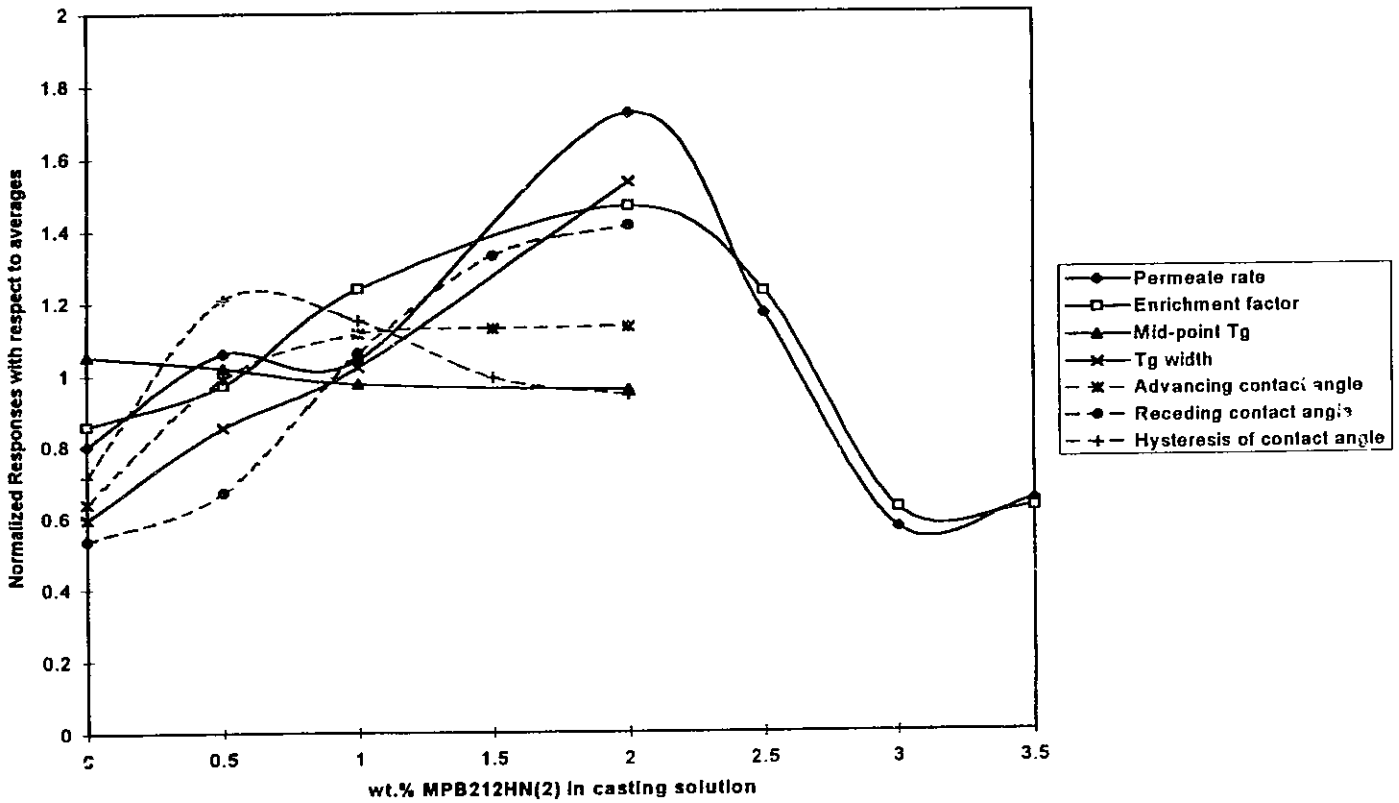

Figure E - 2: Comparisons of normalized response curves of various membrane bulk and surface characteristics (shown in dash line) and membrane selectivity and permeation flux behaviour for MPB212HN(2). PES and PVP in casting solution were kept constant at 25 and 6 wt.% respectively. The curves were artificially smoothed to improve visibility.

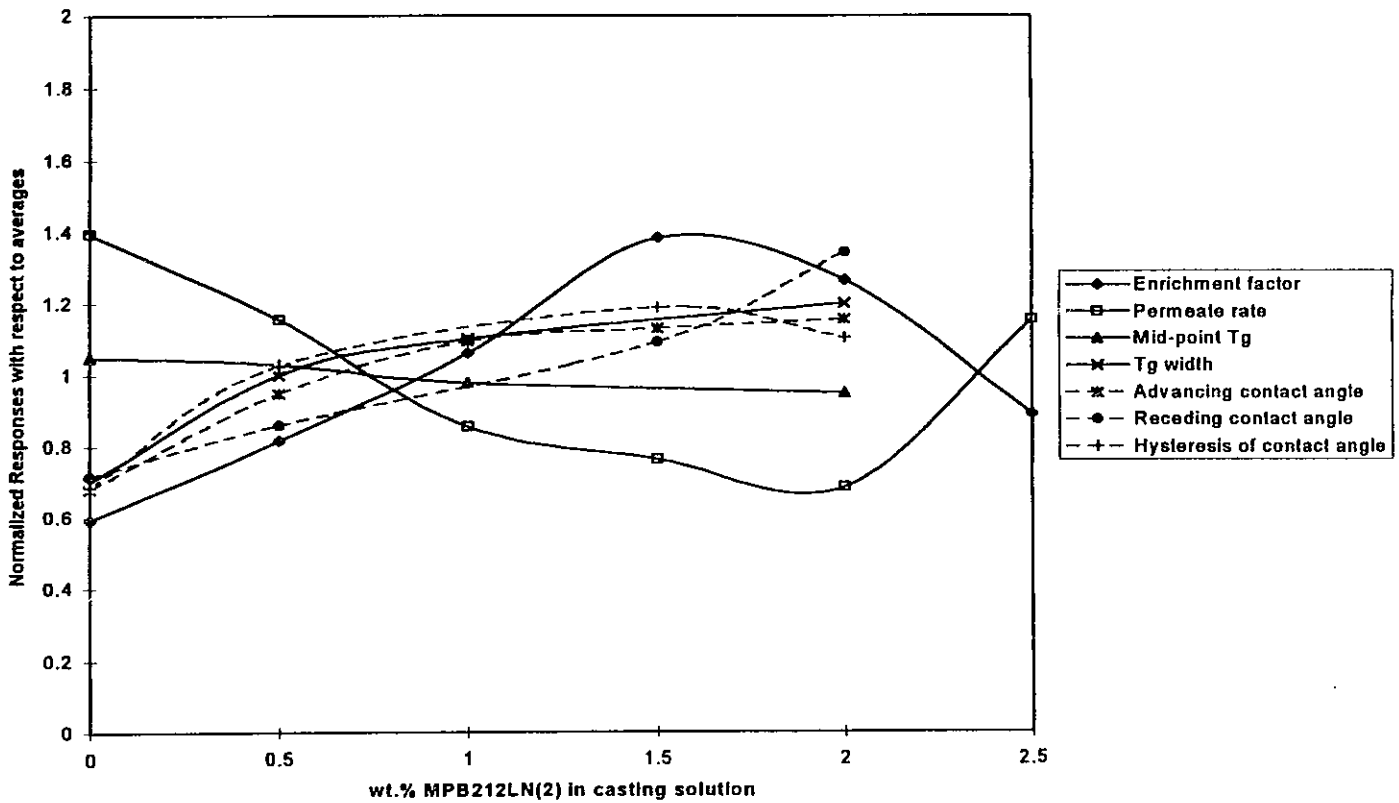

Figure E - 3: Comparisons of normalized response curves of various membrane bulk and surface characteristics (shown in dash line) and membrane selectivity and permeation flux behaviour for MPB212LN(2). PES and PVP in casting solution were kept constant at 25 and 6 wt.% respectively. The curves were artificially smoothed to improve visibility.

Appendix F Suppliers' addresses

Supplier for DuPont products: Van Waters & Rogers, 2700 J.B. Deschamps, Lachine, H8T 1E1, 514-631-941.

Supplier for Eastman Kodak products: Fisher Scientific, 112 Colonnade Road, Nepean, Ontario, K2E 7L6, 613-226-3273.

Aldrich Chemicals, 1001 West Saint Paul Ave., Milwaukee, WI53233, USA

Supplier for BDH products: VWR Scientific Canada, 175 Hanson St., Toronto, Ontario, M4C 1A7, 1-800-561-0789.

ICI Advanced Materials: not available, consult Mr. Y. Fang's Thesis.

Sigma Chemicals: not available, consult Mr. Y. Fang's Thesis.